STUDY OF EPOXY BASED GFRP NANOCOMPOSITES MODIFIED WITH POLYMER FIBER/ELASTOMER

A Thesis submitted

in fulfillment of the requirements

for the award of degree of

DOCTOR OF PHILOSOPHY

By

KARANBIR SINGH
(Registration No. 951208001)

Under the supervision of:

Dr. Tarun Nanda
Associate Professor
Mechanical Engineering Department
T.I.E.T., Patiala

Dr. Rajeev Mehta
Professor
Chemical Engineering Department
T.I.E.T., Patiala

Mechanical Engineering Department
Thapar Institute of Engineering and Technology
Patiala-147004 (Punjab)
January 2019

This Thesis is dedicated to

My mentors, Dr. Tarun Nanda and Dr. Rajeev Mehta, who taught me the principles of life,

My parents, who never stop giving of themselves in countless ways,

My beloved wife, who led me through the valley of darkness with light of hope and support,

My children, whose smile and love has encouraged me to give my best.

My friends, relatives, and in-laws who stood by me when things looked bleak.

You all have successfully made me the person I am becoming.

You will always be remembered and cherished throughout my life.

CERTIFICATE

This is to certify that the thesis entitled, **"STUDY OF EPOXY BASED GFRP NANOCOMPOSITES MODIFIED WITH POLYMER FIBER/ELASTOMER"** submitted by **Mr. Karanbir Singh,** Ph.D. (Part-time) student (Registration Number: 951208001) for the fulfillment of the requirements for the award of degree of Doctor of Philosophy in Mechanical Engineering Department, Thapar Institute of Engineering and Technology, Patiala, is a record of the candidate's own work carried out by him from July 2012 to January 2019 in this institute under our supervision. The matter presented in this thesis has not been submitted in part or full for the award of any degree in any university or institute.

Karanbir Singh

Date: 20/03/2019

(Karanbir Singh)

20/03/2019.

Dr. Tarun Nanda
Associate Professor
Mechanical Engineering Department
T.I.E.T., Patiala

Rajeev Mehta

Dr. Rajeev Mehta
Professor
Chemical Engineering Department
T.I.E.T., Patiala

ACKNOWLEDGEMENT

First and foremost, I would like to thank the Almighty whose countless blessings have made me who I am today. He enabled me with philosophy, perception, and motivation to present this work, after handling the tough times with empathy, professionalism, and clarity.

During the course of this thesis, several personnel directly or indirectly contributed in making this doctoral dissertation possible and I will always remain deeply indebted to them.

Firstly, from the core of my heart, I would like to express special thanks to my esteemed supervisors, Dr. Tarun Nanda (Associate Professor) and Dr. Rajeev Mehta (Professor) for encouraging my research and for allowing me to grow as a research scholar. Their consistent support, dynamic supervision, valuable and innovative suggestions have enlightened my knowledge and skills in the area of nanocomposites. Both of them have been tremendous mentors now and forever.

Besides my supervisors, I wish to express humble and special thanks to Prof. T.P. Singh, Prof. S.K. Mohapatra, and Prof. Ajay Batish for providing me necessary facilities in the department along with their encouragement and constant moral support to accomplish this task. I would also like to acknowledge the valuable suggestions of the members of the Doctoral Committee, Prof. O.P. Pandey, Dr. H.L. Bhowmick, Dr. J.S. Saini for their insightful comments and questions during my presentations. I sincerely appreciate the whole hearted cooperation and valuable help rendered by teaching and non-teaching staff of the Mechanical Engineering Department (MED), TIET, Patiala.

I am grateful to Dr. Sandeep Sharma, Laboratory Superintendent, CHED, TIET, who provided me with the experimental set-up to carry out my research work over the past six years. A special thanks to Dr. Alok Garg, Assistant Professor, CHED, TIET, for also providing me with the equipment for carrying out my research work. Without his benevolent motivation and support it would not have been possible to conduct this research. A thanks also goes to Dr. Rafat Siddique, Dean of Research and Sponsored Projects and Dr. O.P. Pandey (Former, Dean of Research and Sponsored Projects) for providing the possible research facilities.

I owe a special thanks to Dr. Tarun Nanda and his family members for supporting me whenever I needed. Whenever I needed time and inputs from Dr. Tarun Nanda, his family always welcomed me with a smile. It is only with the blessings and help of Ms. Archana Nanda that I was able to complete the present research.

I thank my seniors, Dr. Bikramjit Sharma and Dr. Shilpa Narang, along with fellow research scholars, Dr. Mohit Garg, Ms. Mansi Singh, Mr. Madhav Raturi, Mr. Gaurav Sharma, Mr.

Daksh Shelly, and Mr. Sandeep Sharma with whom I have spent these years of research and enjoyed many interactive sessions.

I am also thankful to all the laboratory staff members who maintained all the machines, sources, and equipment so efficiently which helped me in performing the experiments accurately.

A special thanks is also due to my family members. Words cannot express how grateful I am to my parents for all their sacrifice that they had made on my behalf and who have always been my strongest support and my source of motivation during moments of despair and discouragement. My wife Dr. Gurbinder Kaur who had been always there for me and keep me free from worries by efficiently managing all the odds faced by the family. My children Prabhnoor Kaur and Taskirat Kaur who have always acted as an energy booster for me to keep me motivated to provide more inputs to the research.

I want to thank my relatives and friends who have supported me by any means over the past six years in my pursuit of completing my Doctoral Degree.

I extend my special thanks to all who kept me well-balanced and have tried to make this challenging task a pleasant journey.

Place: *Patiala*

January 31, 2019. ***(*Karanbir Singh)**

ABSTRACT

Commercially used epoxy based glass fiber reinforced polymer composites (epoxy based GFRPs) show good specific strength and stiffness and are employed in many structural applications. However, safe operation of structures for the required lifetime demands that in addition to good static mechanical properties, these composites also possess high impact strength. Among the various approaches studied for an improvement in impact strength of epoxy based composites, significant efforts have been made by addition of nanoclay or polymer/elastomer fillers. Addition of nanoclay is reported to improve almost all properties of epoxy, but the impact strength has not shown significant improvements. Further, addition of elastomers to GFRPs is reported to show significant toughening of epoxy but other properties such as tensile strength etc. show significant deterioration. So, literature reports that addition of nanoclay leads to significant improvements in static properties and addition of polymer/elastomer filler leads to improved toughness of epoxy. Therefore, a combination of both, nanoclay and polymer/elastomer filler in epoxy based GFRPs, may provide a new route for high impact strength along with good tensile properties.

Thus, in the present work, epoxy based GFRP nanocomposites reinforced with clay as the nano-filler and thermoplastic fibers/elastomer particles as the micro-filler were processed using vacuum assisted hand lay-up technique. Polymer fibers namely polypropylene (PP) fibers and polyethylene terephthalate (PET) fibers, and an elastomer namely ethylene propylene diene monomer (EPDM) particles were used separately as the second filler in GFRPs containing nanoclay as the first filler. Nanoclay was added in a fixed amount of 1 phr in various nanocomposites. Low concentration of clay was chosen in order to avoid excessive increase in viscosity of the resulting system on addition of polymer/elastomer micro-fillers along with clay. The amount of PP fibers, PET fibers, and EPDM rubber particles were varied in the range of 0–3 phr, 0–3 phr, and 0–10 phr respectively (‘phr’ is per hundred resin, by weight). As postulated and specified in the present work, the main challenge was to improve the compatibility of polymer/elastomer fillers with other constituents of the nanocomposites. For this, surface treatment (compatibilization) of the micro-fillers was done using two methods (i) coating of silane coupling agents on micro-filler surface, and (ii) ultraviolet assisted maleic anhydride grafting on micro-filler surface. For maleic anhydride grafting of micro-fillers, the optimum treatment time for exposure of MAH-acetone solution to UV radiations was determined to be 30 h, 08 h, and 20 h respectively for PP fibers, PET fibers, and EPDM particles. The processing methodology including the sequence of steps and range of process parameters

used in the present work were effective in fabrication of epoxy based GFRPs possessing significantly improved mechanical performance. XRD results and TEM analysis showed that the processing methodology was effective in dispersing the nanoclay and obtaining the desired exfoliated clay morphology in nanocomposites.

Addition of nanoclay to the reference GFRP slightly improved the impact strength along with significant improvements in tensile strength and modulus. Addition of untreated thermoplastic polymeric fibers (PP fibers/PET fibers) to the nanocomposite system resulted in deterioration of impact strength as well as tensile properties. This decrease was due to the relatively inert nature of thermoplastic fibers resulting in their poor compatibility with other constituents of the nanocomposite system. However, addition of untreated elastomeric particles (EPDM rubber) to the nanocomposite system did improve the impact strength till an optimum concentration of 5 phr elastomer loading. This improvement was mainly due to cavitation of rubber particles in the nanocomposite system. Compatibilization procedures used for surface modification of micro-fillers were successful in enhancing the interfacial adhesion of micro-fillers with other constituents of the composite system and resulted in significant improvements in impact strength of resulting GFRPs. For a given composition, impact strength and tensile properties of nanocomposites reinforced with compatibilized polymer fibers/elastomer fillers was significantly higher than their counterparts reinforced with untreated micro-fillers. The optimum loading of polymer fibers (PET fibers/PP fibers) in the nanocomposite system for maximum improvement in impact strength was 2 phr, with silane treatment. Addition of silane treated PP fibers and PET fibers resulted in maximum improvement of 44% and 19%, respectively in impact strength of resulting nanocomposites with a minor drop in tensile properties. For fiber concentration beyond this optimum value (i.e. at 3 phr), a decrease in impact strength was observed due to poor dispersion of PET fibers/PP fibers in nanocomposites because of concomitant high viscosity of resin at such high concentration of reinforcement. Further, the optimum loading of EPDM filler in nanocomposite system for maximum improvement in impact strength was 5 phr, with silane treatment. Addition of silane treated EPDM rubber particles resulted in maximum improvement of 68% in impact strength of resulting nanocomposites. This increase in impact strength was due to the combined effect of improved compatibility between EPDM filler and glass fibers, along with cavitation phenomenon of rubber particles. Similar to the case of silane treated micro-fillers, addition of MAH grafted micro-fillers also improved the impact strength and tensile properties of nanocomposites compared to when nanocomposites were reinforced with untreated micro-fillers. Further, for a given composition of nanocomposites, improvement in impact

strength with MAH grafted micro-fillers was less than that obtained by silane treated micro-fillers. However, MAH grafting resulted in better recovery of tensile properties of nanocomposites. Thus, for the first time, GFRP nanocomposites with clay as the nano-filler and compatibilized polymer fibers/elastomer particles as the micro-sized filler were fabricated successfully providing improved impact strength without much drop in tensile properties. Processing of these nanocomposites from the highly viscous formulations was a challenging task and great care was taken to prevent any agglomeration.

LIST OF PUBLICATIONS

The results incorporated in this thesis are fully documented. The following publications in peer reviewed SCI Journals have come out from the present experimental work. Some part of the work has also been presented at an International Conference.

A. SCI Journals

Three publications in SCI journals. The details are as follows:

1. **Singh K**, Nanda T, Mehta R. Compatibilization of polypropylene fibers in epoxy based GFRP/clay nanocomposites for improved impact strength. ***Composites Part A: Applied Science and Manufacturing*** 2017; 98: 207–217. DOI: *doi.org/10.1016/j.compositesa.2017.03.027.* ***Impact Factor*** (2017): **4.514.**

2. **Singh K**, Nanda T, Mehta R. Processing of polyethylene terephthalate fiber reinforcement to improve compatibility with constituents of GFRP nanocomposites. ***Materials and Manufacturing Processes***. 2018; 33: 165–173. DOI:*10.1080/10426914.2017.1291955*. ***Impact Factor*** (2017): **2.669.**

3. **Singh K**, Nanda T, Mehta R. Addition of nanoclay and compatibilized EPDM rubber for improved impact strength of epoxy glass fiber composites. ***Composites Part A: Applied Science and Manufacturing*** 2017; 103: 263–271. DOI: *doi.org/10.1016/j.compositesa.2017.10.009.* ***Impact Factor*** (2017): **4.514**.

B. International Conference Proceedings

One publication in international conference. The details are as follows:

1. **Singh K**, Nanda T, Mehta R. Effect of clay reinforcement on the properties of epoxy based polymer matrix nanocomposites. Proceedings of the International Conference on Emerging Trends in Engineering and Management (ICETE 2013); November 8–9, 2013; Continental Group of Institutes, Fatehgarh Sahib, Punjab, India.

ACRONYMS & SYMBOLS

AR	Acrylic Rubber
AS	ɣ-aminopropyltriethoxysilane
ATS	3-aminopropyltrimethoxysilane
ASTM	American Society for Testing and Materials
BP	Benzophenone
BPO	Benzoyl Peroxide
BS	Bis-(3-triethoxysilyl-propyl)-tetrasulfane
CDT	Corona Discharge Treatment
CF	Carbon Fiber
CTBN	Carboxyl-terminated Butadiene Acrylonitrile
CSR	Core Shell Rubber
DCP	Dicumyl Peroxide
DDM	Diaminodiphenylmethane
DGEBA	Diglycidyl Ether of Bisphenol A
DM	Direct Mixing
DMA	Dynamic Mechanical Analysis
DMT	Dimethyl Terephthalate
DPNR	Deproteinized Rubber
DSC	Differential Scanning Calorimetry
EDS	Energy Dispersive Spectroscopy
EPDM	Ethylene Propylene Diene Monomer
EVA	Ethylene-vinyl Acetate
FA	Fly Ash
FE-SEM	Field Emission Scanning Electron Microscopy
FM	Flexural Modulus
FRP	Fiber Reinforced Polymer
FSC	Fatigue Strength Coefficient
FS	Flexural Strength
FSE	Fatigue Strength Exponent

FTIR	Fourier Transform Infrared Spectroscopy
GFRP	Glass Fiber Reinforced Plastic
GNP	Graphite Nano-platelet
GS	ɣ-glycidoxypropyltrimethoxysilane
HCl	Hydrochloric Acid
HDDGE	Hexanediol Diglycidylether
HDPE	High Density Polyethylene
HNT	Halloysite Nanotubes
HP	High Pressure
HPM	High Pressure Mixing
HTAC	Hexadecyltrimethylammonium Chloride
IFSS	Inter-facial Shear Strength
IL	Iconic Liquid
IL-DEP	Iconic Liquid Tributyl (ethyl) Phosphonium (diethyl) Phosphate
IL-TMP	Iconic Liquid Trihexyl (tetradecyl) Phosphonium Bis-2,4,4(trimethylpentyl) Phosphinate
IPDA	Isophoronediamine
MAH	Maleic Anhydride
MAH-g-EB	Maleic Anhydride Grafted Ethylene-1butene Copolymer
MAH-g-EPDM	Maleic Anhydride Grafted Ethylene Propylene Diene Monomer
MAH-g-PP	Maleic Anhydride Grafted Polypropylene
MAH-g-PET	Maleic Anhydride Grafted Polyethylene Terephthalate
MCDEA	4,4'-methylenebis(3-chloro-2,6-diethylaniline)
MMT	Montmorillonite
MS	ɣ-methacryloxypropyltrimethoxysilane
NR	Natural Rubber
OMMT	Organically Modified Montmorillonite
PA6	Polyamide-6
PBS	Poly(butylene succinate)
PCB	Printed Circuit Board
PET	Polyethylene Terephthalate

PETMS	Polyethylene Terephthalate Grafted with ɣ-methacryloxypropyltrimethoxysilane
PETVS	Polyethylene Terephthalate Grafted with Vinyltriethoxysilane
PMMA	Polymethylmetha Acrylate
PMNC	Polymer Matrix Nanocomposite
PP	Polypropylene
PPMS	Polypropylene Grafted with ɣ-methacryloxypropyltrimethoxysilane
PPVS	Polypropylene Grafted with Vinyltriethoxysilane
PTFPTFE	Polytetrafluoroethylene
PVP	Poly(vinylpyrrolidone)
RR	Reclaim Rubber
RS	High Speed at Room Temperature
RIFT	Resin Infusion Under Flexible Tooling
SA	Silane Agent
SEM	Scanning Electron Microscopy
SiR	Silicone Rubber
SR	Skim Rubber
TEM	Transmission Electron Microscopy
TGA	Thermogravimetric Analysis
THF	Tetrahydrofuran
TM	High Temperature with Low-speed Mixing
ToF-SIMS	Time-of-Flight Secondary Ion Mass Spectrometry
THS	High Temperature with High Speed
TPU	Thermoplastic Polyurethane
UTM	Universal Testing Machine
UTS	Ultimate Tensile Strength
UV	Ultraviolet
VARIM	Vacuum Assisted Resin Infusion Moulding
VARTM	Vacuum Assisted Resin Transfer Moulding
VS	Vinylytriethoxysilane
WPE	Waste Polyethylene

XRD	X-Ray Diffraction
E	Young’s Modulus
Phr	Per Hundred Resin
Rm	Room Temperature without Shear
Tg	Glass Transition Temperature
Tm	High Temperature without Shear

TABLE OF CONTENTS

LIST OF FIGURES

LIST OF TABLES

CHAPTER 1
INTRODUCTION

1.1 GENERAL

This chapter presents the general introduction of nanocomposites, polymer nanocomposites, and polymer layered silicate nanocomposites. It discusses the types of clay morphologies obtained in polymer nanocomposites and the general features/limitations of epoxy based nanocomposites. This chapter finally discusses the origin of present research work and the need of compatibilization of polymer fillers before their reinforcement into the epoxy matrix.

1.2 NANOCOMPOSITES

The term 'nanocomposites' describes a family of composite materials involving nanometer size range structures, where properties are of importance due to size of the structures, and are typically different from the bulk matrix [1]. Nanocomposites are multi-phase composite materials in which one of the phases possess at-least one dimension in the nanoscale range (1–100 nm), or have repeat distances between different phases of material in nanoscale [2].

In recent years, usage of nanoscale reinforcement in polymer composites has attracted substantial attention of researchers. Such nanoscale reinforcements possess larger surface area per unit volume, and thus, lead to improvement in performance of composite systems [3]. The large surface area per unit volume of the reinforced particle creates more sites available for bonding, or reaction with the surrounding material, resulting in improvement in chemical, or mechanical, or hydrothermal properties [4]. In other words, nanocomposites have remarkably large surface area-to-volume ratio (aspect ratio) of the reinforcement. This ratio implies that for the same particle loading, nanocomposites will have a much greater interfacial area compared to micro-composites as shown in Figure 1.1. [5]. The constituents of the reinforcing material could be in particle form (e.g. minerals), in the form of laminates (e.g. exfoliated clay stacks), or in fibre form (e.g. carbon nanotubes).

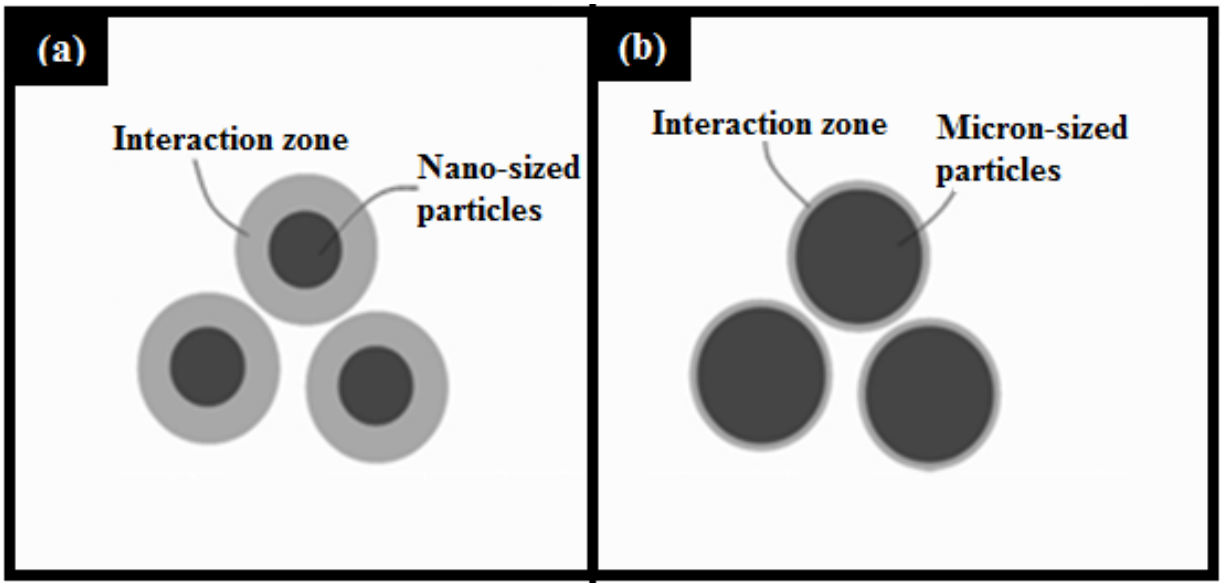

Figure 1.1 Schematic comparison of particle and matrix interaction in (a) nanocomposites, and (b) micro-composites [5].

1.3 POLYMER MATRIX NANOCOMPOSITES

Polymers matrix nanocomposites (PMNCs) are polymers (thermosets/ thermoplastics) reinforced with small concentration of nano-fillers. PMNCs, even at low levels of reinforcement loading (2–3 weight percentage; wt. %) offer similar or even better performance than conventional composites with higher concentration of reinforcing material (30–50 wt. %) [2, 6].

PMNCs are classified on the basis of dimensions of the dispersed particles. Based on the size of dispersed particles, PMNCs are of three main types [2].

(a) Zero dimensional nanocomposites (iso-dimensional nanoparticles) are formed when all the three sizes of the dispersed phase are in the nanometer range. Carbon black, spherical silica, metal particles (aluminium oxide, titanium dioxide, and zinc oxide), semiconductor nanoclusters (silicon carbide) etc. are examples of reinforcement in zero dimensional composites.

(b) One dimensional nanocomposites are formed when two dimensions of the dispersed phase are in the range of nanometer scale, and thus, forming an elongated structure. Examples of reinforcement for these nanocomposites include carbon nanotubes, carbon nano-fibres, and cellulose whiskers.

(c) Polymer layered nanocomposites possess two dimensions of size larger than the nanometer range and the third one in the nanometer scale. The filler is in the form of sheets having

thickness of one to few nanometers to hundred to thousand nanometers long. These materials are prepared by intercalation/exfoliation of polymer inside the spaces between the layers of the fillers (galleries). Examples of reinforcement for these nanocomposites include nanoclays or layered silicates (Montmorillonite, Hectorite, and Kaolinite) and layered double hydroxides [2].

1.4 POLYMER LAYERED SILICATE NANOCOMPOSITES

Amongst all the prospective nanofillers for PMNCs, nanoclays (i.e. layered silicates) are more extensively studied because of their ease of availability at low price and also because their intercalation chemistry has been widely investigated. Polymer nanocomposites reinforced with nanoclay (i.e. polymer layered silicate nanocomposites) are widely used owing to their improved properties over the conventional composites. Some of these improvements include improved tensile modulus and strength, high heat resistance, low gas permeability, and decreased flammability [2, 7–10]. The general structure of layered silicates is presented in Figure 1.2.

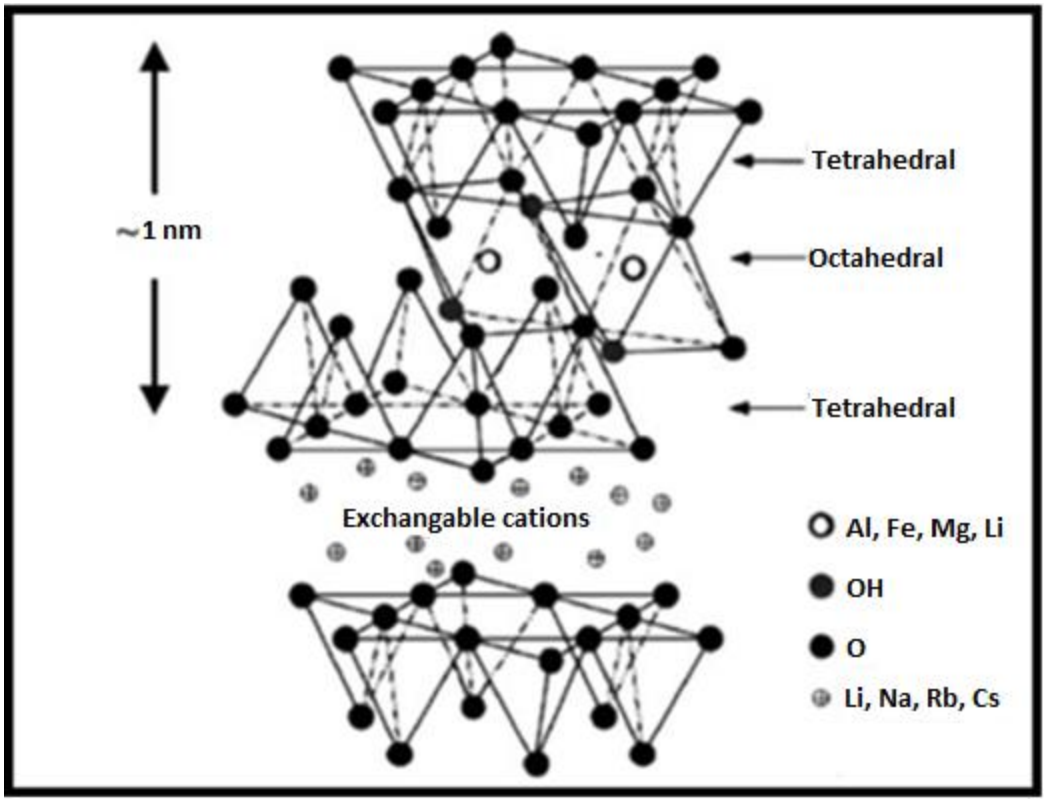

Figure 1.2 Schematic of layered silicate structure [8].

Polymer nanocomposites (reinforced with nanoclay) show improved properties as compared to composites reinforced with conventional fillers because of the strong interface between nano-filler and matrix [2, 11].

1.4.1 Types of clay morphologies in polymer nanocomposites

In polymer layered silicate nanocomposites, three different types of structures can be observed based on interaction of polymer matrix and nanoclay. These three distinct clay morphologies are shown in Figure 1.3 and are discussed in the following section:

i) ***Phase separated***: When polymer-chains are not able to enter between nanoclay layers, a phase separated morphology is obtained. For nanocomposites with this type of morphology, properties do not show much change but stay in the same range as are of conventional composites.

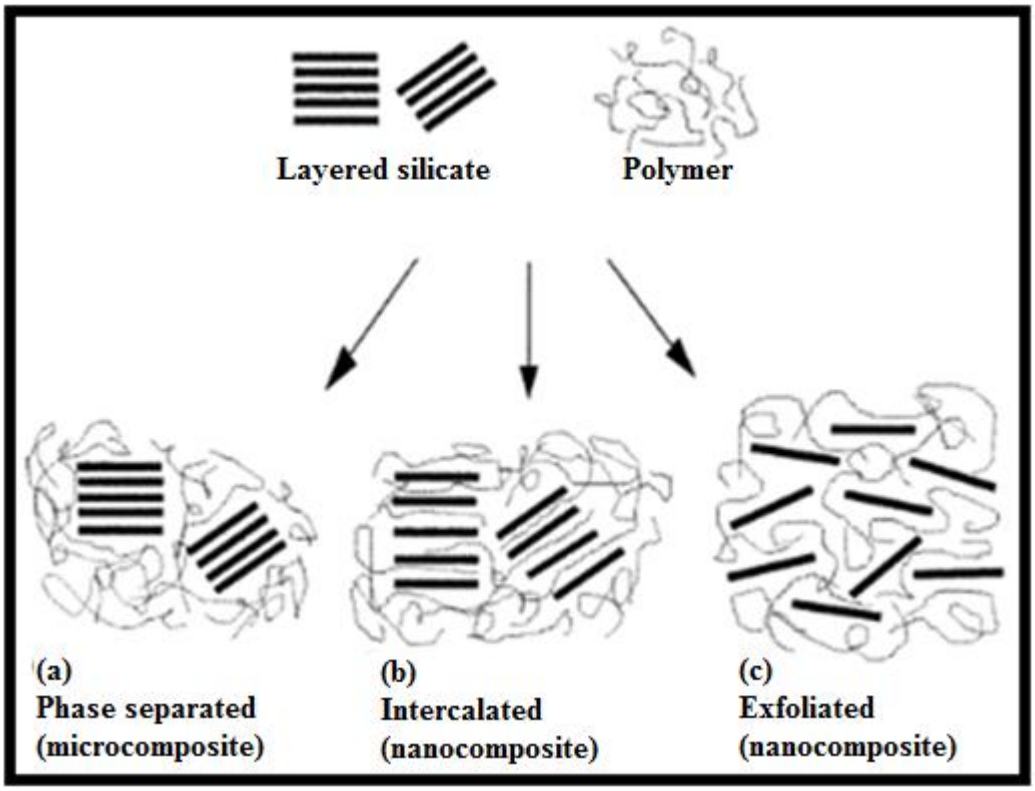

Figure 1.3 Types of clay morphology in polymer nanocomposites based on interaction between matrix and silicate layers [11].

ii) ***Intercalated***: When polymer-chains are able to enter between nanoclay layers resulting in a symmetrically arranged multi-layer structure having alternating layers of polymeric

material and inorganic clay, an intercalated morphology is obtained. In intercalated structures, the inter-layer spacing is increased but the ordered structure of clay layers is retained.

iii) ***Exfoliated***: When polymer-chains are able to intercalate between nanoclay layers resulting in a structure where silicate layers are totally misaligned and homogeneously/completely dispersed in the polymer matrix, an exfoliated morphology is obtained. Exfoliated structures result in formation of a disordered morphology as orientation of clay layers is changed and distance between layers is extensively increased [2, 4, 10, 11].

1.5 EPOXY BASED NANOCOMPOSITES

Epoxy is one of the most important thermosetting resins which is employed as a matrix material for polymer based composites. Due to its low density (1.3 g/cm^3), excellent bonding ability, and good mechanical properties, epoxy is a favourable material for many superior applications, usually as a fibre reinforced composite [1, 12]. Commercially used fiber-reinforced polymer composites (FRPs) have good static mechanical properties but lack in impact strength [13–18]. Most FRPs generally use reinforcements like glass fibers, aramid fibers etc. with epoxy as the matrix [19, 20]. Epoxy based glass fiber reinforced plastics (epoxy based GFRPs) show good stiffness/specific strength etc. and are employed in many structural applications [15, 21–25]. However, structural applications also demand high impact strength in composites (in addition to good static mechanical properties) for safe operations.

Epoxy, on polymerization, acquires a cross-linked structure. This typical structure obtains high modulus/strength etc. in the material but causes increased brittleness, thereby reducing impact performance of FRP composites [26–34]. In this context, the use of nanoclay as reinforcement in polymer matrix composites has offered an interesting route for modifying polymer matrices. Nanoclay reinforced epoxy based GFRPs show significant improvements in properties including tensile, flexural, and hygrothermal properties, but only moderate improvements in impact performance [35–39]. Thus, impact behaviour of nanoclay reinforced epoxy based GFRP nanocomposites is still an area of concern.

1.6 ORIGIN OF THE PRESENT STUDY

Researchers have been investigating methods for epoxy toughening which is a demanding and challenging task for a long period. Attempts have been made in this regard by modifying the epoxy matrices using elastomers [16, 28, 30, 39, 40]. Such modifications have resulted in substantial toughening effects but have caused deterioration in strength etc. and also processing difficulties due to high viscosity [29, 40, 41]. Further, a few researchers have reported improvements in impact strength/thermal properties of epoxy based composites reinforced with thermoplastic fibers [42–44]. However, addition of thermoplastic fibers in epoxy based GFRP composites has not been investigated. Thus, there is still a requirement for developing new toughening methodologies for improving impact strength of epoxy based GFRP composites and epoxy-clay based GFRP nanocomposites.

To improve the impact strength, one of the ways is to use nanoscale reinforcement (nanoclay as the first filler) with soft/ductile polymer fibers/elastomers (as the second filler) in epoxy based GFRPs. It is reported that addition of modifiers (ductile thermoplastic fibers like polypropylene or soft elastomers etc.) which are less rigid than the thermosetting epoxy matrix may behave as excellent toughners for the brittle epoxy based composites [28, 30, 32, 42, 43, 45, 46].

In the light of aforesaid, in the present research work, epoxy based GFRP nanocomposites (epoxy-clay based glass fiber nanocomposite systems) were modified through addition of thermoplastic fibers/elastomers as an additional filler for enhanced impact strength.

1.7 COMPATIBILIZATION

The key to improved properties of a composite materials system lies in good compatibility among its various constituents. One of the main emphasis in the present work was to improve the compatibility of polymer/elastomer filler with other constituents of epoxy based GFRP nanocomposites. It is well reported in literature that interfacial bonding between resin system and fibers (glass fibers, thermoplastic fibers etc.) can be improved by using chemical agents that add active functional groups on the surface of constituents to be compatibilized [47–52]. In this context, one of the important methods is grafting of silane coupling agents to the substrate surface. Silane agents improve interfacial interaction between two different types of materials viz. an inorganic material like glass and an organic material like epoxy or a polymer filler. Active polar

groups from the silane agent are grafted on the surface of substrate in such a way that it chemically reacts with other constituents of the composite system [47, 52, 53]. Another important method is the use of photo-assisted grafting of maleic anhydride (MAH) on the surface of thermoplastic fibers. Maleic anhydride is a poly-functional monomer which on being grafted to polymer/elastomer surface improves its adhesion with polar constituents (viz. epoxy etc.) of the composite system.

The present work investigated the combined effect of nanoclay and polymer/elastomer addition on mechanical properties (especially impact strength) of epoxy based GFRPs. Polymer fibers namely polypropylene (PP) fibers, polyethylene terephthalate (PET) fibers, and an elastomer namely ethylene propylene diene monomer (EPDM) rubber particles were used separately as the second filler in epoxy based GFRPs containing nanoclay as the first filler. These thermoplastic fibers/elastomers are low-cost, light-weight, and ductile in nature.

The novelty of present research work is that proper compatibilization of polymer/elastomer filler added as reinforcement resulted in significant improvements in impact strength of epoxy based GFRPs without any appreciable loss in tensile properties (tensile strength and tensile modulus).

Such nanocomposites would find applications in structural members of marine parts (boats, ship hull frames, decks, propulsion shafts etc.), aerospace components, racing car bodies and chassis, bicycle frames, and sporting goods (surf boards, vault poles, archery bows, and arrows) etc.

1.8 OUTLINE OF THE THESIS

The present research work investigates the effect of addition of soft/ductile fillers (polymer fibers/elastomers) on the mechanical performance (especially impact strength) of epoxy based GFRP nanocomposites. GFRP nanocomposites containing 1 phr nanoclay (where phr is parts per hundred resin) and varying concentration of polymer filler were synthesized using hand lay-up on vacuum assisted resin infusion moulding *set-up* (i.e. VARIM *set-up*). Further, to improve the compatibility of polymer fillers with other constituents of the composite materials system, two different surface modification procedures, viz. (a) silane treatment and (b) ultraviolet-assisted MAH grafting (UV-assisted MAH grafting) were performed on polymer fillers before their addition to the matrix.

This thesis embodies the subject matter resulting out of the present study and is arranged in seven separate chapters. The outline of the chapters is listed below:

- **CHAPTER 1:** The chapter introduces the basic terms involved in the present research viz. nanocomposites, polymer matrix nanocomposites, polymer layered silicate nanocomposites and their various types. This chapter discusses the need for improving the impact strength of epoxy based glass fiber reinforced composites, and thus, presents the origin of present research work. The role of compatibilization (i.e. surface treatment) of polymer fibers/elastomer fillers to improve their interfacial bonding with other constituents of the composites system is also discussed.
- **CHAPTER 2:** The chapter presents a detailed review of literature on the processing and resulting properties obtained in (i) epoxy-layered silicate nanocomposites, (ii) epoxy based GFRP nanocomposites, (iii) polymer/elastomer reinforced composites, and (iv) surface modification of polymer/elastomer fillers reinforced in composites. The chapter also brings out the main gaps in the existing literature in this field of work.
- **CHAPTER 3:** The chapter presents design of the present research work. It discusses the formulation of research objectives based on gaps in the existing literature. The chapter clearly establishes the need for the present research. It includes details of materials, processing methodology, and equipment used for fabrication, testing, and characterization of epoxy based GFRPs. It also describes the procedure of surface treatment/grafting of polymer/elastomer fillers with silane treatment and maleic anhydride to improve the compatibility of these fillers with other constituents of the epoxy based GFRP nanocomposites for enhanced mechanical performance.
- **CHAPTER 4:** This chapter presents the impact testing and tensile testing results of PP fiber reinforced GFRP nanocomposites to determine their optimum composition along with the best surface treatment condition for PP fiber reinforcement providing maximum improvement in properties of resulting GFRPs. Further, the results of characterization procedures of XRD, SEM-EDS, TEM, and FTIR analysis to determine changes in surface morphology of fibers and also interfacial adhesion of constituents in nanocomposites are described in the chapter.
- **CHAPTER 5:** This chapter presents the results of impact testing and tensile testing of PET fiber reinforced GFRP nanocomposites. The results of various characterization techniques

utilized in the present research to ascertain (a) the type of clay morphology obtained in the nanocomposites (XRD and TEM analysis), (b) the chemical and interfacial changes in surface morphology of PET fibers due to compatibilization treatment (FTIR and SEM-EDS analysis) have also been presented.

- **CHAPTER 6:** This chapter presents the results of testing and characterization with regards to epoxy based GFRP nanocomposites processed with the third type of micro-filler reinforcement i.e. EPDM rubber particles. The results of impact testing of nanocomposites are used to determine the optimum composition of nanocomposites and also the surface treatment procedure for elastomer fillers to provide maximum improvement in properties of resulting GFRPs. Further, the results of characterization procedures of XRD, SEM-EDS, TEM, and FTIR analysis to determine changes in surface morphology of fibers and also interfacial adhesion of constituents in nanocomposites are described in the chapter.
- **CHAPTER 7:** This chapter presents the summary of results and significant findings of the experimental work embodied in this thesis. It also discusses the major conclusions to be drawn from the present research. The scope for possible extension of the present work is also discussed.

  As per this outline, a thorough review of the literature is presented in the next chapter.

CHAPTER 2

LITERATURE REVIEW

2.1 GENERAL

This chapter presents an extensive literature review on polymer matrix based nanocomposites (PMNCs). The review is restricted mainly to epoxy resin based matrix systems with layered silicates/glass fibers/polypropylene (PP)/polyethylene terephthalate (PET) or/and elastomers as the reinforcement. The role of different constituents in governing properties of such composite systems, the influence of different processing methods, and the effect of different compatibilization procedures used for surface modification of polymeric/elastomeric fillers on properties of composites are discussed. The review is presented in the following main sections:

- Epoxy-layered silicate nanocomposites
- Epoxy based GFRP nanocomposites
- Polymer/elastomer reinforced composites
- Surface modification of polymeric/elastomeric fillers

2.2 EPOXY-LAYERED SILICATE NANOCOMPOSITES

Lu *et al.* [54] synthesized epoxy-nanoclay composites with varying clay concentration to determine the influence on fracture toughness/Young's modulus (E) of the material by three point bending tests and nano-indentation tests.

Montmorillonite (MMT) nanoclay (Nanomer I.30E) was hand mixed with Epon-82 epoxy for 20 min. Hardener was mixed to this suspension. After thorough mixing, the system was degassed, cured in a mould, and the composite samples were prepared. E value increased to 4.18 GPa for 5 wt. % clay (from 3.06 GPa for no clay). It subsequently decreased to 3.70 GPa for 7 wt. % clay content. E value increased at the cost of reduction in fracture toughness. Fracture toughness of epoxy based system continuously decreased with increase in nanoclay content (2.53 MPa$\sqrt{m}$ at 0% clay loading to 0.90 MPa$\sqrt{m}$ at 7% clay loading).

Yasmin *et al.* [35] synthesized epoxy/clay nanocomposites using three roll milling by varying the clay content (1–10 wt. %) and studied the structure-property relationship of this composite system.

Epoxy diglycidyl ether of bisphenol A (DGEBA)/accelerator (DY070)/hardener (Aradur 917) were taken in weight ratio of 100:90:1. MMT nanoclay (Cloisite® 30B) was mixed in different proportions to the resin system using a three roll mill (500 rpm, 120 g/h). Subsequently, hardener was added at 60 ℃ and then the accelerator. The degassed solution was cast in an aluminium mould and cured (148 ℃, 1 h). XRD/TEM results indicated exfoliated structure/disordered intercalated structure for clay in the nanocomposites.

Tensile tests indicated improvement in Young's modulus at higher clay loadings (Figure 2.1). Tensile modulus improved by 25% and 80% for 1 wt. % and 10 wt. % of clay loading respectively. This improvement was due to (i) well dispersed clay that restricted movement of polymer under loading, and (ii) effective interfacial bonding between epoxy and clay nano-particles.

Further, tensile strength decreased with increased clay loadings because of presence of voids in the viscous material (base material: 64 MPa; nanoclay with 1 wt. % clay: 30 MPa; nanoclay with 10 wt. % clay: 25 MPa). However, with increase in degassing time, drop in tensile strength was less.

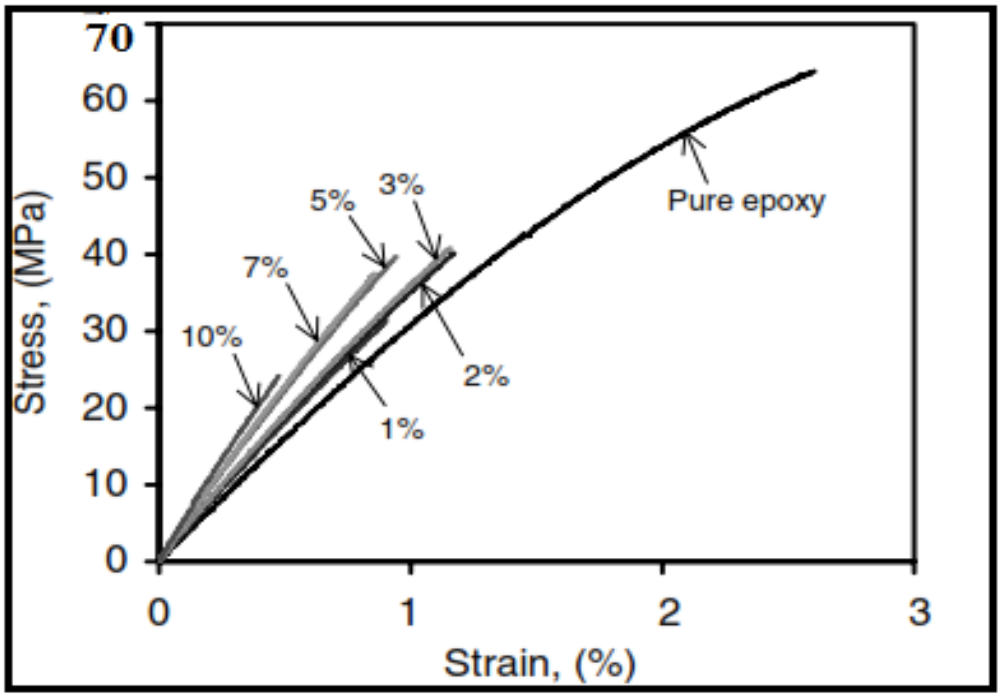

Figure 2.1 Stress-strain behaviour of epoxy-clay PMNCs [35].

Thus, this processing method (using three-roll mill) was able to disperse clay effectively in a small time and was also environmentally friendly as solvent was not required.

Liu *et al.* [55] synthesized epoxy/clay nanocomposites to study influence of clay reinforcement on the performance of nanocomposites. Epoxy (DGEBA) was mixed with nanoclay (Cloisite® 93A). Nanoclay was varied in the range, 1–4 wt. % (homogenization: 10000 rpm, 60 min; ultrasonication: 60 min; degassing: 70 ℃). Hardener (Ethacure 100-A1) was now added in amounts as per supplier recommendations (mixed at 70 ℃ for 30 min under vacuum). The solution was poured into pre-heated glass moulds. The samples were cured and post-cured.

XRD patterns and TEM micrographs of nanocomposites showed exfoliation for epoxy/clay (99/1) system having homogeneously dispersed clay particles or tactoids with size of about 2–5 μm. Storage modulus increased but glass transition temperature ($T_{g)}$ value decreased at higher clay loadings. Fracture toughness increased by about 70% at 4.0 wt. % clay.

SEM analysis of fractured surface of pure epoxy showed smooth surface indicating less energy required for the fracture. For 2 wt. % clay, a rougher surface was obtained which indicated that clay aggregates caused hindrance to crack propagation, and thus, higher fracture toughness value.

Wang *et al.* [56] prepared two types of nanocomposites (one with S-clay and the other with Cloisite 93A) using slurry-compounding process to compare their properties.

S-clay was dispersed in epoxy resin using slurry compounding process. Nanocomposites were prepared using four different clay loadings (1.0/2.5/3.5/and 5.0 wt. %). Clay was dispersed using mechanical stirring (800 rpm, 75 ℃, 10 min) at three different concentrations (1.0, 2.5, and 5.0 wt. %).

For epoxy/93A2.5 nanocomposites, optical micrographs revealed poor dispersion of organoclay. However, optical micrographs for epoxy/S2.5 nanocomposite showed uniform dispersion of clay particles. TEM results revealed completely exfoliated morphology for epoxy/S2.5.

Fracture toughness tests for all epoxy/S-clay specimens showed a significant toughening effect with highest value for epoxy/S-clay2.5. SEM images (fractographic analysis) of this composition indicated that nanoclay layers acted as stress concentrators.

Gupta *et al.* [36] synthesized clay-epoxy nanocomposites using two different methods of preparation (mechanical mixing and shear mixing) to evaluate if the two processing methods

resulted in different structure and mechanical properties (toughness and tensile properties) of the resulting nanocomposites.

Nanocomposites containing Closite® 30B (organically modified MMT; OMMT clay) in 0.125, 0.25, 0.50, 1 and 2 vol. % were synthesized to compare results obtained by two methods: (a) mechanical and (b) shear mixing. Epoxy (D.E.R. 332), dilutent (glycidyl ether), and hardener (D.E.H. 24) were taken as 83.5:12.1:4.4 (vol. %) in all specimens. In the first method, nanoclay was added to the above mixture by mechanical stirring (650 rpm, 50 ℃, 2 h). Similarly, clay was mixed at 180 rpm to the epoxy-hardener-dilutent mixture using a three roll mill.

XRD results showed that nanocomposites synthesized using mechanical mixing exfoliated the nanoclay, thus showing higher modulus and impact strength values. However, shear mixing could obtain only intercalated morphology, resulting in relative lower value of various properties (Figure 2.2).

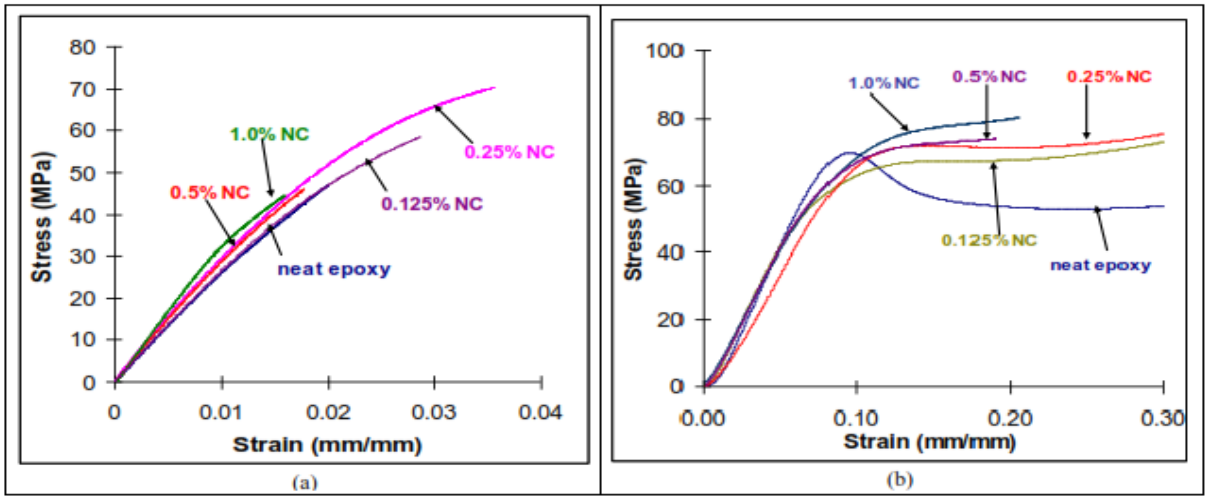

Figure 2.2 Stress-strain curves (a) tensile and (b) compressive for mechanically mixed nanocomposites [36].

Yao *et al.* [37] synthesized SiO_2/epoxy nanocomposites and evaluated their fracture toughness using three-point-bending test. The authors also characterized the nanocomposites using SEM for structure-property correlation.

Matrix (diglycidyl ether of bisphenol F; DGEBF) and toughening agent (PPGDE) were mixed (in 1:1 proportion) by stirring for 2–4 h followed by slight heating. Then, nano-silica (SiO_2) in varying concentration of 0, 1, 3, 5 and 7 wt. %, was added to the prepared mixture by ultrasonic vibrations. Hardener (DETD) was mixed to the system using magnetic stirrer followed by degassing for 30

min. Samples were prepared by pouring the mixture into a mould. The samples were then dried in an oven.

Load-displacement curves of nanocomposites showed a linear trend initially. However, with increase in load, non-linear relation was observed. Fracture test results showed that with 3 wt. % nano-particle loading, both the fracture load and fracture toughness values increased significantly as compared to pure epoxy. For nanocomposites with 5 and 7 wt. % of nanoparticles, the fracture toughness decreased due to agglomeration of nano-silica leading to weakening of bond between nano-particles and matrix. SEM images of fractured surfaces showed that lesser energy was needed for fracture of pure epoxy. For 3 wt. % of nano-silica, composites showed higher toughness due to uniform dispersion of clay. For nanocomposites with higher clay content (5 and 7 wt. %), toughness values were less due to agglomeration.

Ngo *et al.* [57] synthesized epoxy based nanocomposites (reinforced with clay) using different pre-mixing approaches to investigate the role of variations in shear rate and temperature for premixing nanoclay to epoxy.

Epoxy resin, DGEBA (EPON^{TM} 828) was cured with the curing agent (Jeffamine1 D-230). Nanoclay, Cloisite 30B (2 wt. %) was now dispersed in the resin. For curing, two different conditions were used: a) for 2 days at ambient temperature, b) for 2 h at 120 ℃. Samples were then post-cured for 2 h at 140 ℃ irrespective of curing schedule followed. The different pre-mixing conditions included (a) room temperature without shear Rm, (b) high temperature without shear Tm, (c) high pressure HP, (d) high temperature with high speed THS, (e) high temperature with low-speed mixing TM, and (f) high speed at room temperature RS.

XRD results for pre-mixed suspension (by different methods) showed that all the methods were able to intercalate the clay. The modest shear generated by hand mixing facilitated two fold increase in d-spacing of pristine Cloisite 30B. Higher temperature and higher shear rates led to higher d-spacing with very small difference (minimum value = 3.72 nm, maximum value = 3.81 nm) among various mixtures. Pre-mixed nanocomposites were now subjected to curing. Curing was provided to all pre-mixed samples under two separate conditions (at room temperature and at 120 ℃). It was observed that higher curing temperature led to better intercalation/exfoliation because increase in temperature increased the flexibility and movement of epoxy and hardener molecules. Similar effect was observed on the clay morphology when high temperature and high

speed were employed for pre-mixing. Order of intercalation/exfoliation of the nanocomposites was THS>HP>RS>TM>Tm>Rm.

Satapathy *et al.* [58] synthesized layered silicate/epoxy nanocomposites (through in-situ polymerization) to study the role of organic modification of layered silicate on properties of nanocomposites.

MMT (20 g) was added and mixed to distilled water (400 ml) by stirring at 80 ℃. 0.05 moles of modifier (hexadecyltrimethylammonium chloride; HTAC) was added to 4.8 ml HCl in 100 ml distilled water. This solution was mixed to hot silicate water mixture (80 ℃, 1 h). Organo-silicate (OMMT) was obtained after filtering/drying (75 ℃). OMMT and MMT in various concentrations (1, 3, 6, 10 wt. %) were mixed with epoxy by stirring (1 h) followed by sonication (20 min). Amine hardener equivalent to 35 phr was added, and the mixture was degassed. Finally, composites were prepared by casting the solution into silicon moulds and curing at room temperature followed by post-curing (80 ℃, 1 h; and 150 ℃, 2 h).

XRD patterns showed greater d-spacing in OMMT (as compared to unmodified MMT), indicating intercalation of the silicate galleries for OMMT.

Examination of fractured surfaces (SEM analysis) indicated more brittle fracture of neat epoxy as compared to those of nanocomposites. For nanocomposites containing high silicate concentrations (10 wt. % clay), micrographs showed silicate agglomeration resulting in higher stress concentration regions.

Tensile tests showed increase in tensile modulus values (for both MMT and OMMT) with increase in nanoclay content till 6 wt. % (OMMT nanocomposites showed slightly better modulus). Modulus values remained constant for higher loadings. Interestingly, beyond 6 wt. % clay loadings, MMT nanocomposites had better elastic modulus. Further, it was reported that with OMMT (10 wt. %), increase in modulus was 16% as compared to neat epoxy.

Kusmono *et al.* [59] examined the effect of varying clay loading (2–6 wt. %) on mechanical performance of epoxy based nanocomposites.

Clay (Nanomer 1.28E) dried at 80 ℃ for 8 h was mixed to epoxy (DER 331) in varying clay concentrations (2, 3, 4, 5, and 6 wt. %) by stirring for 2 h at 75 ℃ followed by degassing in vacuum for 15 min. Polyaminoamide (curing agent) was mixed to epoxy/clay by stirring for 5 min at 75 ℃.

Finally, the suspension was poured into a steel mould followed by degassing for 10 min. Curing was done at 80 ℃ for 2 h and post-curing was done at 150 ℃ for 2 h.

XRD results showed that d_{001} peak was absent in nanocomposites reinforced with nanoclay till 3 wt. %, indicating exfoliated morphology. Tensile, flexural, impact strength, and fracture toughness values were maximum at clay concentration of 3 wt. % due to the exfoliated structure. These properties showed improvement of 41%, 20%, 95%, and 19% respectively over the corresponding values for neat epoxy. Beyond 3 wt. % clay loading, the properties of nanocomposites deteriorated due to agglomeration of clay particles. SEM analysis showed increased roughness of the fracture surfaces for 3 wt. % nanocomposites as compared to the neat epoxy.

Sharmila *et al.* [60] synthesized epoxy based nanocomposites containing clay using in-situ polymerization to investigate the thermal, mechanical, and barrier properties. Nanoclay was varied in the range of 0–5 phr. Nanoclay (Cloisite 93 A) was added to epoxy (Araldite GY 250) by stirring for 45 min. The mixture was sonicated and degassed for 30 min each. Hardener (HY 951) in amount of 10 phr was mixed (5 min) to the system. Finally, the system was cured (room temperature, 24 h) and post-cured (80 ℃, 4h).

XRD analysis showed that d-spacing for pristine clay was 2.372 nm. For nanocomposites having 0.5 phr/1phr of nanoclay, the d_{001} peak was missing, thus indicating exfoliation for these compositions. However, nanocomposite system containing 5 phr nanoclay showed d_{001} diffraction peak corresponding to d-spacing of 3.242 nm, indicating intercalation. TEM images showed combination of intercalated and exfoliated morphology for nanocomposite with 1 phr of nanoclay (designating it as partially exfoliated-disordered intercalated morphology) whereas that for 5 phr depicted formation of aggregates and thicker Cloisite particles, confirming the presence of intercalated structure. The flexural strength and tensile strength of neat epoxy was 64 MPa and 54 MPa respectively. Flexural properties and tensile properties showed maximum values at 1.5 phr and 1.0 phr clay reinforcement respectively. SEM fractography showed a smooth fracture surface for neat epoxy representing brittle failure. For nanocomposites, a rough fracture surface along with mechanisms like crack pinning, crack deflection, and crack arresting were observed.

Ying *et al.* [61] compared the thermal and mechanical properties of epoxy/clay nanocomposites containing unmodified and modified clay. Sodium montmorillonite (Cloisite Na^+) nanoclay,

(EPON 828) epoxy, Jeffamine D230 (J230) hardener were employed to fabricate the nanocomposites.

The clay was modified and slurry of the clay with acetone was prepared and added to epoxy (80 ℃ , 2 h). Stoichiometric amount of J230 was mixed using a stirrer (10 min). This was followed by outgassing (60 ℃ under vacuum) and pouring into mould. Finally, the system was cured (75 ℃, 2 h) and post-cured (120 ℃, 8 h).

TEM analysis showed uniform distribution of unmodified clay in epoxy without any agglomerates, signifying exfoliated (disordered) morphology. XRD diffractograms showed that unmodified clay and organically modified clay showed peaks at 8° and 6° respectively. Epoxy/modified-clay nanocomposite containing 3 wt. % clay showed no diffraction peak indicating disorderly and highly exfoliated epoxy/clay nanocomposite system. DSC analysis revealed that T_g of neat epoxy (85.5 ℃) increased with increasing clay content. Flexural strength decreased at higher clay loadings under room temperature conditions. However, for high temperature test conditions (80 ℃), flexural strength increased with increased clay content. It increased significantly initially for 1 wt. % clay and thereafter remained almost constant. Further, flexural modulus increased significantly (and linearly) at increased clay content, both under ambient conditions and at 80 ℃.

Sharifi *et al.* [62] prepared epoxy/clay nanocomposites using solution mixing and melt mixing methods to observe the variation in mechanical properties of the prepared nanocomposite powder. Epon 3003 (epoxy), Aradur 2844 (hardener), and Closite 30B (nanoclay) were used as constituents for the nanocomposites. Clay concentration was varied as 1–5 phr.

The mixtures (prepared by the two different methods) were extruded by using a lab twin-screw extruder followed by crushing the extruded material. Finally, the crushed powder was coated on aluminium panel by electro-spraying. The authors compared the clay morphology obtained in nanocomposites with 3 phr clay. XRD/TEM analysis showed that solution method resulted in better exfoliation. With both types of mixing methods, tensile properties and micro-hardness of nanocomposites increased at higher clay loadings, with melt mixed composites showing greater improvement.

Table 2.1 summarizes the literature on epoxy-clay nanocomposites.

Table 2.1 Summary of literature on epoxy-clay composite systems.

S. No.	Summary	References
1.	Several researchers have reported on improvements obtained in properties of the resulting composites with addition of nanoclay till an optimum concentration. The following properties have mainly been investigated:	
	(a) Mechanical properties (tensile/compressive/ flexural strength, fracture toughness, tensile/flexural modulus, impact strength) of epoxy-clay nanocomposites. A few researchers have also studied the effect of reinforcing different types of modified/unmodified nanoclays on the mechanical performance of epoxy layered silicate nanocomposites.	Yasmin *et al*., [35]; Gupta *et al*., [36]; Yao *et al*., [37]; Lu *et al*., [54]; Satapathy *et al*., [58]; Kusmono *et al*., [59]; Sharmila *et al*., [60]; Sharifi *et al*., [62]; Isik *et al*., [63]; Lam *et al*., [64]; Akbari and Bagheri [65]; Lim and Chow [66]; Mouloud *et al*., [67]; Ngo *et al*., [68]; Olad *et al*., [69]; Ying *et al*., [70].
	(b) Dynamic properties (storage modulus, loss modulus) and thermal properties (thermal stability, glass transition temperature, weight loss/weight gain percentage) of epoxy-clay nanocomposites.	Gupta *et al.,* [36]; Liu *et al.,* [55]; Wang *et al.,* [56]; Satapathy *et al.,* [58]; Sharmila *et al.,* [60]; Ying *et al.,* [61]; Isik *et al.,* [63]; Mouloud *et al.,* [67]; Olad *et al.,* [69]; Al-Qadhi *et al.,* [71]; Al-Qadhi *et al.,* [72], Cabezudo *et al.,* [73].
	(c) Barrier properties (oxygen up-take/ permeability, water up-take, oil up-take, hydrogen permeability) of epoxy-clay nanocomposites.	Becker *et al.,* [74]; Mittal [75]; Paul and Robeson [76]; Al-Qadhi *et al*.,[71]; Kusmono *et al*., [59]; Sharmila *et al*., [60]; Al-Qadhi *et al*., [77].
2.	Some researchers have synthesized nanocomposite systems using different processing methods (3-roll milling, mechanical mixing, shear mixing, ultrasonication, solution mixing, melt mixing etc.) and investigated the relative improvements obtained in properties of resulting composites.	Yasmin *et al*., [35]; Gupta *et al*., [36]; Ngo *et al*., [57]; Sharifi *et al*. [62]; Bashar *et al*., [78]. .
3.	Few authors have examined the effect of adding a tertiary filler like polyether polyol, polyether imide, polydimethylsiloxane, polyether sulphone, polyoxypropylene, etc. on performance of epoxy based composites.	Isik *et al*.,[63]; Bucknall and Partridge [79]; Bucknall and Gilbert [80]; Shih *et al*.,[81]; Franco *et al*., [82].

Nanoclay is an easily available and an economical nano-filler for epoxy based nanocomposites. Epoxy-clay nanocomposites provide improved tensile/compressive properties, impact performance, thermal properties, dynamic mechanical properties, and barrier properties over the neat epoxy systems. Various authors have generally worked to obtain the optimum clay loading resulting in maximum improvement in properties under investigation.

Though improvements in mechanical properties over the neat epoxy systems are obtained in epoxy-clay nanocomposites, but for still higher values of tensile properties/impact performance (as are required in composites for structural applications), glass fiber reinforced epoxy-clay nanocomposites were developed. Literature review on such systems is presented in the next section.

2.3 EPOXY BASED GFRP NANOCOMPOSITES

Lee *et al.* [7] examined the influence of adding clay to epoxy based composites having uni-directional glass fiber as reinforcement on the properties of resulting system. Authors also studied the effect of fiber direction on clay distribution.

A flat rectangular mould was used to prepare nanocomposites using VARTM process (vacuum assisted resin transfer moulding) with different clay loadings (0, 1, 3, and 5 wt. %). Cloisite 15A (nanoclay) was mixed with chloroform (solvent) and YD-128 (epoxy) using mechanical stirrer. After removing chloroform and adding D-230 (hardener), the system was finally outgassed. Five layers of glass fiber mat (T-800) were placed in a 70875particular direction (transverse/longitudinal). The mould was kept at a temperature of 50 ℃ during filling with vacuum maintained at 75 cm of Hg. Moulded nanocomposites were cured (ambient temperature, 4h) and post-cured (125 ℃, 3 h).

XRD results showed an increase in basal spacing of clay due to intercalation of epoxy molecules. Fully exfoliated nanocomposites were obtained for clay content below 3 wt. %.

Three-point bending tests indicated that flexural properties increased till 3 wt. % clay content. Un-notched Izod impact tests indicated an increase in impact strength with addition of clay (77.9 J/m for 0 wt. % clay to 100.4 J/m for 5 wt. % clay) into the glass fiber reinforced composites. Thermal stability/storage modulus improved with higher clay loading but T_g was not affected.

SEM images revealed that nanoclay particles were more uniformly distributed when resin flowed along the fiber direction.

Kornmann *et al.* [83] used vacuum bagging along with hand lay-up/hot pressing to fabricate glass fiber-epoxy-clay nanocomposites for evaluating thermal and mechanical properties.

Somasif ME-100 nanoclay was modified organically with deionized water and 37% HCl. It was dried for 2 days at 80 ℃ followed by grinding (average particle size: 80 μm). Organoclay (10 wt. %) was mixed to epoxy (Araldite CY225) by stirring for 1 h at 80 ℃. Hardener (HY925)

was mixed by stirring (80 ℃, 10 min) followed by degassing for 5 min. A thin layer of this mixture was applied on release agent coated aluminium mould. First ply of glass mat (EC9-204) was wetted by the resin using hand-lay-up. The procedure was followed for 8 plies of glass fibers followed by degassing (80 ℃, 5 min) followed by vacuum bagging and placing in hydraulic press (140 ℃, 2 bar). Subsequently, curing (140 ℃, 2 h) and post-curing (140 ℃, 10 h) was done.

XRD and TEM results showed inter-lamellar spacing of about 9 nm indicating presence of non-homogeneous structure/clay agglomerates. SEM images of epoxy/glass mat laminates (without clay) showed that glass fibers deboned from the matrix. However, nanocomposite laminates showed presence of layered silicates at surface of fibers indicating higher toughness over conventional laminates. Further, elastic modulus of the system enhanced by 54% for 10 wt. % clay addition. However, elongation at break and tensile strength deteriorated significantly (84% and 36% respectively). Flexural modulus and strength also showed improvement (6% and 27% respectively). Also, storage modulus increased drastically (45% higher than that of epoxy).

Avila *et al.* [84] synthesized fiber glass-epoxy-nanoclay laminates using wet lay-up method under vacuum and studied the damping behaviour and impact strength of nanocomposites.

Nanocomposites containing epoxy and hardener (in the ratio of 100:20), clay (OMMT in 1, 2, 5, and 10 wt. %) and S2-glass (16 layers) were prepared by wet lay-up method under vacuum. In this method, nanoclay particles were mixed to acetone, were blended into hardener, were degassed (1 h), and mixed to resin. Glass fiber layers were stacked one over the other and were laminated using vacuum assisted wet lay-up to form the nanocomposites. Samples were cured (ambient temperature, 24 h) and post-cured at low temperature.

Impact test results indicated higher area of front face delamination for the clamped condition as compared to the simply supported condition. Study of impact test as a function of energy levels showed that for energy levels of 15–22 J, the area of front face delamination decreased (by 22%) for nanocomposites having 1 wt. % of clay for both cases (clamped as well as simply supported). The area of front face delamination decreased further at higher clay loadings. At energy level of 40 J for different nanoclay levels, damping behaviour improved at higher clay contents.

Tsai *et al.* [85] synthesized epoxy-clay GFRPs to examine the role of organoclay addition on the tensile/compressive properties of composites.

Organoclay (Nanomer I.30E) was dried (90 ℃, 6 h) and blended with epoxy (EPON 828, DGEBA) in varying concentration (2.5, 5.0, and 7.5 wt. %) by mechanical stirring and sonication. Curing agent (32 wt. % of epoxy) was mixed to the suspension by mechanical stirring. Glass fiber/epoxy nanocomposites with 18 layers of E-glass fibers were prepared using vacuum assisted hand lay-up method followed by curing in a hot press under vacuum conditions. The materials system was then transferred to a steel mould and cured (100 ℃, 3 h) and post-cured (125 ℃, 3 h).

Stress-strain curve of the nanocomposites showed that stiffness increased but failure strain decreased at higher organoclay loading. Transverse compressive strength increased constantly with clay loading till 5 wt. %; thereafter, it decreased.

SEM images for the 5 wt. % clay nanocomposite revealed that organoclay promoted interfacial bonding which led to improvement in strength of the nanocomposites. However, for nanocomposites with 7.5 wt. % of clay, the strength decreased as higher clay loading could have increased the viscosity of composites making clay dispersion difficult, and thus, generating defects which could have lowered the strength of nanocomposites(Figure 2.3).

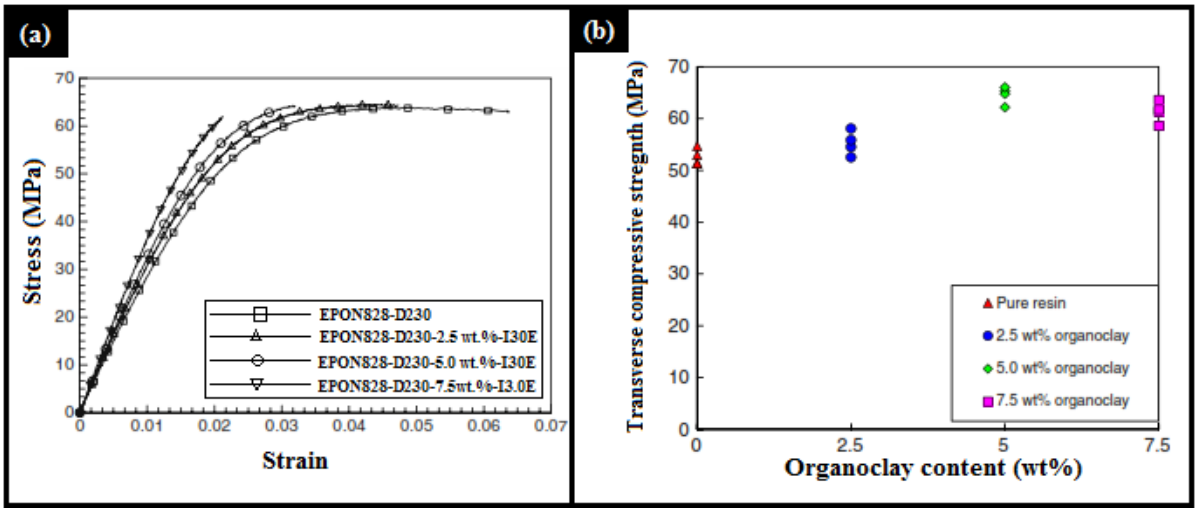

Figure 2.3 (a) Stress-strain curves, and (b) compressive strength for nanocomposites [85].

Manjunatha *et al.* [30] synthesized glass fiber reinforced epoxy composites modified by silica nanoparticles to study the tensile and fatigue behaviour.

Epoxy resin (DGEBA), silica (SiO_2), curing agent (Albidur HE600), E-glass fiber mat were used to fabricate the composites. All components were mixed together in the required amount by stirring

followed by degassing. The degassed resin mixture was used with glass fibers to fabricate the glass fiber reinforced nanocomposites using resin infusion under flexible tooling (RIFT) technique (50 ℃, -1 atm) followed by curing. For comparison, samples without glass fibers were also prepared by pouring degassed mixture in mould followed by curing (100 ℃, 2 h) and post-curing (150 ℃, 10 h).

Elastic modulus & strength values for neat polymer and GFRP enhanced (by 5% & 19%; and 7% & 17% respectively) on addition of nano-silica. The fatigue life of nanocomposite showed a 3–4 folds increase over that for neat epoxy. The fatigue crack growth rate for the nanocomposite was lower as compared to that for neat epoxy, indicating improved fatigue life. Particle debonding and growth of plastic voids were observed as the mechanisms responsible for improvement in fatigue life of composites.

Lingaraju *et al.* [86] synthesized epoxy based glass fiber reinforced nanocomposites with two types of clay (halloysite nanotubes and silica) using hand lay-up method to study the impact strength of nanocomposites.

Epoxy resin, clay, and woven glass fiber mat were used to synthesize the composites. Ultrasonicator was used to disperse the clay (1, 2, and 3 wt. %) in epoxy. Glass fiber reinforced nanocomposites were synthesized with 50 wt. % of glass fiber and were cured (ambient temperature, 24 h).

Impact strength (with 1 mm notch radius) of nanocomposites showed maximum improvement with 2 wt. % halloysite nanotubes (HNT clay) loading (impact strength improved by 28%). With 3 wt. % HNT clay loading, improvement was 20%. Further, impact strength improvement (with 2.5 mm notch radius) was 8% with 2 wt. % HNT clay, but reduced beyond this reinforcement level.

Impact strength of silica reinforced nanocomposites (with 1 mm notch radius) showed maximum improvement of 4 % at 3 wt. % loading. Further, for 2.5 mm notch radius, maximum improvement of 16% in impact strength was observed by reinforcing 3 wt. % silica.

Rafiq *et al.* [77] examined the role of clay addition on properties of glass fiber reinforced nanocomposites with epoxy as the matrix. Clay loading was varied as 0, 1.5, and 3 wt. %. High shear mixer was used for homogenous mixing of silicate layers in epoxy. Epoxy, hardener, clay,

and glass fibers used were GY 6010 RS, Isophoronediamine (IPDA), Nanomer I.30E, and E-CR glass fiber mat respectively.

Clay was hand mixed with epoxy followed by high shear mixing (followed by degassing for 12 h). Hardener was hand mixed to the resin. The mixture obtained was coated on fibers (layer by layer) by hand lay-up.

XRD results confirmed fully/partially exfoliated morphology. Flexural modulus and strength increased till 1.5 wt. % clay content (23% and 15% improvement respectively in modulus and strength). Further, fracture toughness improved by 77% at 1.5 wt. % clay content. Higher stiffness of silicate platelets improved the reinforcing ability of the matrix. Silicate platelets were present at glass fiber surface and resulted in strong interfacial adhesion of fibers with the matrix. Further, the presence of silicate platelets in matrix also deflected the crack, which contributed primarily towards toughening. Also, the presence of silicate platelets acted as an obstacle to crack propagation. Homogenous dispersion of nanoclay in epoxy matrix became very difficult at higher clay loadings (3 wt. %) due to increased viscosity resulting in clay agglomeration. These agglomerates acted as stress concentrators for crack initiation.

Withers *et al.* [87] examined the role of OMMT nanoclay reinforcement on tensile properties of epoxy based GFRPs.

Cloisite 30B nanoclay (2 and 4 wt. %) was mixed to tetraethlyenepentamine/nonylphenol blend using a hot plate/magnetic stirrer. This mixture and the epoxy were mixed and laid-up on glass fibers (6 layers). The laminates were cured for 24 h under ambient conditions while pressing uniformly (550 N) between two plates. Epoxy-glass fiber laminates (without clay) were also fabricated.

Tensile strength and modulus values were highest for nanocomposite having 2 wt. % nanoclay in it. Composite system without nanoclay showed a more brittle nature which made it more prone to fracture. The surfaces of fibers were not surrounded by epoxy matrix, which showed weak fiber/matrix adhesion. The fractured surface of nanocomposite reinforced with clay concentration of 2 wt. % displayed a more ductile/toughened epoxy matrix (strong adhesion of clay reinforced matrix with fibers) which was in confirmation with improvements obtained in properties.

Reddy *et al.* [88] observed the effect of addition of various filler materials (SiO_2, TiO_2, and glass powder) on inter-laminar shear strength of epoxy composites reinforced with glass fibers using

hand lay-up technique. Epoxy LY556 was used as the matrix; SiO_2, TiO_2, and glass powder were used as fillers. LY556 (epoxy) and HY5200 (hardener) with varying content of each filler (SiO_2 etc.) were laid up on woven E-glass fiber mat. This was followed by heating in an oven at 150 ℃ at the rate of 1℃ per min and finally cooling to 60 ℃ at the rate of 1℃ per min. Composite with 10 wt. % of SiO_2 showed highest inter-laminar shear strength value. The strength value of this composite was 28% and 45% higher than that of TiO_2 and glass powder filled nanocomposites respectively.

Sharma *et al.* [9] examined the role of stoichiometry and variation in processing parameters on performance of epoxy-GFRP nanocomposites.

Nanoclay (Cloisite® 15 A) equivalent to 2 phr was mixed to epoxy (Airstone 780 E) by homogenization (3 min) and sonication (10 min). Processing conditions used for mixing of clay are shown in Table 2.2. Hardener (Airstone 786 H) was added to epoxy-clay by mechanical stirring (500 rpm, 2 min, 25 ℃) followed by degassing (30 min). Laminates (with E-glass fiber mat) were fabricated using vacuum-assisted wet lay-up followed by curing (70 ℃, 7 h). All mechanical properties improved significantly in nanocomposites. Post-cured (100 ℃) and non post-cured samples showed almost similar mechanical properties.

Table 2.2 Process parameters utilized for synthesis of nanocomposites [9].

Process conditions	High shear homogenization		Ultrasonic probe amplitude (%)	Whether post-cured/ temperature (℃)	Epoxy: hardener ratio
code	Speed (rpm)	Temperature during mixing (℃)			
PC1	10,000	40	40	No	100:31
PC2	20,000	82	80	No	100:31
PC3	20,000	25	80	No	100:31
PC4	20,000	25	80	Yes/100	100:31
PC5	20,000	25	80	Yes/130	100:31
PC6	20,000	25	80	Yes/150	100:31
PC7	20,000	25	80	No	100:29.5
PC8	20,000	25	80	No	100:28

Table 2.3 summarizes the literature on epoxy-clay GFRP nanocomposites.

Table 2.3 Summary of literature on epoxy-clay GFRP composite systems.

S. No.	Summary	References
1.	Several researchers have examined the role of clay addition in varying content on hygrothermal/mechanical/fatigue/thermal/ & tribological properties of GFRPs.	
	Authors have used different techniques like VARTM/ VARIM/vacuum assisted wet lay-up method/hand lay-up combined with vacuum bagging etc. for synthesis of GFRPs. The following properties have mainly been investigated:	Lee *et al*., [7]; Manjunatha *et al*.,[30]; Rafiq *et al*., [77]; Kornmann *et al*., [83]; Avila *et al*., [84]; Tsai *et al*., [85]; Withers *et al*., [87]; Lin *et al*., [89]; Bozkurt *et al*., [90]; Kumar *et al*., [91]; Agubra *et al*., [92].
	a) Mechanical properties (tensile strength, tensile modulus, flexural strength, flexural modulus, fatigue strength, impact strength) of epoxy-clay based GFRP nanocomposites.	
	b) Thermal properties (thermal stability, T_g and weight loss/weight gain percentage) of epoxy-clay based GFRPs.	Chow,[12]; Lin *et al*., [89]; Bozkurt *et al*., [90].
	c) Tribological, hygrothermal properties and dampening behaviour of epoxy-clay GFRPs.	Kornmann *et al.*, [83]; Lingaraju *et al.*, [86]; Bozkurt *et al.*, [90].
2.	A few researchers have investigated the effect of adding different filler materials (SiO_2, TiO_2, glass powder, asbestos, hematite, fly ash, Al_2O_3, $Mg(OH)_2$ etc. on the inter-laminar shear properties, tensile properties, flexural strength, hardness, impact strength, bending strength of GFRPs.	Reddy *et al*., [88]; Devendra and Rangaswamy [93], Channapagoudra *et al*., [94]; Shettar and Chauhan [95].
3.	A few researchers have studied the influence of operating/mixing parameters, curing/post-curing procedure/time-periods, and stoichiometry on mechanical/thermal characteristics of GFRPs.	Sharma *et al.*, [9]; Cid *et al*., [96]; Kumar *et al*., [97]; Minty *et al.*, [98]; Sharma *et al*., [99].

Majority of the fiber reinforced polymers (FRPs) consist of an epoxy matrix reinforced with glass fibers. Epoxy-clay based GFRP nanocomposites possess high specific strength but suffer from

increased brittleness and hence poor impact strength. The safe operation of structures demands that epoxy based GFRPs also possess high impact strength in addition to their good static properties. To improve the impact performance, one of the ways is to use nano-scale reinforcement (nanoclay) along with soft/ductile thermoplastic polymer/elastomer as the second filler in GFRPs. Few authors have utilized ductile thermoplastic fillers (PET, PP, elastomers etc.) as reinforcement in composite systems. Literature review on composite systems containing polyethylene terephthalate (PET), polypropylene (PP), or elastomer filler is presented in the next section.

2.4 POLYMER FILLER/ELASTOMER MODIFIED COMPOSITES

A) Polyethylene terephthalate (PET) based literature

Santos and Pezzin [100] presented an experimental study on composites containing polypropylene (PP) as matrix and recycled PET as the reinforcement. PP/PET composites with varying concentrations of PET fiber reinforcement (3, 5, and 7 wt. %) were fabricated using combination of extrusion and injection moulding.

PET fibers were incorporated in PP matrix using a mono-screw extruder at 11.8 rpm. The temperature was kept between 106 ℃ and 160 ℃. Finally, the samples were cooled and pelletized in a knife mill.

The mechanical performance was assessed by measuring the tensile strength, surface hardness, and Izod impact strength values. Results showed that PET addition showed a nominal increase (3.7% increase with 5% PET fiber loading) in the tensile strength of the system. However, incorporation of PET fibers dramatically decreased the elongation at break for all compositions (about 80% drop in all composites compared to pure PP sample). Impact testing results showed improvement in impact strength for all concentrations of PET loading (maximum improvement of 18.9% for 7 wt. % of PET fiber loading). Surface hardness values of the composite system did not show any change as compared to pure PP.

Guan *et al.* [101] synthesized PET/MMT nanocomposites using in-situ poly-condensation and converted these to fiber form using melt spinning. The fibers were characterized using XRD, DSC, TEM, TGA and were tensile tested for performance.

MMT was modified using poly(vinylpyrrolidone) (PVP) and was designated as PVP-MMT. PVP-MMT was uniformly dispersed in hundred parts by weight of dimethyl terephthalate (DMT)

followed by addition of 72 parts of ethylene glycol and zinc acetate (as catalyst). Methanol generated from the mixture was removed by heating the mixture to 180 ℃. Antimony trioxide was added as the catalyst, the temperature was increased to 280 ℃, and vacuum of 0.1 mm of Hg was applied to produce PET/PVP-MMT nanocomposite. Fibers of pure PET (containing no nanoclay) were also prepared through melt spinning.

TGA results showed that PVP-MMT did not show any appreciable weight loss below 400 ℃. XRD analysis showed improvement in inter-layer spacing from 1.2 nm to 3.2 nm when untreated MMT was compared to PVP/MMT. Also, a strong shear stress during melt spinning caused MMT to exfoliate. However, it was observed that there were difficulties in processing of melt spinning with increasing amount of MMT. Further, for 5% elongation of PET/PVP-MMT nanocomposite drawn fiber, it was observed that MMT layers dispersed uniformly, restricting the movement of PET macromolecules, and thus leading to increase in tensile strength. Also, the DSC results showed that heat shrinkage of the resulting nanocomposite got lowered, which was advantageous.

B) Polypropylene (PP) based literature

Dutra et al. [42] synthesized epoxy/PP±EVA blend (PP and ethylene-vinyl acetate i.e. EVA copolymer) and investigated the mechanical properties of resulting composites.

The fiber (PP) was wrapped on a carton cylinder having a fissure. To prepare the laminates, vacuum method was employed to apply mixture of epoxy resin (CY260) and curing agent (HY561) on the PP fibers. The resulting pre-impregnated specimens (40–45 vol. % fiber fraction) were stacked for required number of plies, under vacuum. This was followed by curing (350 kPa, 120 ℃, 2 h). Epoxy/PP fiber composites were also prepared for comparison. Fourier transform infrared spectroscopy (FTIR) of the prepared composites indicated presence of carbonyl group of EVA component and existence of mercapto group near surface of fibers facilitating good adhesion between various components of the system. Impact test results for composites having PP±EVA fiber showed a significant increase in impact resistance as compared to composite with PP fibers (without EVA).

Dutra *et al.* [43] synthesized epoxy based hybrid composites with carbon fibers and PP fibers/ PPEVA blend as reinforcement to study the effect of PP fiber reinforcement on the resistance to impact loading and storage modulus of the resulting system.

PP fibers and blends of PP fibers/EVA (95:5) phr were synthesized using melt spinning. Prepreg layers of each filler (carbon fibers/PP/PPEVA) were prepared by applying the epoxy system (CY260/HY561) on fibers wrapped around a container having fissures. Then, composites were prepared by stacking 6 layers (6 layers of PP/PPEVA prepreg or 3 layers each of carbon fiber and PP/PPEVA prepregs) of the prepregs into an open mould and applying vacuum. Finally, the composites were cured (350 kPa, 120 ℃, 120 min).

Impact test results showed that PP fiber reinforced system (EP/PP) displayed higher impact strength (259±38 J/m) than the (EP/CF) carbon fiber composite (209±32 J/m). The improvement was attributed to the ductile nature of PP fibers. The addition of both PP and carbon fibers (EP/PP/CF) led to improvement in impact strength (246±18 J/m) over carbon fiber composites without PP fibers. Epoxy composites with PPEVA and carbon fibers showed comparatively higher impact strength (352±78 J/m) but lesser than the EP/PPEVA (951±148 J/m) system. SEM images of impact tested surface of carbon fiber composites showed that carbon fiber fractured in a brittle manner. However, hybrids having PP fiber showed characteristics of a relatively ductile failure. PPEVA-CF hybrid composites showed good interfacial adhesion as the fiber debonding was not so extensive due to presence of mercapto groups which promoted good matrix-fiber interaction. PPEVA-CF hybrid composites showed higher storage modulus values also.

Prabhu *et al.* [44] synthesized epoxy/PP fiber composites with different fiber loadings to study the thermal degradation characteristics through TGA results.

Varied concentration of PP fibers (5–15 wt. %), DGEBA (epoxy), and hardener were mixed together with gentle stirring to prepare composites with mould covered with teflon sheet. The system was thereafter cured (room temperature, 24–26 h).

TGA results of composites showed the onset of thermal degradation between 275–375 ℃ for 5 wt. % PP composite, 250–380 ℃ for 10 wt. % fiber content, and 265–380 ℃ for 15 wt. % fiber content. Derivative weight loss curve showed that complete decomposition occurred at 520 ℃ for 5 wt. % fiber, 530 ℃ for 10 wt. % fiber, and 600 ℃ for 15 wt. % PP fiber composites. The results indicated that PP fiber reinforcement reduced the thermal degradation due to binding of fiber to epoxy. The improvement in thermal properties was maximum for fiber content between 5–10 wt. %. Reinforcement beyond 10 wt. % reduced the performance of the system as a minimum amount of matrix was essential for the composite.

SEM images showed brittle fracture for neat epoxy. For composites, more ductile failure resulted from increased fiber loading. Most of the fibers were together without any damage, indicating that the matrix contributed to failure of the composites.

Arikan *et al*. [102] fabricated glass fiber reinforced composites using two different types of matrix (a) thermosetting (epoxy/hardener), and (b) thermoplastic (polypropylene) to study the impact performance of resulting composites.

Epoxy-composite plates were fabricated using vacuum infusion method and polypropylene-composites were fabricated by hot pressing. Impact test results showed that thermoplastic composites absorbed 4% more energy as compared to the thermoset type. Deflection was more in case of polypropylene based composites. For both types of composites, failure of fiber initiated at 2 kN force. However, the maximum force which the materials could bear was higher (16 kN) for thermoset matrix as compared to thermoplastic matrix (8.9 kN). Deflection of composite plates at 8 kN contact force was observed as 3.5 mm and 8.1 mm for epoxy based and polypropylene matrix composites respectively. Bending stiffness values for epoxy based and polypropylene based composites were 2225 N/mm and 940 N/mm respectively.

Both types of composites absorbed nearly same impact energies. However, contact force of thermoset matrix was able to withstand contact force nearly double the contact force of thermoplastic matrix. However, less stiffness and ductility of thermoplastic matrix resulted in comparable absorbed energy.

C) Elastomer based literature

Balakrishnan and Raghavan [27] dispersed acrylic rubber to prepare epoxy based clay reinforced hybrid nanocomposites. Mechanical properties of the resulting system were evaluated. Mixture of C18 clay (Na Cloisite), epoxy resin, acrylic rubber, and tetrahydrofuran were mixed together by sonication (30 min). This suspension was degassed using vacuum oven (60 ℃, 4 h) and hardener (pyridine) was added by hand mixing. The suspension was transferred to a silicon mould and cured (120 ℃, 16 h). Similarly, epoxy, rubber toughened epoxy, and clay filled composites were also prepared.

Stress-strain plots indicated that pristine epoxy showed a brittle failure. Introduction of clay to epoxy improved its capability to bear load due to good stress-transferring ability of silicate layers. For the rubber-dispersed systems (with or without clay), the fracture behaviour was observed to

have a smooth transformation from a region of linear variation of load with displacement to a maxima, followed by yielding, and failure.

From tensile test results (Table 2.4), it was evident that addition of clay particles led to improved modulus. However, dispersion of rubber to the system resulted in reduced modulus and strength with improved failure strain, as compared to pristine epoxy. Reduction in properties as a result of addition of rubber was offset by addition of clay and reduction in failure strain resulting from addition of clay was offset by addition of rubber.

Table 2.4 Results of tensile testing of samples [27].

Type of Material	Tensile Strength (MPa)	Tensile Modulus (MPa)	Tensile Break Strain (%)
Epoxy Resin	160.5	2256.5	8.3
Clay Composite	177.5	2775.9	8.2
Rubber Dispersed Epoxy	143.3	1976.2	9.98
Rubber Dispersed Clay Nanocomposite	161.1	2352.8	11.5

Liu *et al.* [40] synthesized epoxy based composites modified with nanoclay and rubber to study the influence on morphology and mechanical properties.

Composites were prepared, both with and without carboxyl-terminated butadiene acrylonitrile (CTBN) rubber. Two different methods: a) direct mixing (DM), and b) high pressure mixing (HPM) were used to mix clay (Nanomer I.30.E) to epoxy (DGEBA). Desired amount of CTBN rubber (20 phr) was added to this mixture by mechanical stirring (100 rpm, 2 h) followed by degassing.

High pressure applied in HPM led to better dispersion of nanoclay as compared to DM. Clay agglomerates were observed in nanocomposites processed through DM. High pressure used in HPM method was able to break the clay agglomerates. XRD results showed increase in d-spacing (2.37–3.52 nm) after mixing clay/epoxy using HPM, indicating exfoliation. XRD patterns of CTBN reinforced composites (20 phr CR and 6 phr clay) with curing at different temperatures showed that high temperatures benefited the formation of exfoliated nanocomposites.

All compressive properties improved at higher clay content (without CTBN). However, in CTBN dispersed composites, improvement in strength (ultimate as well as yield strength) was noted at

higher clay contents (other properties did not change). Nanocomposites without CTBN possessed higher hardness values; these values did not show significant improvement with increased clay content for the system with CTBN. Addition of 20 phr CTBN led to 15 % decrease in hardness (this was largely recovered with addition of 6 phr clay).

Balakrishnan *et al.* [28] dispersed rubber to epoxy/clay nanocomposites for investigating influence of clay/rubber content on mechanical performance of prepared composites.

Epoxy DGEBA, clay Na Cloisite (NaMMT), and acrylic rubber dispersion were used to synthesize the composites. Rubber toughened epoxy nanocomposites were prepared by mixing organoclay, rubber dispersion, epoxy and swelling agent tetrahydrofuran (THF) followed by sonication (35 ℃, 30 m). The system was kept in vacuum oven (60 ℃, 4 h) to remove THF followed by hand mixing with curing agent. The suspension was filled in a silicone mould and cured (120 ℃, 16 h). The composites were prepared with content of rubber ranging from 0–16 phr and organoclay ranging from 0–5.5 wt. %. For comparison, pristine epoxy samples were also prepared.

Tensile behaviour of prepared composites showed that addition of clay improved strength and modulus (11% and 23% respectively), though it did not have any impact on elongation at break. Further, incorporation of rubber alone led to decrease in both tensile strength (11%) and modulus (15%) of epoxy. However, 20% improvement in elongation at break was observed by addition of rubber to pristine epoxy. Incorporation of both (rubber and clay) resulted in an increase in elongation at break by 39% with negligible change in tensile properties of pristine epoxy.

Lee *et al.* [29] synthesized epoxy/clay/rubber based composites to study the influence of incorporation of clay and rubber on morphology and properties of composites. Authors also studied the change in properties after using gamma-ray irradiation for accelerating the aging.

Clay (Cloisite A) was mixed to epoxy (DGEBA) for 5 h followed by ultrasonication (20 min). Rubber (CR) in varying concentrations (7 and 15 wt. %) was mixed to epoxy-clay suspension by stirring (2 h), and adding hardener (Jeffamine D-230). The system was kept in an oven for degassing. Degassed system was then injected to mould, cured (130 ℃, 3 h), and post-cured (120 ℃, 12 h). For accelerated aging, the specimens were exposed to gamma rays (500–1500 kGy) under the conditions of 8kGy/h and ambient temperature.

XRD patterns showed an increase in inter-layer spacing (20 Å to 35.7 Å) of clay after incorporation to epoxy and 15 wt. % CR. Tensile test results showed that with increase in dose of absorption,

the tensile strength of specimens decreased. Addition of clay increased the modulus but decreased the tensile strength. Nanocomposites having 7 wt. % CR exhibited tensile strength values lower than that of epoxy. However, for incorporation of higher content of CR (15 wt. %) to epoxy-clay, the tensile strength observed was 10% higher than epoxy without irradiation, 50% higher than the system irradiated at 500 kGy, 90% increase over the system irradiated at 1000 kGy, and 20% increase over the specimens irradiated at 1500 kGy. FE-SEM of fractured surface showed brittle fracture surface for epoxy, whereas that for epoxy-clay was rough due to excellent mechanical strength. All fractured specimens showed hard surfaces with increase in absorption dose due to the cross-linking developed by irradiations. For CR modified samples, the fracture surface possessed a typical morphology (two phase) having a rubbery phase (spherical particles) and a rigid continuous phase.

Manjunatha *et al.* [41] synthesized glass fiber reinforced polymer composites based on rubber modified epoxy matrix to observe influence of this modification of epoxy on cyclic fatigue behaviour of the prepared composites.

Epoxy (DGEBA), liquid rubber (CR), curing agent (Albidur HE 600), and non-crimp E-glass fibers were used to prepare the composites.

Epoxy (LY556), hardener (Albidur HE 600), and CR rubber (9 wt. %) were mixed and degassed (50 ℃, 1 atm, 1 h). The prepared mixture was transferred into a mould and cured (100 ℃, 2 h) followed by post-curing (150 ℃, 10 h). The mixture was used with glass fiber using RIFT (resin infusion using the flexible tooling) method to fabricate GFRPs.

Tensile modulus (E) and ultimate tensile strength (UTS) of the polymer and GFRPs decreased with addition of CR. Fatigue test results showed 3–4 fold increase in fatigue life of epoxy by incorporation of rubber. Presence of rubber led to 35% and 13% increase in fatigue strength coefficient (FSC of bulk epoxy and GFRP respectively). Fatigue strength exponent (FSE) of the epoxy decreased by 16% with incorporation of CR. However, for GFRP, the FSE did not show any significant change.

SEM images of fatigue tested specimens showed smooth surface for epoxy polymer without any indication of large plastic deformation. In rubber modified system, cavitation of rubber particles with plastic deformation of surrounding material was observed. It was concluded that energy

absorbing mechanisms of cavitation and shear deformation led to improvement in fatigue life of the materials system.

Dafdar and Ghadami [32] synthesized glass fiber reinforced composites by adding carboxyl-terminated butadiene acrylonitrile, CTBN rubber (5, 10, and 15 phr) to epoxy for examining the influence of CR on mechanical and fracture properties of composites.

DGEBA (epoxy resin), Aradur 917 (curing agent), and rubber (CTBN liquid rubber) were mixed in a stoichiometric ratio and degassed. The degassed mixture was cast in a mould followed by curing (80 ℃, 4 h) and post-curing (160 ℃, 8 h) in an oven. GFRP composite sheets (using E-glass fiber) were prepared by hand lay-up method using the degassed mixture.

Fracture surface of CTBN-epoxy showed increase in cavities with increased CTBN concentration, and thus, increased fracture toughness. Tensile properties of all the composites deteriorated with increase in rubber concentration as compared to un-reinforced system because CTBN has lower modulus as compared to matrix.

Wang *et al.* [87] prepared nanocomposites having acrylic rubber (AR) and varying concentration of montmorillonite (MMT) clay in epoxy to investigate the influence of varying concentration of clay (0–5 wt. %) on the thermal, dynamic mechanical, and physical properties of nanocomposites. AR (50 wt. %), DGEBA (epoxy), and diaminodiphenylmethane (DDM) (hardener) were stirred in acetone to prepare a solution. Nanoclay (0, 1, 3, 5 wt. %) was mixed to the solution by sonication and was then cast. The prepared solution was then coated over Polytetrafluoroethylene (PTFE) substrate using a coating machine and cured (120 ℃, 4 h). Epoxy/AR/MMT nanocomposites led to increased T_g of epoxy phase. Modulus of composites improved with increase in clay content with maximum improvement of 61%.

Carolan *et al.* [103] prepared epoxy based nanocomposites containing core shell rubber (CSR)/silica particles and reactive dilutent (hexanediol diglycidylether, HDDGE) to study microstructure and fracture performance of the prepared system.

Araldite LY556 (epoxy), Albidur HE600 (hardener), SiO_2 (nanoparticles), HDDGE, and CSR particles were used to prepare the nanocomposites. Nanocomposites were prepared by casting into steel moulds followed by curing (90 ℃, 1 h) and post-curing (160 ℃, 2 h).

Addition of 25 wt. % of HDDGE led to significantly higher fracture energy (38%) of epoxy. Addition of 20 wt. % CSR without HDDGE sharply raised (six folds increase) the fracture energy

of epoxy. Further, when both CSR (20 wt. %) and HDDGE (25 wt. %) were added, the fracture energy of the system increased extensively by around 9 times as compared to neat epoxy. Addition of silica to the nanocomposites having both silica and CSR led to modest increase in the fracture energy of epoxy polymer.

Nguyen *et al.* [104] modified the epoxy by addition of CSR particles to study the effect of incorporation of different phosphonium ionic liquids (IL) on properties of epoxy. Epoxy (DER332), hardener (4,4'-methylenebis(3-chloro-2,6-diethylaniline)) designated as MCDEA, various ILs: tributyl (ethyl) phosphonium (diethyl) phosphate (IL-DEP), and trihexyl (tetradecyl) phosphonium bis-2,4,4(trimethylpentyl) phosphinate (IL-TMP). Core-shell rubber particles, Genioperl P52 (CSR) were used to prepare the materials system. CSR in varying concentration (10 and 20 phr) was dispersed in epoxy at 60 ℃ by stirring at 200 rpm for 1 h followed by sonication for 15 min. MCDEA (54 phr) and IL-TMP/IL-DEP (10 phr) were mixed to epoxy-CSR mixture followed by decanting into moulds and curing and post-curing as presented in Table 2.5.

Table 2.5 Curing schedule followed with different agents [104].

Curing agent	Curing	Post-curing
MCDEA	150 ℃, 1 h and 180 ℃, 2 h	200 ℃, 1 h
IL-TMP	80 ℃, 2 h and 120 ℃, 3 h	200 ℃, 1 h
IL-DEP	80 ℃, 2 h and 120 ℃, 3 h	200 ℃, 3 h

It was observed that ILs had a vital influence on CSR particle dispersion in the matrix. ILs also influenced the morphology of CSR modified system leading to effective dispersion of rubber as compared to amine cured systems. Reinforcement of IL-TMP resulted in significant increase in fracture toughness by 27% and 54% respectively over epoxy/hardener and epoxy/IL-DEP system (with 20 phr rubber).

Table 2.6 summarizes the literature on polymer fiber or elastomer reinforced epoxy based composites.

For the polymer filler/elastomer reinforced composites, literature indicated that surface modification of polymer filler/elastomer can result in improved properties of resulting composites. The next section presents the literature review on surface modification (compatibilization) procedures for polymer/elastomer fillers.

Table 2.6 Summary of literature on polymer fiber or elastomer filler reinforced epoxy based composite systems.

S. No.	Summary	References
1.	**PET reinforced composites**	
	Researchers have investigated the effect of reinforcing PET fibers in epoxy based composites on the mechanical properties (tensile properties, flexural properties, impact performance, and strain at break etc.) of prepared systems. A few authors have also investigated the mechanical properties of composites containing PET as the reinforcement with polymethylmetha acrylate (PMMA) or polypropylene (PP) as the matrix.	Santos and Pezzin [100]; Teh *et al*., [105]; Khanchaitit and Aht-Ong [106]; Jindal [107]; Raturi [108].
2.	**PP reinforced composites**	
	Researchers have investigated the role of polypropylene fiber addition in epoxy/PP, epoxy/PP/EVASH, and epoxy/carbon fibers/PP composite systems. Authors have examined the influence of PP reinforcement on the mechanical (flexural properties, impact resistance etc.), dynamic mechanical properties (storage modulus etc.), and thermal degradation characteristics of composite systems.	Dutra *et al*., [42]; Dutra *et al*.,[43]; Parbhu *et al*., [44]; Arikan *et al*. [102].
3.	**Elastomer reinforced composites**	
	Researchers have investigated acrylic particle dispersed epoxy-clay nanocomposites, core shell rubber reinforced epoxy-clay nanocomposites, CTBN rubber reinforced glass fiber epoxy based systems to examine the influence of elastomer reinforcement on mechanical properties (yield strength, ultimate tensile strength, failure strain, hardness, fatigue strength, and fracture toughness) and also on the storage modulus and T_g values of resulting composites. A few researchers have also investigated the effect of addition of reactive dilutent/phosphonium ionic liquid to epoxy based composites reinforced with core shell rubber and reported enhancement in fracture properties of composites.	Balkrishnan and Raghavan, [27]; Balakrishnan *et al*., [28]; Lee *et al*., [29]; Dafdar and Ghadami [32]; Liu *et al*., [40]; Manjunatha *et al*., [41]; Carolen *et al*., [103]; Nguyen *et al*., [104]; Wang *et al*., [109].

2.5. SURFACE MODIFICATION OF POLYMER/ELASTOMER FILLER

A) Surface modification of polyethylene terephthalate (PET)

Demir *et al.* [110] treated PET powder with three different silane coupling agents (SCA) to study the effect on properties of high density polyethylene (HDPE) composites reinforced with PET (5, 10, 15, and 40 wt. %).

HDPE granules (S0464) and PET powder (prepared from soft drink bottles) were used to prepare HDPE/PET composites. PET was treated with three different silane coupling agents viz. ɣ-glycidoxypropyltrimethoxysilane (A-187), vinyl-tris-(beta-methoxyethoxy) silane (A-172), and ɣ-methacryloxypropyltrimethoxysilane (A-174). SCA (2 wt. % of PET) was taken in ether solution and was applied onto surface of PET powder followed by heating in an oven (45 ℃, 8 h) to vaporise ether. Compositions with varying concentration of PET (5, 10, 15, and 40 wt. %) in HDPE were prepared by mixing in a brabender. Composites were prepared by compression-moulding (200 ℃, 20,000 psi, 1 min). Pure HDPE samples were also prepared for comparison by similar process.

Addition of both treated/untreated PET led to improved tensile strength values. However, for composites having 5 wt. % of PET fibers, UTS decreased as compared to HDPE, irrespective of treatment. Weak adhesion among the polymers was observed as the reason for low value of UTS of PET (untreated) filled HDPE. However, for SCA treated PET filled composites, a considerable increase was observed in UTS for 15% PET loading. Further, impact performance also improved for SCA treated PET filled composites.

Cioffi *et al.* [111] fabricated PET/polymethylmetha acrylate (PMMA) composites using filament winding equipment. PET fibers were treated with oxygen-plasma. Contact angle measurements were done to assess optimum time for plasma treatment. Further, tensile testing and SEM analysis were carried out to investigate the mechanical behaviour and morphological changes with different treatment times.

For treatment, PET fibers (diameter: 13 μm; elastic modulus: 14 GPa) were kept in a cold plasma reactor for different time periods (0, 5, 20, 30, and 100 s). Contact angle of fibers was measured using Rame-Hart goniometer. The composite (PET/PMMA was fabricated using filament winding process and tensile testing of different samples was done using universal testing machine (UTM).

Non-treated fibers exhibited a contact angle of 90º. Contact angle reduced with increase in

treatment time. For 5 s and 20 s, respective values of contact angle were 31º and 7º (beyond 20 s time, no significant change in contact angle was observed).

SEM micrographs indicated that an increase in treatment time till 20 s resulted in higher adhesion between fibers and matrix (5 s treated fibers showed no traces of matrix after failure whereas those with 20 s displayed resin adhered to them after failure). However, for greater exposure times (greater than 20 s), intense degradation of fiber surfaces was observed. Further, the UTS values of the composite (PMMA reinforced with PET) improved for treatment time till 20 s. However, maximum value was obtained for treatment time of 5 s.

Teh *et al.* [105] fabricated composites of aromatic epoxy with 1 wt. % of PET fibers with the objective to study the toughening mechanism and fracture behaviour of composites for optimizing the treatment time required for NaOH treatment of PET fibers.

PET fibers of diameter 20 μm and length 2–3 mm were taken. For surface modification, PET fibers were kept in NaOH solution with water (50% w/v) at temperature of 80 ℃ for varying time periods of 0–30 min. Subsequently, NaOH was washed off from the samples using distilled water. ToF-SIMS technique was used to scan the surface topology and internal structure of PET fibers during hydrolysis (surface modification) before adding them to epoxy. The fibers were mixed to epoxy by mechanical mixing followed by homogenization. The blends prepared were then degassed, cured (100 ℃, 2 h), and post-cured (180 ℃, 5 h). Samples (thickness: 6.25 mm; width: 12.5 mm) as per ASTM E399 were taken for mechanical testing (three point bending test) at room temperature.

SEM and ToF-SIMS investigations revealed that unmodified fibers showed smooth and featureless surface while the surface of modified fibers appeared with shallow pitting and some cracks for treatment time periods of 2.5 min. Fibers treated with NaOH for 20 min resulted in irregular surface and did not remain straight (Figure 2.4).

The results showed an increase of 33% in toughness with addition of 1 wt. % un-treated PET fibers which increased to 88% on addition of 1 wt. % treated (with NaOH for 2.5 min) fibers. On increasing the time of surface treatment, toughness decreased because prolonged alkaline hydrolysis led to large accumulation of pits resulting in crack initiation and internal hydrolysis.

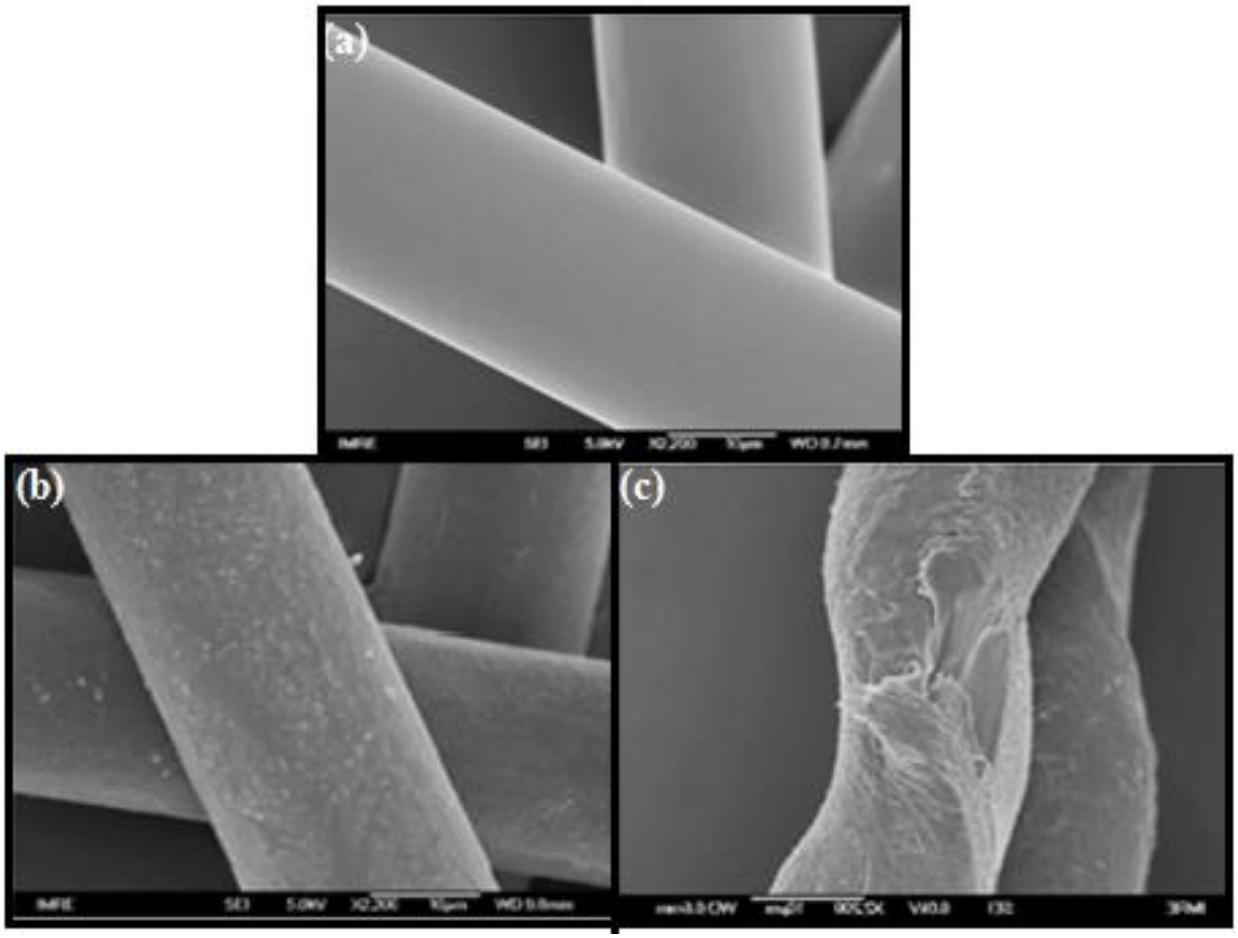

Figure 2.4 SEM images of (a) unmodified fibers, (b) modified fibers with 2.5 min, and (c) 20 min NaOH treatment [105].

Fractured surface of failed composites were also investigated with SEM. Observations revealed that non-treated fibers showed pull-out, leaving clean holes in the epoxy, which represented poor adhesion between fibers and epoxy. The fractured surface of composites with treated fibers (2.5 min) showed typical breakage and river like structures on the surface, which indicated that a lot of energy was utilized during the fracture. However, in the sample with treated fibers for a prolonged period (20 min), the river like structure was less apparent, thus concluding that less energy was consumed.

Khanchaitit and Aht-Ong [106] fabricated a PET reinforced epoxy composite using UV/ozone surface modification of PET fibers. The effect of exposure to UV radiations and different types of gases (oxygen/ozone, nitrogen, oxygen, air/ozone, and air) and also the influence of varied time of exposure (2, 5, and 10 min) on PET fiber chemistry/morphology was investigated.

Multi-filament PET fiber samples having filament diameter of 10 μm were used for the study. Surface modification was done in a 1 m long tubular stainless steel reaction chamber. The reaction chamber was equipped with hemispherical sealable lids on both ends. Gas species were split by using three different inlets. The inlet gases were further split into 18 flows (each) by nozzles. The gas type to be used for modification was passed through the centre of the chamber having fibers to be treated, leading to increased number of collisions on the surface of the fibers. For UV treatment, low-pressure mercury lamps were used. For the ozone treatment, ozone generators having three corona discharge generators were used. EPOTEC YD 582 (epoxy) and XDH 125 (hardener) were mixed in weight ratio of 3:1. This mixture was poured into a casting mould containing PET fibers (10 vol. %).

Both, gas type as well as exposure time, did not show any effect on tensile properties. SEM images did not show any considerable changes in the surface roughness at micro level. Changes due to surface modification were observed at the nano level. The results suggested that to influence the tensile properties of composites, interfacial properties needed an improvement. Tensile strength of composites reinforced with untreated fibers and treated fibers were compared, and the properties of latter were observed to be better. Composites with fibers treated for 5 min showed maximum improvement in tensile properties (with increase of at-least 25 MPa in tensile strength). With treatment time increased till 10 min, reduction in tensile properties was observed. SEM micrographs helped in drawing conclusions with regards to various failure mechanisms (like improvement in interface was indicated by increased roughness of pulled-out fiber surface).

Blazquez *et al.* [112] treated PET fibers by plasma treatment and studied the effect on interfacial adhesion between epoxy resin and PET fibers.

PET fibers (diameter: 200 μm) and epoxy (DER 331) were used for the study. PET fibers were subjected to oxygen plasma treatment for different time periods (till maximum value of 20 min). Interfacial failure decreased with increasing plasma treatment time. As a result, interfacial shear strength (IFSS) of fibers improved with increase in treatment time. IFSS showed a maximum increase of 200% for 10 min of plasma etching. Further increase in the treatment period did not affect the IFSS value.

Jindal [107] synthesized nanocomposites with epoxy resin (M Brace), MMT nanoclay (Closite® 30B), and PET fibers (Recron®) as reinforcement to investigate the mechanical properties by varying only the PET fiber content. PET fibers used were of 15 μm diameter and 3 mm length. Nanocomposites consisted of MMT clay (3 wt. %), PET fibers (0, 0.25, 0.5, 0.75, and 1.0 wt. %) and epoxy resin. PET fibers were kept immersed in NaOH solution (for 2.5 min and rinsed thoroughly by distilled water) to roughen the fiber surface and facilitate enhanced interfacial bonding of fibers with matrix. All properties showed an appreciable change with change in treated PET fiber content. XRD was conducted to ascertain distribution of clay. XRD results showed that epoxy chains were intercalated into the nanoclay layers. Tensile strength of nanocomposite system showed increase with increase in concentration of PET fibers till an optimum level (0.5 wt. %), and thereafter decreased gradually. Modulus of elasticity decreased continuously with increase in PET fiber content. Both, bending and impact strength showed increasing trend with increase in PET fiber content. Impact strength of composite system increased further with reinforcement of treated fibers. The results exhibited that PET imparts ductility to composites.

Liu *et al.* [113] investigated/compared the influence of surface modification of PET using ultraviolet (UV) radiations and other techniques like corona discharge treatment (CDT) and alkaline treatment on mechanical properties of PET reinforced composites. The fabrication of composites was done using laminates of PET fabric and TPU (thermoplastic polyurethanes).

The adhesion between TPU and PET fabric was measured using T-peel test of the laminates. It was observed that alkali treatment led to decrease in tensile strength and elongation values of composites. However, CDT treatment led to retention of the properties as no appreciable loss was observed in the properties of composites. UV treatment provided good adhesion between PET and TPU as it provided a matrix friendly surface to the fibers. Good adhesion was achieved through covalent and hydrogen bonding between fiber and matrix, and improved surface roughness of fibers.

Raturi [108] studied the effect of addition of PET fibers (Recron 3s; 0–1.5 wt. %) and nanoclay (MMT; 0–2.25 wt. %) on mechanical properties of epoxy based nanocomposites (epoxy: GY 257; hardener: HY 837). PET was used as reinforcement (both, in untreated form as well as after alkaline treatment for different time periods and different temperatures).

Nanoclay was dispersed in the resin by homogenization followed by ultrasonication, each for 10 min. PET fibers were treated using alkali (NaOH) treatment. For treatment, PET fibers were

dipped in alkaline solution (50 g of NaOH in 100 ml of water i.e. 50% w/v ratio) with treatment time of (2.5–15 min) at temperatures of 31 ℃, 50 ℃, and 80 ℃ respectively. Untreated/treated fibers were added to epoxy-clay suspension by stirring for 5 min. Finally, hardener was added to the system by mechanical stirring for 5 min. The prepared system was poured in aluminium mould for curing. Optimum condition for surface modification (NaOH treatment) of PET fibers was treatment time of 15 min at temperature of 80 ℃.

PET fiber blend containing 1.5 wt. % PET (maximum fiber content) and no clay showed 12% increase in tensile strength over the neat polymer. With increase in clay content (from 0.5625 to 1.6875 wt. %), for the same concentration of PET (1.125 wt. %), tensile strength decreased (39.5 to 34.3 MPa). This drop was attributed to stress concentration due to agglomeration of clay at higher concentration.

The maximum bending strength observed for the nanocomposite system was 83.3 MPa for 2.25 wt. % clay with no PET addition. Improvement in flexural modulus was observed for the epoxy-clay blend containing maximum weight percentage of clay and was about 10% more than the base material.

Nanocomposites containing both, PET as well as clay, in their higher ranges (wt. %), deteriorated the flexural modulus considerably. The epoxy-hardener system was not able to accommodate both the fillers simultaneously in large amounts as presence of both the fillers led to decrease in all the mechanical properties.

B) Surface modification of polypropylene (PP)

Jiang *et al.* [114] prepared blends of PP/epoxy (70/30) and PP/MAH grafted PP/epoxy (60/10/30) to investigate the effectiveness of MAH as a compatibilizing agent. MAH grafted PP (with 1 wt. % MAH content) was used to prepare the blends.

DGEBA (epoxy) and MAH-g-PP (i.e. MAH grafted PP) were kept in a vacuum oven (80 ℃, 8 h). Blends of PP/MAH-g-PP with epoxy were mixed in a rheometer (190 ℃, 50 rpm, 10 min). EMI-2,4 (hardener) was added and mixed to the system for 10 min (total mixing time). Finally, the specimens were compression moulded (195 ℃, 10 min) followed by cold pressing.

It was observed that torque at equilibrium for PP/MAH-g-PP/epoxy (60/10/30) blends was higher than the PP/epoxy (70/30) blends. Reaction of functional group and resultant co-polymer led to increase in torque of 60/30/10 composition. SEM micrographs of 70/30 blend showed that epoxy

was present as spherical particles in the PP matrix. For the 60/10/30 blend, epoxy was present as fine particles in the matrix with unclear boundaries at the interface. The results indicated that presence of MAH-g-PP led to improved interaction between PP and epoxy.

Adding epoxy (30 wt. %) to PP matrix led to improvement in flexural modulus at the cost of deterioration in other properties because of poor compatibility between PP and epoxy. Incorporation of 10 wt. % MAH-g-PP resulted in improved tensile strength and flexural modulus.

Pan *et al.* [115] compared the efficiency of two techniques for MAH grafting on PP. The techniques included (i) photo-initiated grafting using benzophenone (BP) as the initiator, and (ii) thermally initiated grafting using benzoyl peroxide (BPO) as the initiator.

For photo-initiated grafting using benzophenone (BP) as the initiator, solution method was used and for thermally initiated grafting using benzoyl peroxide (BPO) as the initiator, melt method was used.

For solution method, a solution of MAH, PP with benzene was poured into Pyrex glass reactor followed by keeping it in irradiation chamber (having 175.8 W mercury vapour lamp). Finally, benzene solution containing initiator (BP) was poured into the reactor. For melt method, grafting was performed by photo-irradiation of PP mixture having BPO and MAH in molten state (above 190 ℃) for different time periods ranging from 30 s to 8 min.

Photo-assisted grafting showed a high level of grafting and also reduced consumption of initiator.

Abacha and Fellahi [116] functionalized PP by grafting MAH onto its surface and incorporated it in varying concentrations (2.5–10 wt. %) to glass fibre reinforced nylon 6 composites (containing 30 wt. % of glass fibers) for studying the effect on impact performance.

MAH was grafted onto PP in an internal mixer (200 ℃, 7 min). PP was placed in a rheometer for melting and then the initiator, dicumyl peroxide (DCP) was added to the rheometer.

Fourier-transform infrared (FTIR) spectrometry confirmed the grafting reaction, and titration showed that 0.6 wt. % was grafted. Incorporation of compatibilized PP (i.e. MAH-g-PP) led to improvement in mechanical properties of the system. Impact resistance of blends increased significantly in comparison to that of blends without compatibilization.

Aboudzadeh *et al.* [117] modified PP plates with two different silane agents (i) GS (ɣ-glycidoxypropyltrimethoxy silane), and (ii) AS (ɣ-aminopropyltriethoxy silane) to study the effect of silane treatment on the bonding between acrylic lacquers and treated PP surfaces.

PP plates (1.5 mm thick), silane agents (GS and AS), acrylic lacquers (hydroxyl functional: SM518; carboxyl functional: SC133) and hardener (Desmodur N75 MPA) were used for the study. All samples were flame treated by exposing them to direct flames before the silane treatment. 0.5, 1.0, and 2.0 wt. % silane solutions were prepared using standard procedure. PP samples were immersed into each solution for 30 min. Finally, the immersed samples were washed with distilled water to remove excess (un-grafted) silane.

FTIR analysis revealed presence of carbonyl group for flame treatment and also confirmed the silane treatment of flame treated and silane treated PP respectively. Contact angle measurements revealed that flame treatment made the PP surface hydrophilic and also increased the surface free energy and surface roughness of PP. It was observed that adhesion strength of the materials system improved substantially with silane treatment. GS silane treatment showed higher adhesion strength as compared to AS silane treated PP/acrylic lacquer system.

Castel *et al.* [118] prepared PP/montmorillonite nanocomposites using silane treated PP to study the effect of silane treatment of PP on clay dispersion and mechanical performance of composites. Nanocomposites having 5 wt. % clay and varying concentration (5, 10, and 20 wt. %) of treated PP were prepared.

Polypropylene homopolymer, OMMT (Cloisite®15A) organoclay, PP grafted with vinyltriethoxysilane (PPVS) were used to prepare the nanocomposites.

For fabrication of nanocomposites, PP was pre-mixed with clay and PPVS in a tumbling mixer. The mixture was melt blended using a screw extruder (170–195 ℃, 80 rpm).

XRD patterns of nanocomposites revealed no significant change in d-spacing of montmorillonite due to low (0.4 wt. %) content of grafting. However, TEM images revealed homogeneous dispersion. Tensile modulus of PP increased by 34% with addition of OMMT. High modulus as well as high aspect ratio of the reinforcing material (clay) led to improvement in tensile modulus of PP based system. Interestingly, significant increase in tensile modulus (50%) was observed with introduction of clay and silanized PP to PP matrix.

Roh *et al.* [119] examined the role of reinforcing graphite nano-platelets (GNPs) and polypropylene grafted with maleic anhydride (MAH-g-PP) into polypropylene (PP) on the properties of resulting system. Nanocomposites with constant concentration of GNPs

(8 wt. %) and varying concentration of MAH-g-PP (0–20 wt. %) were prepared with PP as the matrix.

For composite fabrication, the constituents (PP, GNPs, and MAH-g-PP) were hand-mixed. The mixture was melt-compounded in a screw extruder (210 ℃, 350 rpm). The extrude was quenched and then chopped. Finally, the chopped pellets were moulded using an injection moulding machine (220 ℃, 120 MPa, 15 s).

Addition of MAH-g-PP (10 wt. %) and GNPs (8 wt. %) showed maximum value of tensile strength (TS), flexural strength (FS), and flexural modulus (FM) of 27.7 MPa, 46.4 MPa and 2407.9 MPa respectively. The increase in properties over nanocomposites without MAP was 20%, 28.6%, and 11.8% in TS, FS, and FM respectively. However, for 20 wt. % of MAH-g-PP content, all properties showed a substantial decrease. Impact strength value decreased with increase in MAH-g-P content.

Tsuji *et al.* [120] provided surface modification to PP by coating 3-aminopropyltrimethoxysilane (ATS) silane agent onto PP (substrate). It was then modified using oxygen plasma treatment to examine the role of treatment on gas barrier properties of the system.

Initially, PP substrate (0.1 mm thick film) was treated for 30 s by bombarding it with plasma ions. ATS silane agent was coated on PP using a spin coater (3000 rpm, 60 s). Finally, radio frequency (RF) plasma equipment was used for the plasma treatment of this silane treated PP (ATS/PP). In this process of plasma treatment, the operating parameters included power of 200 W for 60 s at a pressure of 13.3 Pa and temperature value maintained below 50 ℃.

From oxygen permeation measurements, it was observed that gas barrier properties of the ATS/PP showed a 15 folds improvement after oxygen plasma treatment.

C) Surface modification of elastomer

Kaynak *et al.* [121] modified recycled rubber using different silane agents (SAs) for improved adhesion between the two components of epoxy-rubber system.

Seven different silane agents (Table 2.7) were used to modify the recycled rubber. Hardener (HY917), accelerator (DY062), and recycled rubber were used to prepare the composites.

SAs (2 wt. % of rubber) were dissolved in diethylether followed by mixing of rubber particles to the solution prepared. The solution was kept in an oven (50 ℃, 1 h) for solvent evaporation. Epoxy, hardener, and accelerator in weight ratio of 10:9:0.2 were mixed to form slurry. The

untreated/treated rubber particles (5 % by volume) were added to slurry and were hand mixed for 3–4 min. The slurry was transferred into moulds and kept in oven (90 ℃, 1 h) followed by curing (140 ℃, 3 h).

Table 2.7 Silane agents used and their designation [121].

S. No.	Silane agent	Designation
1.	Methyl tri methoxy silane	SA1
2.	Vinyl tri ethoxy silane	SA2
3.	3 Amino propyl tri ethoxy silane	SA3
4.	3 (Tri methoxy silyl) propyl methacrylate	SA4
5.	Hexa decyl tri methoxy silane	SA5
6.	Octa decyl tri methoxy silane	SA6
7.	Hexa decyl tri chloro silane	SA7

Addition of untreated rubber deteriorated all the mechanical properties. This deterioration was attributed to lack of compatibility of untreated rubber with epoxy. Silane treatment of rubber with some of the silane agents resulted in improved bonding of rubber particles with epoxy, and led to improvements in tensile properties of composites. Addition of rubber treated with SA2, SA3, and SA6 showed the highest increase in tensile properties of composites.

Pasbakhsh *et al.* [122] prepared epoxy nanocomposites containing halloysite nanotubes (HNT) and maleic anhydride (MAH) grafted ethylene propylene diene monomer (MAH-g-EPDM) to investigate the tensile characteristics of composites.

For surface modification, EPDM was mixed in a mixer (180 ℃, 60 rpm, 5 min) with MAH (2.5 wt. %), and dicymyl peroxide (DCP, 0.25 wt. %). HNT in varying concentration (0–100 phr) was added to epoxy. Nanocomposites were prepared by adding all the components to a two-roll mill (ambient temperature, 20 min) followed by compression moulding at 150 ℃.

Tensile strength of nanocomposites containing MAH-g-EPDM was higher for all clay loadings (except 100 phr) as compared to EPDM/HNT nanocomposites. This was attributed to improved bonding of HNT and EPDM as a result of compatibilization. Tensile strength of nanocomposite with 100 phr HNT concentration was almost similar for compatibilized and un-compatibilized systems due to non-uniform dispersion at high concentration of filler. For HNT loading above 10 phr, elongation at break decreased with addition of MAH-g-EPDM.

Satapathy *et al.* [123] synthesized composites from waste polyethylene (WPE), reclaimed rubber (RR), and flyash (FA) to examine the influence of silane treatment of flyash on the mechanical performance of composites.

RR (0–70 wt. %) was melt mixed with WPE (30–100 wt. %) using a brabender (180 ℃, 500 rpm, 5 min) followed by roll milling to prepare the sheets. Silane agent Si-69 was used to modify the surface of FA. Treated FA (50 wt. %)/untreated FA (10–50 wt. %) was added to WPE blend with RR (15 wt. %) and the constituents were melt mixed. Though RR concentration was varied in the range of 0–70 wt. % but it was observed that blends containing 15 wt. % of RR provided the best combination of mechanical properties. For further investigations, RR content was at 15 wt. % and FA concentration was varied. Maximum improvement was observed for 50 wt. % of FA concentration. The improvements observed were 15% and 30% in tensile and flexural strength respectively with addition of 50 wt. % FA to WR15-WPE system. With addition of silane treated FA, the improvement in properties enhanced significantly. The improvements observed were 30% and 70% in tensile strength and flexural strength respectively over WR15-WPE blends.

Zhou *et al.* [124] prepared ternary blends containing HDPE (high density polyethylene), MAH-g-EPDM (maleic anhydride grafted EPDM), and PA6 (polyamide-6) to investigate the mechanical performance.

Firstly, MAH and initiator DCP were dissolved in acetone and this solution was added to EPDM. The blends were then extruded and pelletized. The extrudate was heated and dissolved in xylene followed by cooling to room temperature. Finally, the MAH grafted EPDM was precipitated and filtrated.

PA6/MAH-g-EPDM/HDPE ternary blends displayed substantial improvements in elongation at break. Tensile and flexural properties of the blends decreased with addition of untreated/treated

EPDM. Impact performance of PA6 enhanced by a factor of 10 when taken in the ternary blend form.

Sarkawi *et al.* [125] investigated filler-to-filler and filler-to-rubber interactions in silica reinforced rubber to study the effect of surface treatment of rubber using silane agent. Silane agent used in the study was Bis(triethoxysilylpropyl) tetrasulfide. Three different types of rubber viz. natural rubber (NR), deproteinized rubber (DPNR), and skim rubber (SR) were used to prepare rubber-silica vulcanizates having silica (Ultrasil 7005). All ingredients were mixed in a mixer (60 rpm, 0.7 fill factor, 150 ℃, 14 min). Curatives were mixed to the mixture using a two-roll mill followed by curing (150 ℃) to prepare valcunizates.

TEM images of the system without silane showed cavities around the silica particles. These cavities represented weak interaction of silica and NR. Cavities were more clearly visible in DPNR and skim rubber systems without silane. With silane treatment, the interactions of silica and rubber were found to improve as was evident from absence of cavities in TEM images. Absence of cavities was associated with the improvement in adhesion of filler and rubber. For untreated NR and DPNR systems, the filler-to-filler interactions were strong. It was concluded that proteins were able to hydrophobize the silica surface and decreased filler-to-filler interactions.

Jantanasakulwong *et al.* [126] prepared two different blends of poly(butylene succinate) designated as PBS with (i) MAH-g-EPDM and the other with (ii) MAH-g-EB (i.e. MAH grafted ethylene-1butene copolymer).

PBS and elastomer were taken in weight ratio of 40:60 and blended using melt mixing method (160 ℃, 100 rpm, 10 min).

Low modulus values were observed for PBS/MAH-g-EB blend over PBS/MAH-g-EPDM. However, strain recovery was better for PBS/MAH-g-EB blend. Strain recovery values were 40%, 70%, and 20% for PBS/MAH-g-EPDM, PBS/MAH-g-EB, and PBS respectively. Elongation at break/tensile strength values for both the modified systems were lesser than the values for PBS.

Bazli *et al.* [127] prepared nanocomposites using silicone rubber (SiR), EPDM, and Cloisite 15 A (nanoclay) using melt compounding with the help of a two-roll mill. The influence of nanoclay addition and MAH grafting of EPDM on the visco-elastic behaviour of the system was investigated.

For MAH grafting of EPDM, the initiator DCP (0.1 phr) and the compatibilizer MAH (2 phr) were mixed in an internal mixer (130 ℃, 50 rpm, 2 min). Un-grafted/grafted EPDM and nanoclay in varying loading (3, 6, and 9 phr) were mixed using a two-roll mill (50 ℃, 3 min). SiR was added to the mixture along with DCP (1 phr) with the help of two-roll mill (15 rpm, 2 min) followed by compression moulding (160 ℃, 15 min) and curing (150 ℃, 2 h).

Incompatibility of SiR and nanoclay led to agglomeration of clay. System with treated/untreated EPDM having 9 phr clay showed a linear viscos-elastic behaviour for a strain rate up-to 25%. These observations were evident of good adhesion between clay and EPDM. However, the compatibilizing effect was observed only when clay was present in the blends.

Combination of intercalated and exfoliated clay morphology in EPDM and agglomeration in SiR was observed through XRD analysis. Presence of MAH as compatibilizer in the system improved the dispersion of filler in SiR/EPDM blend composites. Interfacial tension between the rubbers was notably reduced with addition of either clay or MAH-g-EPDM. However, the effect of clay addition was more pronounced.

Table 2.8 summarizes the literature on surface modification procedures used for polymer/ elastomer fillers reinforced in composites.

Table 2.8 Summary of literature on surface modification procedures used for polymer fibers or elastomer fillers reinforced in composites.

S. No.	Summary	References
1.	**Surface modification of PET**	
	(a) Several researchers have worked on the surface modification of PET fibers for enhanced fibre/matrix adhesion in the resulting composites. The surface modification procedures for PET fibers reported in literature include oxygen-plasma treatment, alkaline hydrolysis using NaOH aqueous solution, UV/ozone surface modification procedure, corona discharge treatment.	Teh *et al*., [105]; Khanchaitit and Aht-Ong [106]; Jindal [107]; Raturi [108]; Cioffi *et al*., [111]; Blazquez *et al*., [112]; Liu *et al*., [113]; Hadhjizadeh *et al*., [128].
	(b) Limited research is available that reports on surface modification of PET fibers using silane coupling agents for improved fiber-matrix interfacial adhesion in composite systems. Apart from this, a few researchers have utilized silane treatment for improving the reactivity and water repellence of PET.	Demir *et al*., [110]; Fadeev and Mc Carty [129]; Kusuktham *et al*., [130]; Goh *et al*., [131].
2.	**Surface modification of PP**	
	Researchers have reported on the role of surface modification of PP fibers on the impact, tensile, flexural, and barrier properties of PP/epoxy and PP/nanoclay composites. Two main compatibilization procedures have been used for surface modification of PP fibers. These include (i) silane treatment, and (ii) MAH grafting. For MAH grafting of PP fibers, a few authors have also compared the effectiveness of photo initiated MAH grafting with thermally initiated MAH grafting.	Jiang *et al*. [114]; Pan *et al*., [115]; Abacha and Fellahi [116]; Aboudzadeh *et al*., [117]; Castel *et al*., [118]; Roh *et al*., [119]; Tsuji *et al*., [120]; Paunikallio *et al*., [132]; Zhou *et al*., [133]; Jiang *et al*., [134]; Hujuri *et al*., [135]; Igarza *et al*., [136].
3.	**Surface modification of elastomers** Researchers have mainly used two main compatibilization procedures for surface modification of elastomers. These include (i) silane treatment, and (ii) MAH grafting. Surface modification of elastomer reinforcement has been reported to result in improved interfacial adhesion among various constituents of composites. Different researchers have reported improvements in various properties viz. impact strength, tensile properties, flexural properties, and fracture toughness because of the improved interfacial adhesion.	
	(a) Researchers have used various silane coupling agents for compatibilization (surface modification) of elastomer fillers and reported improved interfacial adhesion of elastomer with the matrix (epoxy, waste polyethylene/flyash etc.).	Kaynak *et al*., [121]; Satapathy *et al*., [123]; Sarkawi *et al*., [125].
	(b) Researchers have used MAH grafting onto EPDM surface and reported improved interfacial adhesion of MAH grafted EPDM with the matrix of composite systems including EPDM/nanoclay, silicon rubber/EPDM/nanoclay, polyamide/EPDM/HDPE, PBS/EPDM, composite systems.	Pasbaksh *et al*., [122]; Zhou *et al*., [124]; Jantanasakulwong *et al*., [126]; Bazli *et al*., [127].

2.6. GAPS IN THE EXISTING LITERATURE

The detailed review of literature carried out in this research work (as discussed in the above sections) presents the following main gaps in the existing literature:

a) For epoxy based polymer matrix composites containing clay as the nano-filler (i.e. epoxy-clay nanocomposites), several processing techniques (slurry compounding, in-situ polymerization, melt mixing etc.) and various mixing methods (mechanical mixing, shear mixing, hand stirring, high-speed homogenizing, etc.) have been discussed in literature for different epoxy-clay nanocomposites. However, in most of the reported work, these techniques/methods have not been compared on similar materials to evaluate their relative performance.

b) For epoxy based polymer matrix composites, very limited work has been reported using PET fibers as the reinforcement. A few authors have modified epoxy-clay nanocomposites with reinforcement of PET fibers and reported improvements in tensile properties and impact performance. However, PET fiber reinforcement in epoxy based GFRPs has not been reported.

c) For epoxy based polymer matrix composites, very few authors have discussed the effect of PP fiber addition on mechanical and thermal properties of epoxy/PP fiber and epoxy/PP/ carbon fiber composite systems. No work has been reported on the role of PP fibers in epoxy-clay based nanocomposite systems and epoxy based GFRPs.

d) For epoxy based polymer matrix composites, several authors have studied the effect of elastomer addition to epoxy, epoxy-clay, and epoxy-GFRP based composites and reported improvements in strain at break, fracture toughness etc. However, to the best of researcher's knowledge, epoxy based GFRPs containing both, clay and elastomer, have not been investigated.

e) Several researchers have discussed surface modification procedures for polymeric filler (PET, PP)/elastomer modified composites for improved fiber/matrix interfacial adhesion. However, limited literature is available reporting on compatibilization (surface modification procedures) of the fillers in epoxy-clay nanocomposites or epoxy based GFRPs.

The next chapter presents design of the present experimental work. It discusses in detail the origin of present research, objectives and key issues, and the materials and methods used in the research work.

CHAPTER 3

DESIGN OF THE STUDY

3.1 GENERAL

This chapter discusses the establishment of research objectives on the basis of limitations in the reviewed literature. The chapter also discusses the details of materials to be used for the research work, the key issues, and the methodology. In addition to this, the details of equipment used for fabrication, testing, and characterization have also been discussed.

3.2 NEED OF THE PRESENT WORK

It has been observed from the reviewed literature that epoxy based glass fiber reinforced polymers (GFRPs) find extensive applications as structural composites due to their good static mechanical properties. However, the brittleness induced in such composites due to cross-linking of epoxy limits their use in applications such as vault poles, racing car bodies, bumpers of cars, ship hull frames, masts, propeller shafts, etc. which are subjected to impact load during their operation [15–18, 22]. Such applications require high toughness along with good static properties for superior performance [21, 22, 25, 26]. Significant efforts have been made to improve the toughness/impact strength of epoxy based composites by addition of clay or polymer fillers like PP/PET or an elastomer. Though addition of clay has been reported to improve almost all the properties of epoxy, the impact strength has not shown significant improvement [35–39]. Further, addition of elastomers to GFRPs has been reported to show significant toughening of epoxy but other properties such as tensile strength etc. show significant deterioration [29, 40, 41]. So it was observed from literature review that addition of clay leads to significant improvements in static properties and addition of polymeric filler/elastomer leads to improved toughness of epoxy. Therefore it was considered that, combining both, reinforcement of clay and soft polymer filler/elastomer in epoxy based GFRPs may provide a new route for high impact strength along with good tensile properties. Thus, in the present work, nanoclay reinforcement along with soft and ductile polymer/elastomer filler were used in epoxy based GFRP system to obtain high impact strength along with good tensile properties.

However, the key to improved properties of composite system lies in good compatibility among various constituents i.e. improved interfacial adhesion of constituents at the interface of the composite system [19, 52, 137]. Thus, for such complex systems combining multi-scale reinforcement (clay as nano-filler and polymer fiber/elastomer filler as micro-filler), compatibility among various fillers is very important. With regards to compatibility, literature reports on the various surface treatment procedures used in various polymer systems. These include NaOH treatment, corona discharge treatment, ozone treatment, silanization, and maleic anhydride (MAH) grafting. These procedures, in general, have been successful in modifying the surface of polymer/elastomer fillers [105, 106, 110–113, 115–117, 120, 128, 130–135, 138, 139]. Among the above-mentioned treatments, silane treatment and MAH grafting are reported to be more effective, and thus are commonly used for various types of fillers in different polymeric systems.

In the light of aforesaid, in the present research work, epoxy based GFRP nanocomposites (epoxy/clay/glass fiber nanocomposite systems) were modified through an addition of thermoplastic fibers/elastomers as additional fillers for enhanced impact strength. For improving compatibility, silane treatment and UV-assisted MAH grafting of polymer/elastomer filler was also studied.

The present work investigated the combined effect of nanoclay and polymer/elastomer addition on the mechanical properties (mainly impact strength) of epoxy based GFRPs. Polypropylene (PP) fibers, polyethylene terephthalate (PET) fibers, and ethylene propylene diene monomer (EPDM) rubber particles were used separately as the second filler in epoxy based GFRPs containing nanoclay as the first filler. These thermoplastic fibers/elastomers are low-cost, light-weight, and ductile with regards to the brittle epoxy matrix.

The novelty of the present research work is that proper compatibilization of polymer/elastomer filler added as a reinforcement results in significant improvements in impact strength of epoxy based GFRPs without any appreciable loss in tensile properties. Such nanocomposites with improved impact strength would find applications in a wide range of products ranging from electronics goods to aviation industry where traditionally only GFRPs are used.

3.3 OBJECTIVE

The overall objective of the present research was to '*improve the mechanical properties of epoxy/clay/glass fiber nanocomposites (mainly impact strength) with an addition of polymer fiber or/and elastomer through selection of an optimum composition'.*

The key issues to meet the overall objective were as follows:

- To synthesize epoxy/clay/glass fiber nanocomposites with varying concentrations of polymer fiber or/and elastomer content.
- To optimize the content of polymer fiber or/and elastomer in the polymer matrix nanocomposites to attain optimum combination of mechanical properties (with main focus on impact strength).
- To characterize the fabricated nanocomposites through various characterization techniques for correlating the structure and morphology with processing and properties.

3.4 METHODOLOGY

The constituents of the nanocomposites processed in the present study and their range of concentrations are shown in Table 3.1. The procedure adopted for processing, testing, and characterization of epoxy based GFRP nanocomposites is as follows:

a) Processing of GRPPs

— Nanoclay was dispersed into the base resin using a homogenizer (20,000 rpm; 10 min) and ultrasonicator probe (amplitude: 80%; pulse on time: 40 s, pulse off time: 20 s).

—Thermoplastic fibers (PP fibers, PET fibers) and elastomer filler (EPDM rubber particles) were compatibilized (silane treatment, UV-assisted MAH grafting) using procedures as per supplier recommendations and/or details reported in literature.

— Treated/untreated thermoplastic fibers were added to the resin system by mechanical stirring (500 rpm; 10–15 min). Treated/untreated EPDM rubber was added to the base resin with the help of a homogenizer (20,000 rpm; 10 min).

Table 3.1. Constituents of the epoxy based GFRP nanocomposites synthesized in the present work.

S. No.	Constituents of GFRP nanocomposite system	Specifications	Concentration/quantity used in GFRP nanocomposite system	Compatibilization treatment used for thermoplastic fibers/elastomer filler
1.	***Nano-clay***	Cloisite®15A (OMMT); Sheet thickness: 1nm; Platelets aspect ratio (l/w): 200– 400	1.0 phr	No compatibilization treatment was used. However, the clay used was an organically modified clay
2.	***Glass fibers***	E-Glass fiber; Cross-weaved mat	(i) 2 mat layers each for tensile test specimens (ASTM D3039) (ii) 12 mat layers for impact test specimens (ASTM D256–02)	No compatibilization used
3.	***Polymer fibers/Elastomer filler***			
a)	Polyethylene terephthalate (PET)	PET fibers; 3.0 mm length	0–3 phr concentration *(in increments of 1 phr)*	Treatment with a) MS# silane agent b) VS* silane agent c) UV-assisted MAH grafting
b)	Polypropylene (PP)	PP Fibers; 3.0 mm length	0–3 phr concentration *(in increments of 1 phr)*	Treatment with a) MS# silane agent b) VS* silane agent c) UV-assisted MAH grafting
c)	Elastomer	Ethylene propylene diene monomer (EPDM) rubber	0–10 phr concentration *(in increments of 2.5 phr)*	Treatment with a) BS* silane agent b) UV-assisted MAH grafting
4.	***Epoxy***	Araldite	Balance	----------

- ***phr***: per hundred resin (by weight); ***MS#***: ɣ-methacryloxypropyltrimethoxysilane; ***VS****: vinylytriethoxysilane; ***BS****: bis-(3-triethoxysilyl-propyl)-tetrasulfane

— Hardener was added to this modified resin system by vigorous stirring with the help of a mechanical stirrer (500 rpm; 10 min).

— Suspension prepared was used with glass fiber mat to fabricate the epoxy based glass fiber reinforced nanocomposites by vacuum assisted hand lay-up method using a VARIM *set-up* (Vacuum Assisted Resin Infusion Moulding).

b) Testing of GFRPs

— Mechanical properties (impact strength, tensile strength, and tensile modulus) of various nanocomposite sheets were evaluated to determine the optimal composition of constituents of nanocomposites i.e. optimum concentration of PET fibers, PP fibers, EPDM rubber in the nanocomposite system. The compatibilization procedures were also optimized.

c) Characterization of materials and GFRPs

— Prepared nanocomposites (and treated thermoplastic fibers) were characterized using XRD, FTIR, SEM-EDS, TEM etc. to ascertain the dispersion of nanoclay and also to understand the structure-processing-property relationship.

The details of these procedural steps are available in Section 3.6.

3.5 MATERIALS

The epoxy matrices used in the present research were diglycidyl ether of bisphenol-A (DGEBA) based resins. Epoxy resin 'Araldite LY 1564' with a density of 1.1–1.2 g/cm^3 (at 20 ℃) and viscosity of 1200–1400 mPa.s (at 25 ℃) and hardener 'Aradur 3486' were used for polypropylene (PP) and polyethylene terephthalate (PET) reinforced nanocomposites. For elastomer reinforced nanocomposites, epoxy resin 'Araldite CY-230' having a density of 1.1–1.2 g/cm^3 (at 20 ℃) and viscosity of 1350–2000 mPa.s (at 25 ℃) was used as the matrix material and 'HY-951'was used as the hardener. These were supplied by Huntsman Advanced Materials (India) Pvt. Ltd. An organically modified clay Cloisite®15A (Nanoshell, USA) was used as the nano-filler. Glass fiber reinforcement was in the form of E-glass fiber mat, 'Advantex® WR360' (Owens Corning Inc., India).

For polymer reinforcement, PP fibers of 3 mm length and PET fibers of 3 mm length were supplied by Reliance Industries Ltd, India. For elastomer reinforcement, ethylene propylene diene monomer

rubber (EPDM) having particle size of 400 µm was used. The elastomer particles were supplied by Arihant Oil and Chemicals, India. Further, for surface treatment of polymer/elastomer fillers, the two silane agents namely γ-methacryloxypropyltrimethoxysilane (MS) and vinylytriethoxysilane (VS), and the maleic anhydride (MAH) granules used for MAH grafting were supplied by TCI Chemicals (India) Pvt. Ltd. The third silane agent used for EPDM rubber particles was 'bis-(3-triethoxysilyl-propyl)-tetrasulfane' (BS) and was supplied by Chemtech India Pvt. Ltd., India.

3.6 PROCESSING OF EPOXY BASED GFRP COMPOSITES

Epoxy resin having an epoxide group, 'diglycidyl ether of bisphenol-A' (DGEBA) is one of the most widely used epoxies. For fabrication of composites, epoxy resin is mixed with hardener (amine hardener was used in the present study). On mixing with hardener, the resin gets polymerized by a cross-linking reaction between resin and hardener.

The detailed procedure for processing of composites is described as follows:

3.6.1 Preparation of epoxy-hardener system

Epoxy resin and curing agent were weighed in pre-determined amounts and were placed in separate beakers. Curing agent (hardener) was added to epoxy resin and mixed for 10 min at 500 rpm with the help of a mechanical stirrer. The mixture was kept in a desiccator (connected to a vacuum pump) and was degassed for 30 min to remove any entrapped air. Figure 3.1 shows the equipment used for processing of epoxy-hardener system.

Figure 3.1 Desiccator with vacuum pump used in the present work.

3.6.2 Dispersion of nanoclay into epoxy resin

Nanoclay was taken in an amount equivalent to 1 phr (per hundred resin by weight) and was mixed to epoxy by homogenization (T25 IKA Inc.) at a speed of 20,000 rpm for 10 min. The suspension was further subjected to ultrasonication (700W; 80% amplitude; pulse on time: 40 s, pulse off time: 20 s) for 10 min using a probe sonicator (QSonica Q-700). To prevent rise in temperature during sonication, the beaker containing the suspension was kept in an ice-water bath. Finally, the suspension was subjected to degassing for 30 min. Figure 3.2 shows the equipment used for dispersion of nanoclay into the epoxy resin.

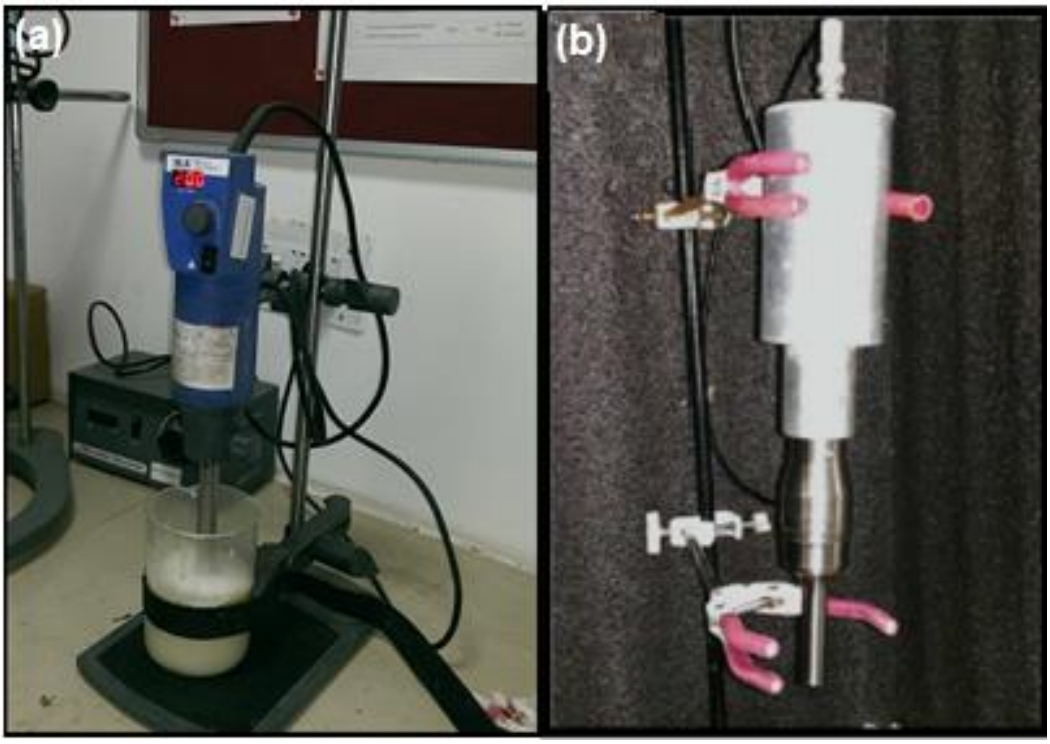

Figure 3.2 a) Homogenizer and b) ultrasonicator probe used in the present work.

3.6.3 Compatibilization of fillers

For surface treatment, polymer/elastomer fillers were treated with specific compatibilizers. The compatibilized fillers were then used as reinforcement for composite fabrication. For polymeric fillers (PP and PET), two separate silane agents (i) γ-methacryloxypropyltrimethoxysilane (MS) and (ii) vinylyriethoxysilane (VS) agents were selected for surface treatment [110, 117, 118, 130, 140, 141]. For elastomer filler (EPDM rubber particles), surface treatment was done using bis-(3-triethoxysilyl-propyl)-tetrasulfane silane agent [58,125,142,143]. Further, polymer/elastomer

fillers were also treated using maleic anhydride (MAH) grafting. However, MAH grafting of polymer/elastomer fillers was not done for all the nanocomposites. Nanocomposites reinforced with MAH grafted fillers were fabricated only for specific filler concentrations. Polymer/elastomer filler concentration at which silane treatment resulted in maximum improvement in impact strength of nanocomposites (for each case of PP, PET, and EPDM reinforcement) were selected for MAH grafting of fillers.

3.6.3.1 Compatibilization of fillers using silane treatment

Silane agents are multi-functional chemicals in which one end forms bond with an organic surface and the other end forms bond with an inorganic surface [130,144–146]. Thus, in the present study, silane treatment of fillers was done to improve the compatibility of these polymer/elastomer fillers with other constituents of the GFRP nanocomposites. Silane treatment of polymer/elastomer fillers was done as per the supplier recommendations. For this, ethanol solution (95%) with water was used. The pH of the ethanol solution was adjusted to be in the range of 4.5–5.5 by adding acetic acid. Silane agent was added to the ethanol solution (in an amount equivalent to 2% volume of ethanol solution). Polymer/elastomer fillers to be treated were dipped in the prepared ethanol-silane solution and allowed to react for 5 min. After the reaction, the fillers were rinsed twice with ethanol to remove the excess silane/unreacted silane. The treated and rinsed fibers were then cured in oven at 110 ℃ for 10 min. These silane treated fillers were used as reinforcement in the GFRP formulations.

3.6.3.2 Compatibilization of fillers using MAH grafting

Maleic anhydride (MAH) is a poly-functional monomer which on being grafted to polymer/elastomer surface improves its adhesion with polar constituents (viz. epoxy etc.) of the composite system [147–149]. MAH on being exposed to UV radiations transforms to excimer. The MAH excimer can abstract hydrogen atoms from polymer/elastomer filler molecules which induces cross-linking reaction leading to grafting of substrate with MAH [148, 150]. Thus, in the present study, UV-assisted MAH grafting was employed for compatibilization of polymer/elastomer fillers. For the UV-assisted MAH grafting, the exposure/treatment time of fillers to UV radiations had to be optimized because excessive exposure to UV radiations is expected to damage the filler [105]. Initially, four different exposure time periods (10, 20, 30, and

40 h) were taken for UV-assisted MAH grafting of polymer fillers [115, 151]. Thereafter, for each polymer/elastomer filler, an optimum exposure time was determined.

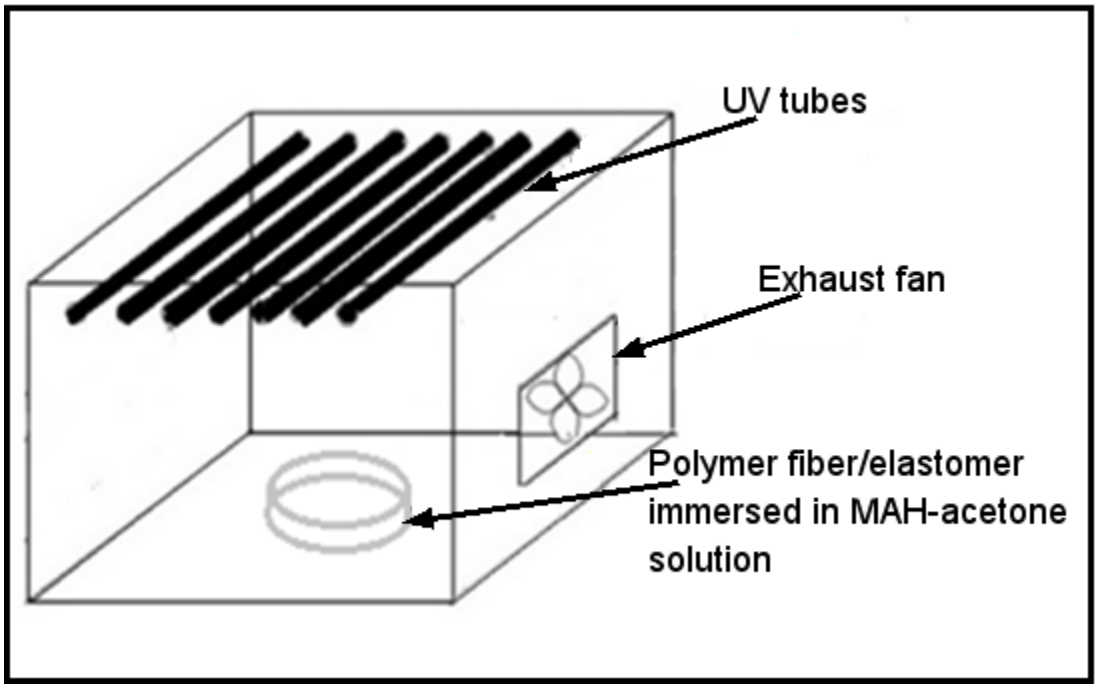

Figure 3.3 Schematic of UV *set-up* used for MAH grafting.

For MAH grafting, maleic anhydride (taken in an amount equivalent to twice the weight of filler) was dissolved in acetone. The required amount of fillers were kept in a petri dish and were completely immersed in MAH-acetone solution. This solution was exposed to ultraviolet radiations. For this, the dish was kept in a UV apparatus for UV-assisted MAH grafting. The UV apparatus as shown in Figure 3.3 consisted of 7 UV tubes of 36 W each. The distance of dish from the UV tubes was kept constant at 30 cm for the entire study. MAH grafted samples were rinsed with acetone to remove the excess/un-grafted MAH. The treated fibers were weighed to calculate the weight gain. Samples treated for the time period showing maximum weight gain were selected for reinforcement.

A) Optimum exposure time for MAH grafting of PP fibers

The exposure time to UV-radiations had to be optimized because excessive exposure to radiations was expected to damage the fillers. To determine the optimum treatment time for UV-assisted MAH grafting of PP fibers, four different exposure time periods (10, 20, 30, and 40 h) were

investigated [115, 151]. The treatment time for which the fibers showed maximum weight gain after MAH grafting was considered as the optimum exposure time. Table 3.2 shows the percentage weight gain by PP fibers after MAH grafting for different exposure time periods. Maximum weight gain was observed for treatment time of 30 h (Table 3.2). Thus, PP fibers (dipped in MAH-acetone solution) exposed to UV-radiations for a treatment time of 30 h were used as reinforcement for fabrication of MAH grafted PP fiber reinforced nanocomposites.

Table 3.2 Weight gain by PP fibers as a function of exposure time during UV-assisted MAH grafting.

Grafting time (h)	Initial weight before grafting (g)	Final weight after grafting (g)	Weight gain by PP fibers (g)	Percent weight gain by PP fibers (%)
10	2.00	3.31	1.31	65.5
20	2.00	3.88	1.88	94.0
30	**2.00**	**4.18**	**2.18**	**109.0 (max.)**
40	2.00	3.21	1.21	60.5

B) Optimum exposure time for MAH grafting of PET fibers

To determine the optimum treatment time for UV-assisted MAH grafting of PET fibers, the fibers were initially exposed to UV rays for four different time periods of 10, 20, 30, and 40 h respectively [115, 151]. The treatment time for which the fibers showed maximum weight gain after MAH grafting was considered as the optimum exposure time. Table 3.3 shows the weight gain by PET fibers after UV-assisted MAH grafting for time periods in the range of 10–40 h.

Table 3.3 Weight gain by PET fibers as a function of exposure time (10–40 h) during UV-assisted MAH grafting.

Grafting time (h)	Initial weight before grafting (g)	Final weight after grafting (g)	Weight gain by PET fibers (g)	Percent weight gain by PET fibers (%)
10	**2.00**	**2.80**	**0.80**	**40**
20	2.00	2.58	0.58	29
30	2.00	2.50	0.50	25
40	2.00	2.35	0.35	17.5

For this the fibers were again subjected to UV-assisted MAH grafting with exposure time in the range of 1–10 h (Table 3.4). Optimum exposure time for MAH grafting of PET fibers was determined as 8 h.

Table 3.4 Weight gain by PET fibers as a function of exposure time (1–10 h) during UV-assisted MAH grafting.

Grafting time (h)	Initial weight before grafting (g)	Final weight after grafting (g)	Weight gain by PET fibers (g)	Percent weight gain by PET fibers (%)
1	2.00	2.08	0.08	4
2	2.00	2.12	0.12	6
3	2.00	2.24	0.24	12
4	2.00	2.47	0.47	24
5	2.00	2.62	0.62	31
6	2.00	3.00	1.00	50
7	2.00	4.35	2.35	117.5
8	**2.00**	**5.00**	**3.00**	**150 (max.)**
9	2.00	3.42	1.42	71
10	2.00	2.80	0.80	40

C) Optimum exposure time for MAH grafting of EPDM particles

The same procedure was followed to determine the optimum treatment time for UV-assisted MAH grafting of elastomer particles. Maximum weight gain was observed for treatment time of

20 h (Table 3.5). Thus, EPDM particles exposed to UV-radiations for a treatment time of 20 h were used as reinforcement for fabrication of MAH grafted EPDM reinforced GFRP sheets.

Table 3.5 Weight gain by EPDM particles as a function of exposure time during UV-assisted MAH grafting.

Grafting time (h)	Initial weight before grafting (g)	Final weight after grafting (g)	Weight gain by EPDM particles (g)	Percentage weight gain (%)
10	4	6	2	50
20	**4**	**9**	**5**	**125 (max.)**
30	4	8	4	100
40	4	7	3	75

3.6.4 Preparation of epoxy-clay-filler suspension

Pre-determined amounts of treated/untreated polymer fibers were added to the epoxy resin/clay suspension and mixed with the help of mechanical stirrer (500 rpm; 15 min). For mixing EPDM to epoxy resin/clay suspension, homogenization was done (20,000 rpm; 10 min).

Finally, the stoichiometric ratio of hardener was added to the epoxy resin/clay/filler suspension as described in Section 3.6.1. Fabrication of epoxy based GFRP laminates was done using vacuum assisted hand lay-up technique on a VARIM *set-up* as described in the next section.

3.6.5 Fabrication of epoxy based GFRPs

Glass fibers were cut (from the glass fiber mat roll) as per the required dimensions so that four tensile specimens (as per ASTM D3039) and four impact specimens (as per ASTM D256–02) were prepared for a given composition after fabrication of nanocomposite laminates. The sequence of steps followed for the preparation of epoxy based GFRP composites on the VARIM mold is described in Figure 3.4. In this process, the VARIM mold surface was cleaned (cleaning agent: PMC; Supplier: DBA Agencies Pvt. Ltd.) and the release agent (release agent: Freekote NC 770; Supplier: DBA Agencies Pvt. Ltd.) was applied. Connections of vacuum ports were made with the help of a breather cloth. The first layer of glass fiber mat was placed on the VARIM table and the prepared suspension (epoxy-clay-filler-hardener suspension) was applied by hand lay-up. Now the second layer of glass fiber mat was kept on the coated first layer and was again laid-up using hand lay-up. The processing was repeated for a number of mat layers as per the test requirements. For

tensile specimens, two layers of glass fiber mat were used and for impact specimens, 12 layers of glass fiber mat were used.

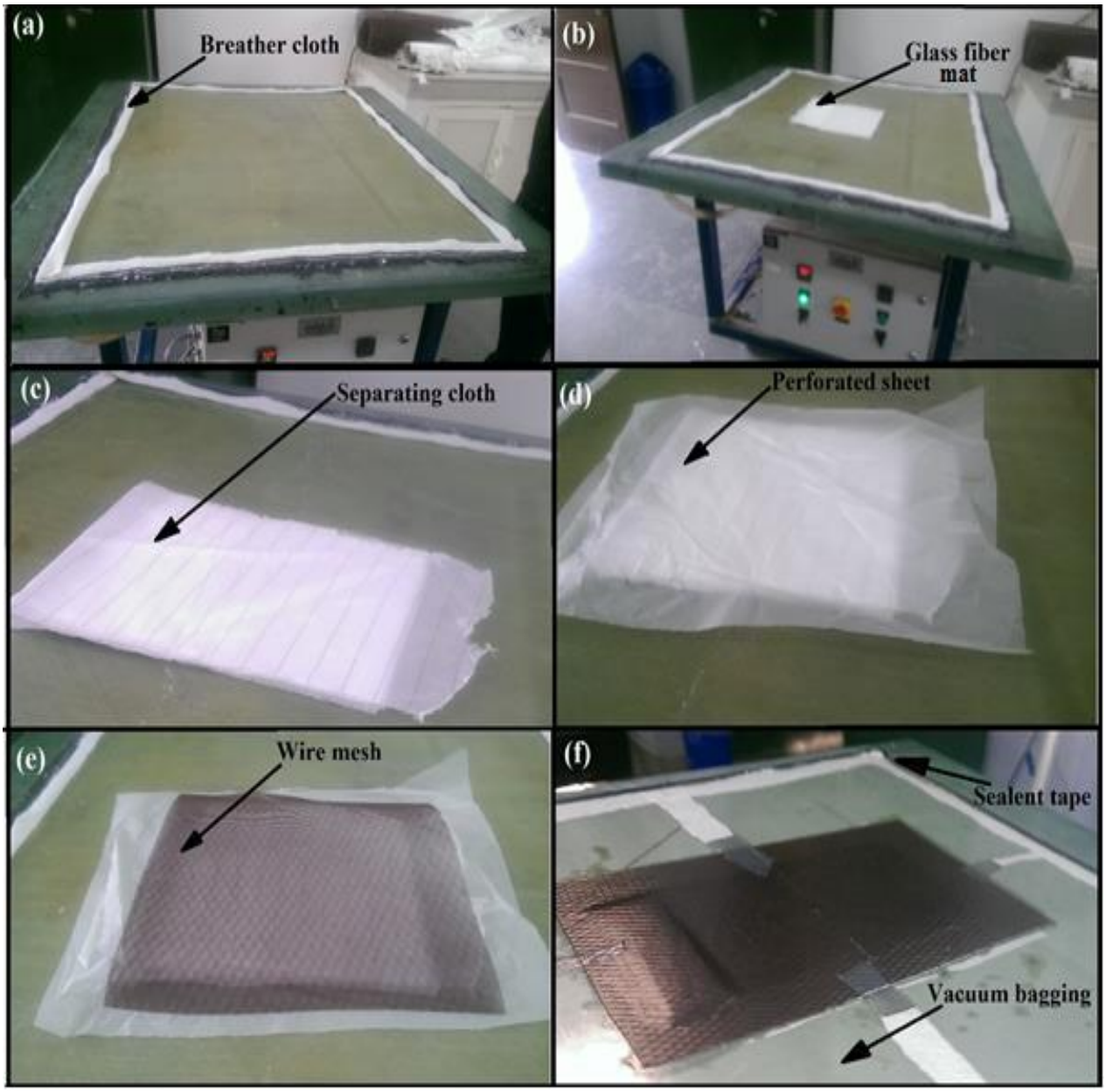

Figure 3.4 Procedure for fabrication of GFRP composites on the VARIM mold.

After the lay-up, the material was covered with a separating cloth. This was followed by spreading the perforated sheet, and finally the wire mesh over the materials system. The entire assembly was connected to vacuum port bridges with the help of a breather cloth. The VARIM table was covered with vacuum bagging film by fixing it on sides of the table using a sealant tape to provide air-tight

bagging. Vacuum pump was switched on to maintain a vacuum of the order of 1 mbar. Curing schedule as given by the supplier was followed. For the LY1564 resin, this included curing at 60 ℃ for 4 h followed by post-curing for 16 h at 60 ℃ without vacuum. For CY230 resin, this included curing at ambient temperature for 6 h with vacuum followed by post-curing at 60 ℃ for 6 h without vacuum.

The sample designations used for various nanocomposites processed in the present work are presented in Table 3.6.

3.7 TESTING AND CHARACTERIZATION

For each test (tensile and impact), the four specimens obtained for a given composition were tested and the average values were obtained. Also, error bar and standard deviation of values were calculated. Tensile tests were conducted with a crosshead speed of 2mm/min on a universal testing machine (UTM Z010 TN Proline, Zwick/Roell, Germany) having a load cell of 10 kN.

Izod impact testing was done on an impact testing machine (ATS FAAR, Italy) equipped with a load cell of 15 J. XRD (XPERTPro, JDX-8030, PANalytical, Almelo, Netherlands) and TEM (H-7500, Hitachi, Japan) analysis were used to ascertain the type of clay morphology (phase separated, intercalated, or exfoliated) obtained in the developed nanocomposites. For XRD, $0.6°min^{-1}$ and 0.1° were used as the scanning speed and step size respectively. The diffraction patterns were collected in the small angle range of 1–10°.

Further, to confirm the silanization treatment of fillers, SEM-EDS (scanning electron microscopy-energy dispersive spectroscopy) was used (JEOL JSM 6510LV, Japan). Similarly, to confirm MAH grafting on filler surface, SEM micrographs were analyzed. To confirm the MAH grafting on fillers, FTIR analysis was also conducted using FTIR Spectrometer (Perkin–Elmer FTIR Spectrometer RX-IFTIR, Massachusetts, USA) having a scanning range of 4000–400 cm^{-1}. In order to prepare the samples, the fibers/elastomer particles were mixed with potassium bromide (KBr). The mixture was pressed into a pellet and scanned in the range of 4000 to 400 cm^{-1} with resolution of 4 cm^{-1}.

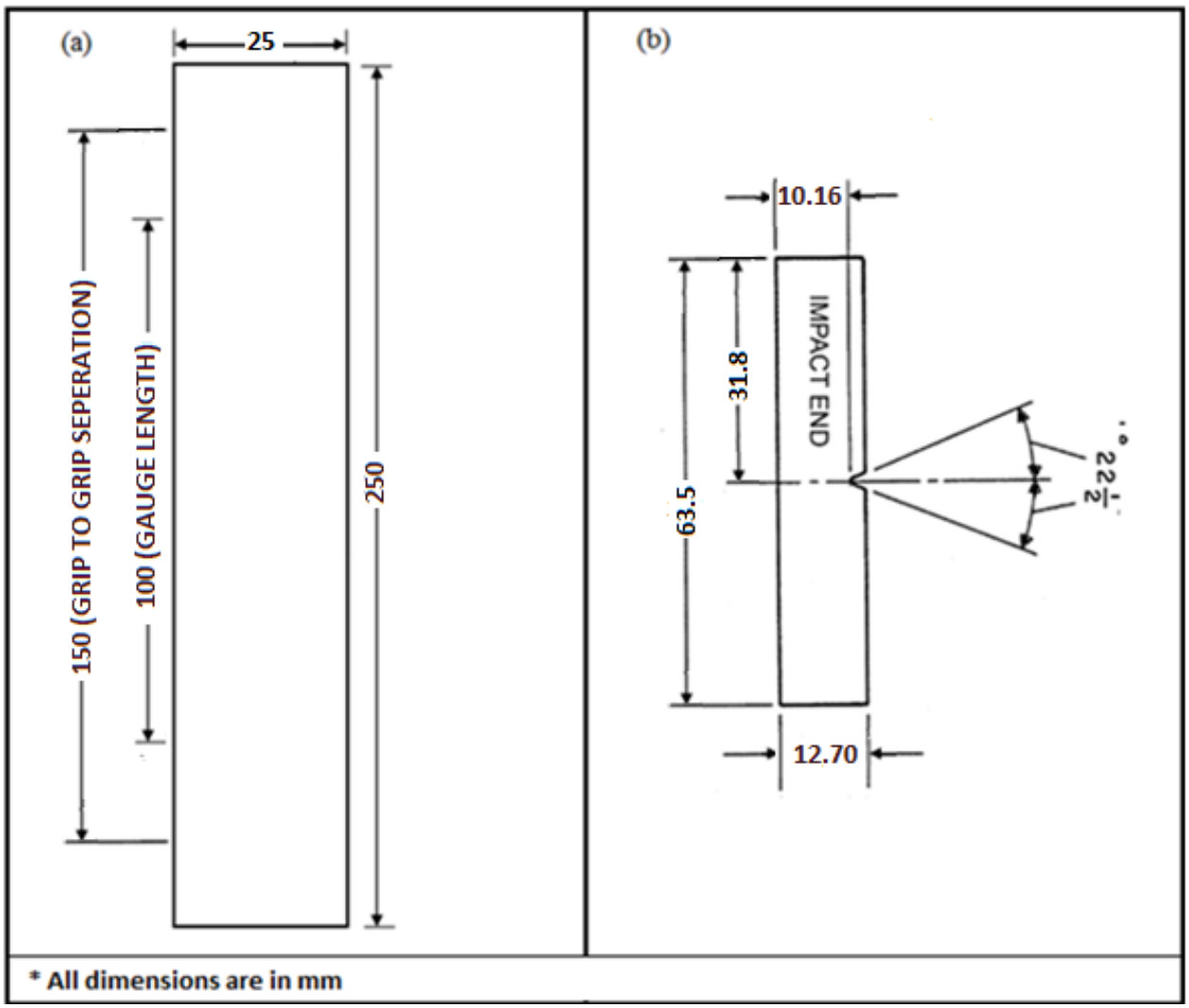

Figure 3.5 Schematic of a) tensile testing specimen and b) impact testing specimen.

Table 3.6 Sample designations used for various nanocomposites processed in the present work.

1.POLYMER FIBER (PP or PET) REINFORCED EPOXY BASED GFRP NANOCOMPOSITES		
SAMPLE DESCRIPTION	**SAMPLE DESIGNATION**	
A. REFRENCE SAMPLE		
Epoxy based GFRP without clay or polymer filler	**NE**	
B. GFRP NANOCOMPOSITE CONTAINING ONLY NANOCLAY		
Epoxy based GFRP with 1 phr clay without polymer fiber/elastomer filler	**E1C**	
C. POLYMER FIBER REINFORCED GFRP NANOCOMPOSITES WITH (GFRPs containing both nanoclay and polymer filler)	***PP fiber as reinforcement***	***PET fiber as reinforcement***
Epoxy based GFRP with 1 phr clay and 1 phr untreated polymer fiber	**E1C1PP**	**E1C1PET**
Epoxy based GFRP with 1 phr clay and 1 phr MS treated polymer fiber	**E1C1PPMS**	**E1C1PETMS**
Epoxy based GFRP with 1 phr clay and 1 phr VS treated polymer fiber	**E1C1PPVS**	**E1C1PETVS**
Epoxy based GFRP with 1 phr clay and 2 phr untreated polymer fiber	**E1C2PP**	**E1C2PET**
Epoxy based GFRP with 1 phr clay and 2 phr MS treated polymer fiber	**E1C2PPMS**	**E1C2PETMS**
Epoxy based GFRP with 1 phr clay and 2 phr VS treated polymer fiber	**E1C2PPVS**	**E1C2PETVS**
Epoxy based GFRP with 1 phr clay and 2 phr MAH grafted polymer fiber	**E1C2PPMAH**	**E1C2PETMAH**
Epoxy based GFRP with 1 phr clay and 3 phr untreated polymer fiber	**E1C3PP**	**E1C3PET**
Epoxy based GFRP with 1 phr clay and 3 phr MS treated polymer fiber	**E1C3PPMS**	**E1C3PETMS**
Epoxy based GFRP with 1 phr clay and 3 phr VS treated polymer fiber	**E1C3PPVS**	**E1C3PETVS**
2. ELASTOMER (EPDM) REINFORCED EPOXY BASED GFRP NANOCOMPOSITES		
A. REFRENCE SAMPLE		
Epoxy based GFRP without clay or elastomer	**NE_R**	
B. GFRP NANOCOMPOSITE CONTAINING ONLY NANOCLAY		
Epoxy based GFRP with 1 phr clay without polymer fiber/elastomer filler	**$E1C_R$**	
C. *ELASTOMER REINFORCED GFRP NANOCOMPOSITES (GFRP nanocomposites containing both nanoclay and elastomer filler)*		
Epoxy based GFRP with 1 phr clay and 2.5 phr untreated elastomer	**E1C2.5R**	
Epoxy based GFRP with 1 phr clay and 2.5 phr BS treated elastomer	**E1C2.5RS**	
Epoxy based GFRP with 1 phr clay and 5 phr untreated elastomer	**E1C5R**	
Epoxy based GFRP with 1 phr clay and 5 phr BS treated elastomer	**E1C5RS**	
Epoxy based GFRP with 1 phr clay and 5 phr MAH grafted elastomer	**E1C5RMAH**	
Epoxy based GFRP with 1 phr clay and 7.5 phr untreated elastomer	**E1C7.5R**	
Epoxy based GFRP with 1 phr clay and 7.5 phr BS treated elastomer	**E1C7.5RS**	
Epoxy based GFRP with 1 phr clay and 10 phr untreated elastomer	**E1C10R**	
Epoxy based GFRP with 1 phr clay and 10 phr BS treated elastomer	**E1C10RS**	

The next chapter presents the results and discussion with regards to impact strength and tensile properties displayed by epoxy-clay based GFRPs reinforced with polypropylene fibers i.e. the first type of micro-fillers chosen in the present research.

CHAPTER 4

RESULTS AND DISCUSSION OF POLYPROPYLENE FIBER REINFORCED GFRP NANOCOMPOSITES

4.1 GENERAL

This chapter presents the results of impact testing and tensile testing of PP fiber reinforced GFRP nanocomposites. The results of various characterization techniques utilized in the present research to ascertain (a) clay morphology in the nanocomposites (XRD and TEM analysis) and (b) the interfacial and chemical changes in surface morphology of PP fibers due to compatibilization treatment (SEM and FTIR analysis) have also been presented.

4.2 IMPACT STRENGTH

This section presents the results of impact testing of PP fiber reinforced GFRP nanocomposites. Table 4.1 shows the results of various mechanical properties evaluated for PP fiber reinforced GFRP nanocomposites.

The impact strength of epoxy based GFRP composite without nanoclay and PP fibers (reference sample, NE) was 161 kJ/m^2. On addition of 1 phr clay to the reference sample (i.e. E1C nanocomposite), a slight increase of 4% in impact strength (167 kJ/m^2) was observed. Further, on addition of untreated polypropylene fibers (PP) to this nanocomposite system, impact strength of the resulting nanocomposites viz. E1C1PP, E1C2PP, and E1C3PP (Table 3.6 provided details of these compositions) decreased (148 kJ/m^2, 149 kJ/m^2, and 129 kJ/m^2, respectively with an addition of 1 phr, 2 phr, and 3 phr untreated PP fibers). It is evident that impact strength deteriorated even on addition of a more ductile component i.e. untreated PP fibres. This may be attributed to lack of compatibility of PP fibers with other constituents of the composite system. For improving the compatibility, PP fibers were treated with two different silane agents separately viz. methacryloxypropyltrimethoxysilane (MS) and vinylytriethoxysilane (VS). The results showed that addition of silane treated PP fibers (as compared to untreated PP fibres) to the composite system significantly increased the impact strength of GFRPs for a given composition (Table 4.1 and Figure 4.1). Further, interestingly it was observed that for all cases with PP fiber reinforcement

(treated or untreated), the impact strength of GFRPs showed improvement till 2 phr PP fiber loading, and after this limit (i.e. for 3 phr PP loading), the impact strength deteriorated.

Table 4.1. Mechanical properties of PP fiber reinforced GFRP nanocomposites.

Sample Designation		Impact Strength (kJ/m^2)	Tensile Strength (MPa)	Tensile Modulus (MPa)
NE	*Avg**	161±2	269±3	7315±40
	s	4	7	81
E1C	*Avg**	167±15	313±6	7780±133
	s	30	12	265
E1C1PP	*Avg**	148±8	215±4	5410±20
	s	16	8	93
E1C1PPMS	*Avg**	178±8	292±3	6110±22
	s	16	6	43
E1C1PPVS	*Avg**	177±12	278±8	5970±58
	s	23	16	115
E1C2PP	*Avg**	149±13	247±8	5835±76
	s	25	17	152
E1C2PPMS	*Avg**	**232±21**	242±2	5225±86
	s	42	5	148
E1C2PPVS	*Avg**	185±8	258±2	5225±38
	s	16	4	76
E1C2PPMAH	*Avg**	181±1	266±8	6515±131
	s	2	17	262
E1C3PP	*Avg**	129±5	183±4	4385±136
	s	9	8	273
E1C3PPMS	*Avg**	150±6	215±10	4708±54
	s	11	19	108
E1C3PPVS	*Avg**	142±7	205±6	4415±64
	s	15	13	129

*Avg** = Mean value ± Range of values; *s* = Standard deviation of values

This decrease in impact strength of GFRP nanocomposites with 3 phr PP loading can be attributed to the poor dispersion of PP fibers in the composite system because of the concomitant high viscosity of resin at such high concentration (i.e. 3 phr). For such systems, poor dispersion leads to lower aspect ratio of aggregates, and thus, lowers the impact strength.

Impact strength of reference sample was significantly improved with addition of treated PP fibers (i.e. compatibilized PP fibers). Maximum improvement of 44% in impact strength was achieved for GFRPs with reinforcement of 2 phr MS treated PP fibers. Since, maximum improvement in impact strength was observed for 2 phr PP loading (E1C2PPMS), only this PP concentration was selected for the further study of PP fibers i.e. UV-assisted grafting of maleic anhydride (MAH) on PP fibers. When maleic anhydride grafted PP fibers were used as reinforcement (2 phr of MAH grafted PP fibers), the resulting GFRP (E1C2PPMAH) showed a significant improvement in impact strength (12%; second only to E1C2PPMS) as compared to the reference sample.

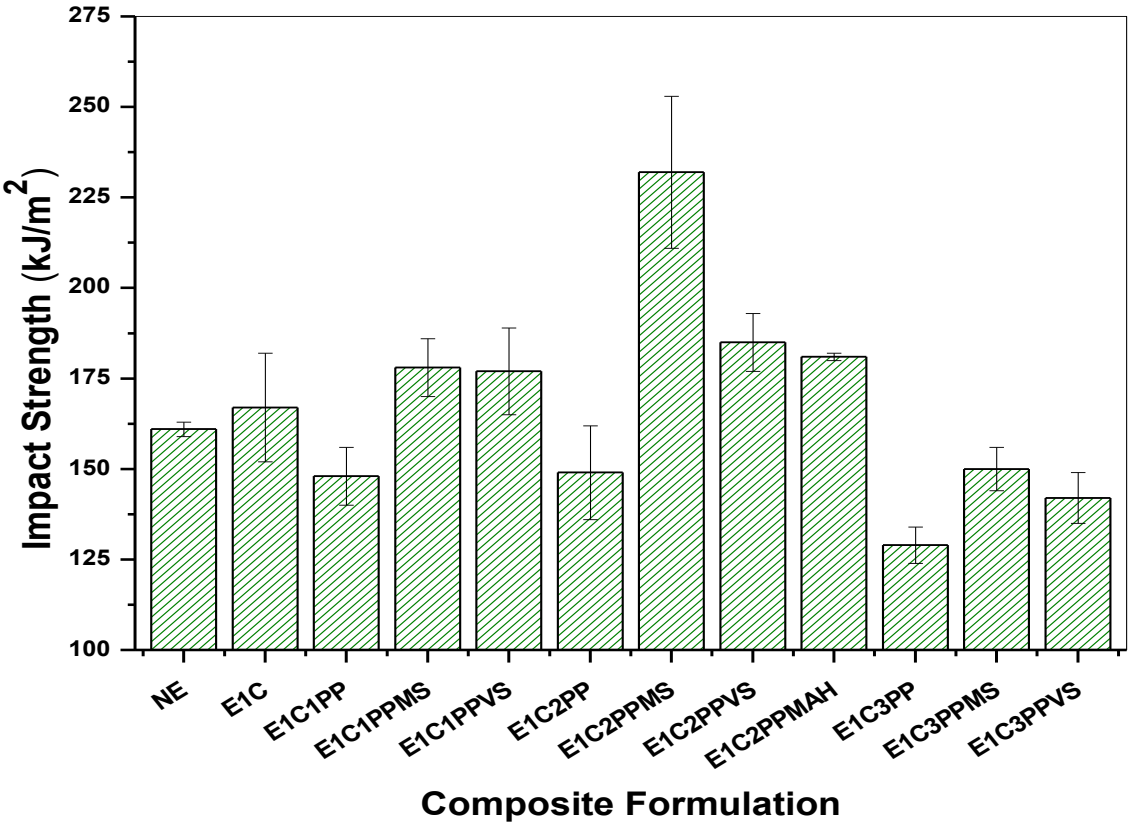

Figure 4.1 Impact testing results of PP fiber reinforced GFRP nanocomposites.

4.3 TENSILE PROPERTIES

The tensile strength and tensile modulus values of the reference sample were observed as 269 MPa and 7315 MPa, respectively. On addition of 1 phr clay to the reference sample (i.e. E1C nanocomposite), an increase of 16% and 6% in tensile strength and modulus respectively was observed. Further, on addition of untreated PP to this nanocomposite system (viz. E1C1PP, E1C2PP, and E1C3PP), tensile strength and modulus values of the resulting nanocomposites decreased. Significantly, addition of treated PP fibers, restored the tensile properties of nanocomposites in most cases (as compared to untreated PP fiber reinforced nanocomposites for a given composition); however, the values were below those for the reference sample (NE).

For the nanocomposite at which maximum improvement in impact strength was observed (i.e. E1C2PPMS), the tensile strength and modulus values were 4% and 28% lower as compared to the reference sample. However, for the optimum concentration of 2 phr PP fiber loading, the MAH grafted PP fiber reinforcement led to a recovery in tensile properties of nanocomposites. For this E1C2PPMAH nanocomposite, tensile strength value was almost the same and modulus value was 10% lower as compared to the NE composition. Thus, the objective of significantly improving the impact strength of epoxy based GFRPs with addition of soft/ductile second phase filler (here PP fibers) without considerable loss in tensile properties was successfully achieved. The optimized composition of GFRP combining 1 phr clay and 2 phr PP fiber treated with MS silane agent, showed a significant improvement of 44% in impact strength over the reference sample and a very slight drop in tensile strength. A detailed investigation was done to understand the reasons for the increase in the impact strength. These are discussed in the following sections (Section 4.4–4.7).

4.4 COMPATIBILIZATION

The main purpose of the present research was to enhance the impact strength of epoxy based GFRP nanocomposites. For improving the impact strength, second phase fillers in the form of PP fibers were added to the GFRP nanocomposite system containing nanoclay as the first filler. The results showed that addition of treated PP fibers (up to 2 phr) led to improvements in impact strength of the composite system. For nanocomposites reinforced with silane treated PP fibers, impact strength improvement was attributed to the improved compatibility between the inorganic glass fibers and the organic PP fibers. It is well reported in literature that silane agents can react with a variety of

materials (viz. organic and inorganic material surfaces via covalent bonds etc.) to increase the compatibility/coupling between them. Silane agents have two types of functional groups viz. hydrolyzable group (OR group) and organo-functional group (X group). The Si-OR bonds hydrolyze quickly with water (even with moist air) to make silanol Si-OH groups which condense and result in formation of Si-O-Si bonds. This allows chemical compatibilization of dissimilar material surfaces [152, 153]. Further, for MAH grafted PP fibers, there was improvement in impact strength with appreciable restoration of tensile properties of nanocomposites. The enhancement in impact strength was attributed to the improved bonding of MAH grafted PP fibers to the epoxy matrix. It is reported that functional groups of MAH grafted PP fibers react with the hydroxyl or epoxy groups of the epoxy resin [114, 134]. Figure 4.2 shows the schematic of possible coupling reaction of MAH grafted PP fibers with epoxy in the nanocomposite system.

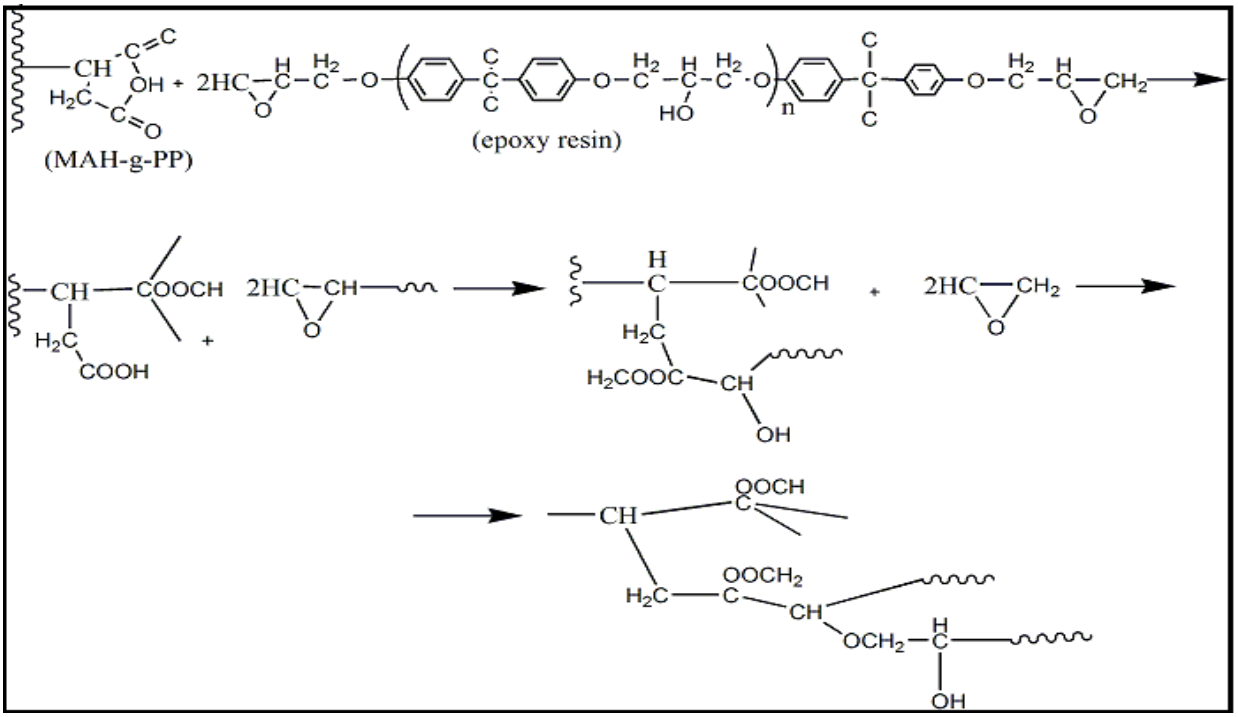

Figure 4.2 Schematic of coupling reaction between MAH grafted polypropylene and epoxy [134].

4.5 DISPERSION OF CLAY IN NANOCOMPOSITES

X-ray diffraction (XRD) and transmission electron microscopy (TEM) were conducted to examine the type of clay morphology (phase separated, intercalated, or exfoliated) obtained in the nanocomposites as a result of processing methodology. This analysis helped in determining if the

processing methodology used was able to achieve the desired clay morphology (i.e. exfoliated morphology) in the nanocomposites.

4.5.1 XRD analysis

XRD analysis was carried out for pristine nanoclay and for 'E1C' nanocomposite. 'E1C' composition was selected because the same processing method for clay dispersion was followed for all other nanocomposites as was used for the 'E1C' nanocomposite.

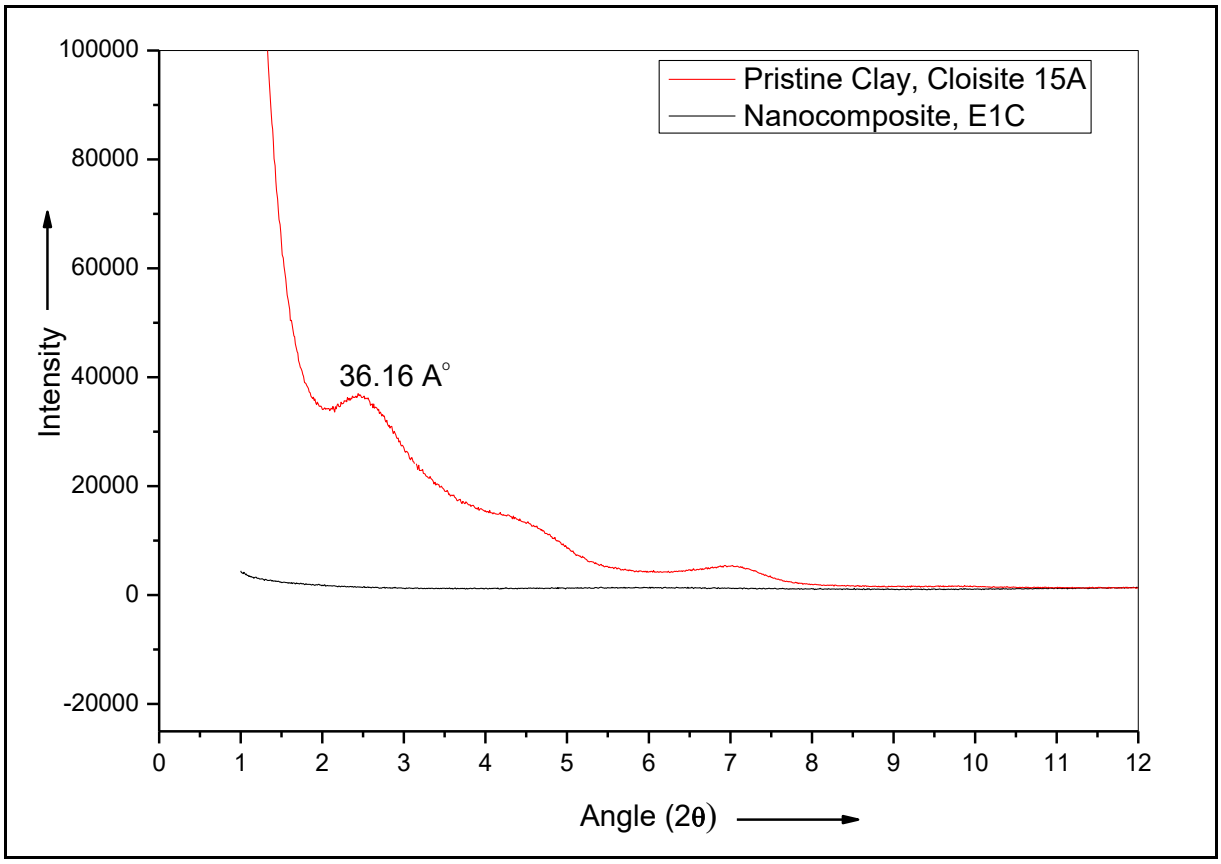

Figure 4.3. XRD patterns for the pristine nanoclay and the nanocomposite system.

It is well reported in literature that for nanocomposite systems, absence of peak in the XRD spectrum indicates exfoliated morphology [60, 71]. Figure 4.3 shows the XRD patterns of pristine nanoclay (Cloisite 15A) and the 'E1C' nanocomposite. XRD pattern of pristine clay showed peak (d_{001}) at 2.44 degree ($2\theta = 2.44°$) and d-spacing was calculated as 36.16 Å. However, XRD pattern of the nanocomposite system (E1C) showed absence of peak, indicating an exfoliated morphology of silicate layers in the nanocomposite system.

4.5.2 TEM analysis

To confirm the results obtained through X-ray diffraction pattern, TEM analysis was carried out for 'E1C' nanocomposite. Figure 4.4a–b presents the TEM micrographs of 'E1C' composition at two different regions in the nanocomposite system. The dark/black lines represent the clay platelets and the grey background represents the epoxy matrix.

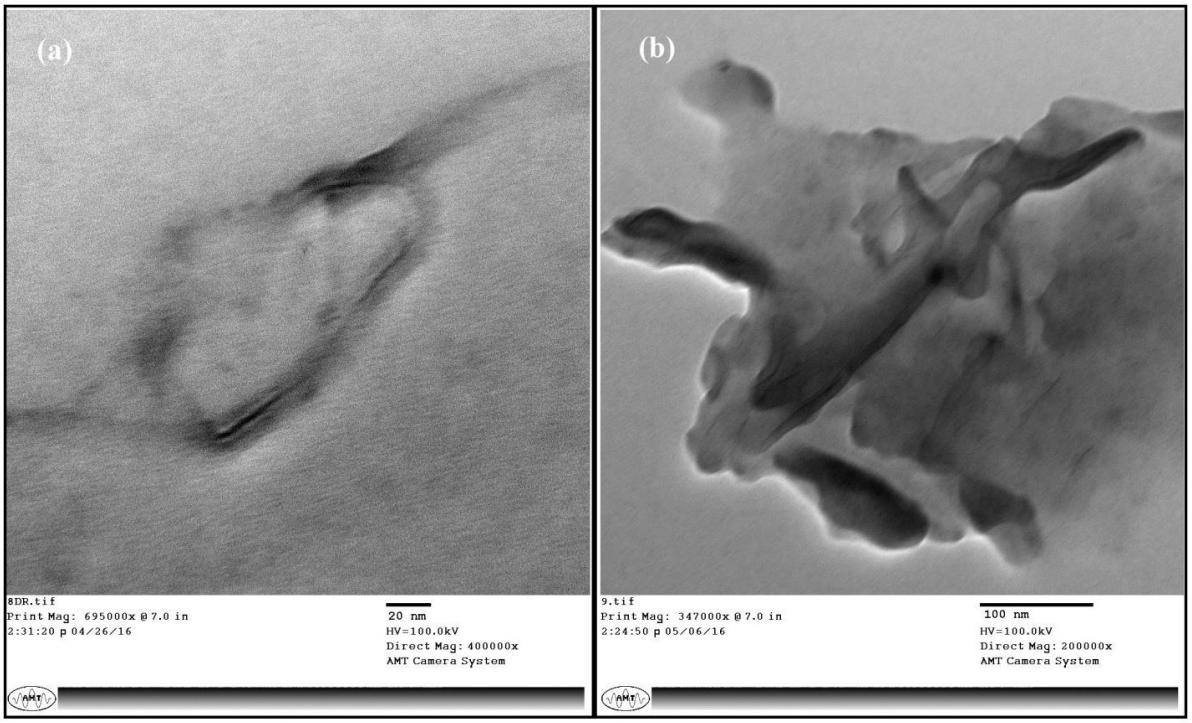

Figure 4.4 TEM micrographs of the epoxy-clay nanocomposite showing clay morphology.

Figure 4.4a shows that clay layers are non-parallel and randomly aligned. Figure 4.4b shows a mixed type of clay morphology where some clay layers are evenly spaced with large inter-lamellar spacing, whereas others are randomly aligned. Thus, TEM images largely showed presence of exfoliated clay morphology with uniform dispersion, interspersed with intercalated layers also [78, 87, 154–157]. XRD and TEM analysis justified that the processing method used in the present research was effective in dispersing the clay in the nanocomposite system.

4.6 CHANGES IN SURFACE MORPHOLOGY OF PP FIBERS

This section describes the changes observed in the surface morphology of PP fibers as a result of surface treatment of these fibers including silane treatment and MAH grafting.

4.6.1 SEM analysis of untreated fibers

SEM images of the as-received glass fibers and PP fibers are presented in Figure 4.5. Glass fibers showed a circular cross-section (diameter ~ 15 μm) whereas PP fibers showed a rectangular cross-section (width ~ 35 μm). These details were helpful to differentiate between the glass fibers and PP fibers during SEM analysis of nanocomposite samples which contained both types of fibers.

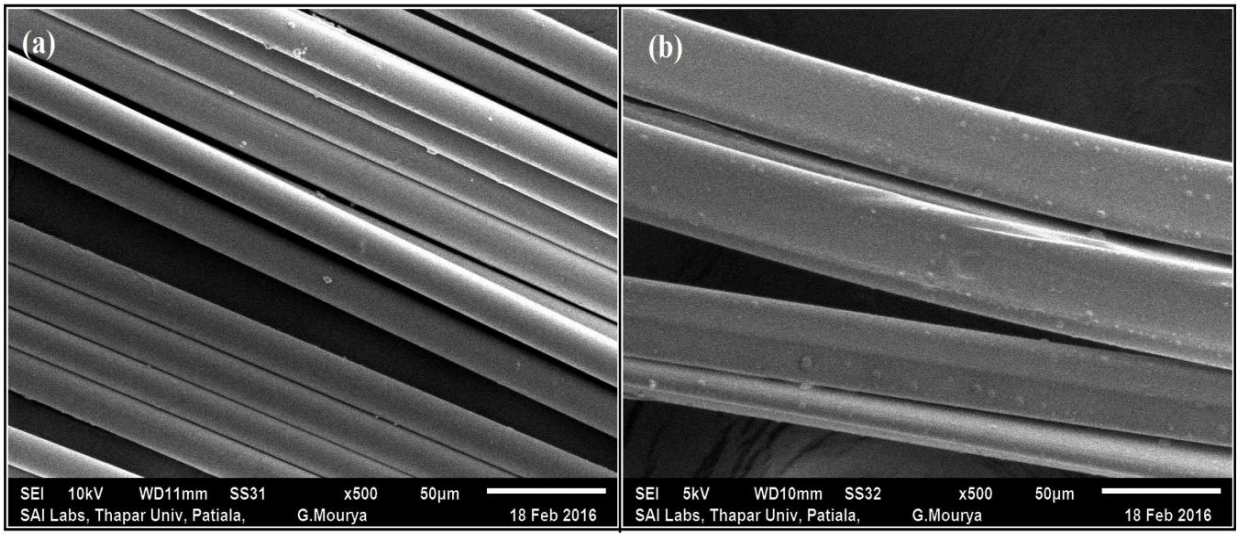

Figure 4.5 SEM images of the as-received (a) glass fibers, and (b) polypropylene fibers.

4.6.2 SEM-EDS of silane treated polypropylene fibers

Figure 4.6 shows the SEM images of untreated PP fibers (Figure 4.6a) and those treated with MS silane agent and VS silane agent respectively (Figure 4.6b–c).

SEM micrographs confirmed the presence of coating on the treated PP fibers. The composition of this coating was obtained from the energy dispersive spectroscopy (EDS) analysis. From EDS, it was confirmed that the coating present on the silane treated PP fibers was of silane agent as was evident by presence of silicon in the EDS spectra. Figure 4.7a–c shows the results of EDS analysis. The amount of silicon in the untreated, MS treated, and VS treated PP fibers was observed as 0, 1.25, and 1.47 wt. % respectively. The presence of silicon on the surface of treated PP fibers confirmed successful silane coating on the PP fibers.

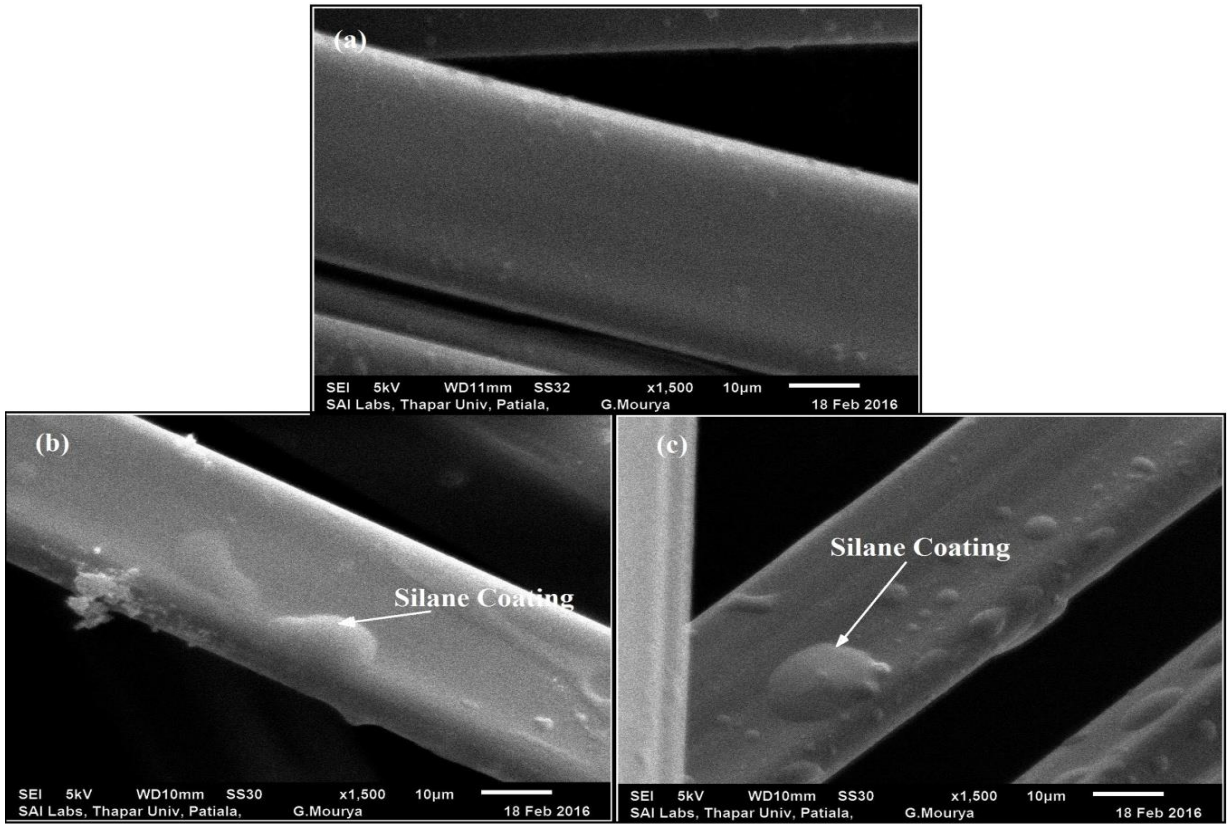

Figure 4.6 SEM micrographs showing surface of polypropylene fibers in the condition (a) untreated, (b) VS silane treated, and (c) MS silane treated.

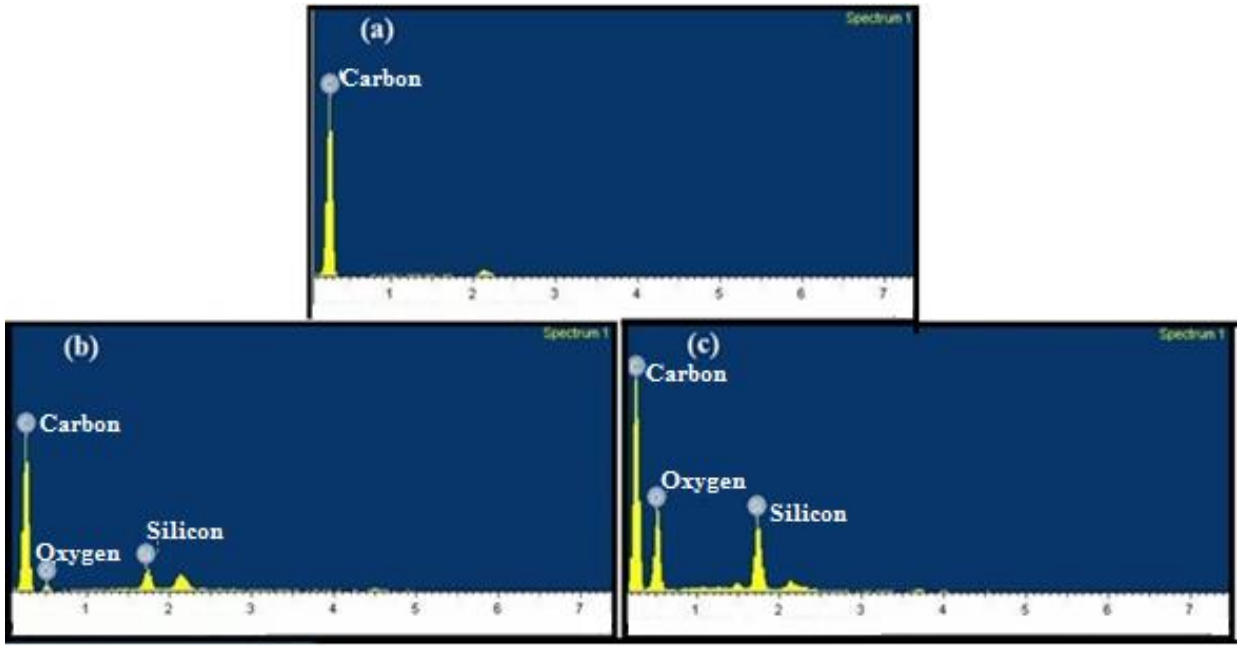

Figure 4.7 Results of EDS of polypropylene fibers in the condition (a) untreated, (b) treated with VS silane agent, and (c) treated with MS silane agent.

4.6.3 SEM and FTIR analysis of MAH grafted polypropylene fibers

As discussed earlier in Section 3.6.3.2, UV-assisted MAH grafting of PP fibers showed maximum weight gain for a treatment time of 30 h (2.18 g; Table 3.2). So, for MAH grafting of PP fibers, the optimum treatment time was selected as 30 h. To confirm MAH grafting on PP fiber surface, SEM analysis of MAH grafted fibers exposed to UV-rays for different treatment time periods (10, 20, 30, and 40 h, respectively) was conducted.

SEM results confirmed the observations of weight gain (Figure 4.8). SEM micrograph of the 30 h sample showed uniform grafting with minor pitting on the surface of PP fibers (Figure 4.8c). The minor pitting observed along with uniform grafting also improves adhesion of polymeric fibers to the constituents of composite system [105]. For treatment time periods of more than the optimum period of 30 h, the SEM micrograph (Figure 4.8d) showed ruptured surfaces which was due to excessive exposure to UV radiations.

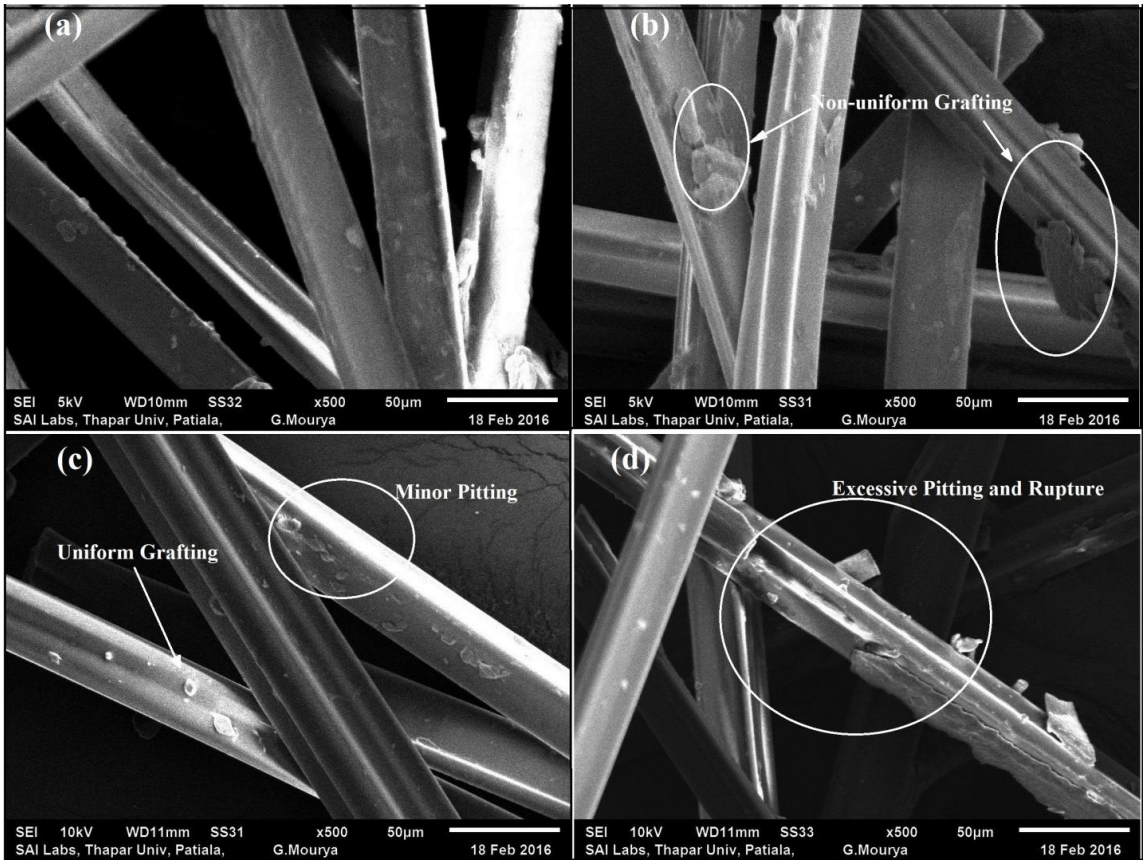

Figure 4.8 SEM micrographs showing polypropylene fibers subjected to UV-assisted MAH grafting for exposure time period of (a) 10 h, (b) 20 h, (c) 30 h, and (d) 40 h.

Further, FTIR (Fourier transform infrared spectroscopy) was conducted for MAH grafted PP fibers to confirm the grafting. Figure 4.9 presents the FTIR results for both the untreated PP fibers as well as the MAH grafted PP fibers (treated for optimum period of 30 h). For MAH grafted samples, peaks at 841 cm^{-1}, 1168 cm^{-1}, 1265 cm^{-1}, and 1636 cm^{-1} could be recognized as peaks due to C–H alkenes, –OH aromatic, C=C aromatic ring, and C=C alkenes, respectively. Further, the difference in shape of band between 3000–3600 cm^{-1} could be because of modification of self-association of –OH group due to hydroxyl group involved in interactions with maleic anhydride [158]. Absorption bands at around 1707 cm^{-1} and 1887 cm^{-1} correspond to the asymmetric C=O stretching and carboxylic acid respectively and indicated grafting of maleic anhydride on polypropylene fibers [116, 134, 149, 159]. Thus, MAH grafting on PP fibers was confirmed by the FTIR study.

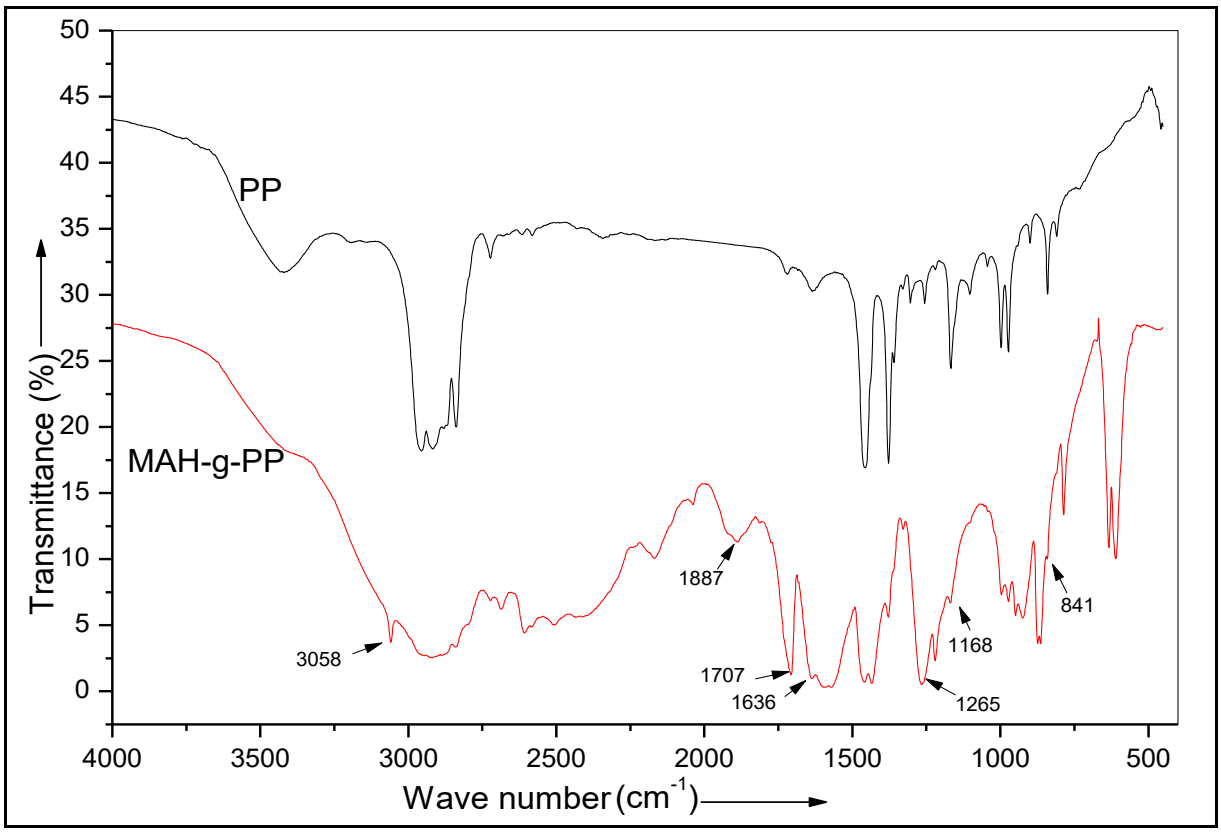

Figure 4.9 FTIR results of untreated and MAH grafted polypropylene fibers. PP = untreated polypropylene fibers, MAH-g-PP = MAH grafted polypropylene fibers.

4.7 SEM ANALYSIS OF FRACTURED IMPACT SPECIMENS

SEM micrographs of the fracture surface of impact tested specimens were investigated for some typical compositions (NE, E1C, and all nanocomposites containing 2 phr untreated/treated PP fibers) to understand the failure behaviour of composites.

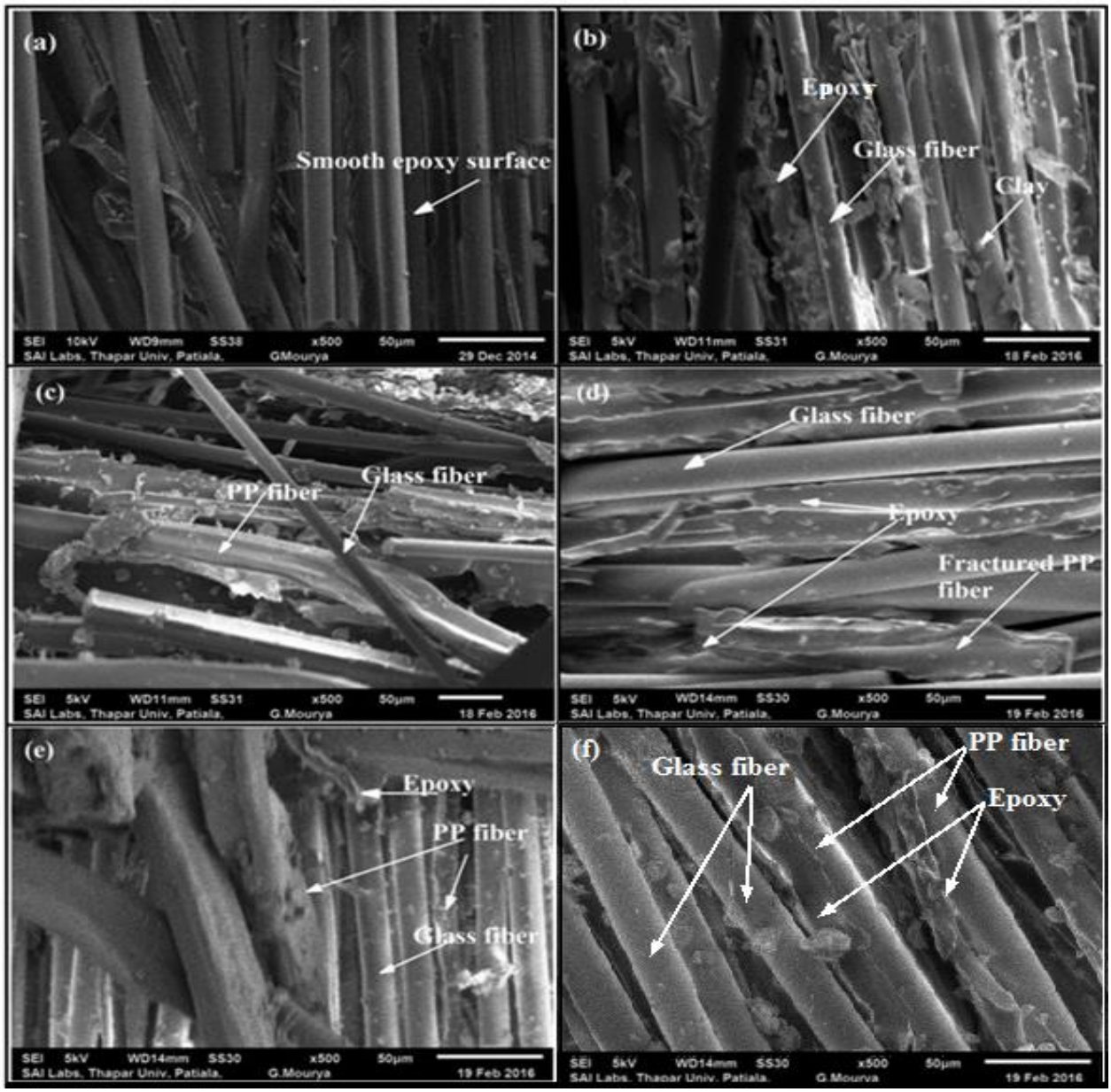

Figure 4.10 SEM micrographs showing fracture surfaces of impact specimens of (a) reference GFRP without clay and PP fibers (NE), (b) nanocomposite without PP fibers (E1C), (c) nanocomposite with 2 phr untreated PP fibers (E1C2PP), (d) nanocomposite with 2 phr MS treated PP fibers (E1C2PPMS), (e) nanocomposite with 2 phr VS treated PP fibers (E1C2PPVS), and (f) nanocomposite with 2 phr MAH grafted PP fibers (E1C2MAHPP). PP = polypropylene.

Figure 4.10a–f presents the SEM micrographs showing fracture surfaces of impact specimens of various GFRPs.

Figure 4.10a shows the fracture surface of the reference sample 'NE'. The micrograph revealed a lack of interaction between glass fibers and epoxy resin. Also, the surface of epoxy appeared quite smooth which indicated less resistance to failure under impact loading [83, 90].

Figure 4.10b shows the fracture surface of 'E1C' nanocomposite. As compared to 'NE', the surface of epoxy in 'E1C' composite was more rough indicating greater resistance to impact loading before failure. Also, epoxy-nanoclay was observed on the glass fibers indicating better interaction among the 'E1C' constituents.

SEM image of fracture surface of epoxy-clay GFRP nanocomposite containing 2 phr of untreated PP fibers (E1C2PP) is presented in Figure 4.10c. It was observed that there is negligible interaction of PP fibers with other constituents which could be attributed to the inert nature of PP [160, 161]. This lack of interaction resulted in poor impact strength.

Figure 4.10d–e shows the SEM images of fracture surfaces of epoxy-clay GFRP nanocomposite samples containing 2 phr silane treated PP fibers (E1C2PPMS and EIC2PPVS respectively).

The micrographs showed improved interaction of the silane treated PP fibers with other constituents of the nanocomposite system. For the 'E1C2PPMS' nanocomposite containing 2 phr of MS silane treated PP fibers, a few regions even showed fractured PP fibers (Figure 4.10d). This indicated that silane treated PP fibers used as reinforcement in the nanocomposites resisted the impact loading more effectively, thereby resulting in higher impact strength of the nanocomposite system.

Figure 4.10f shows the SEM image of the impact tested surface of epoxy-clay GFRP nanocomposite sample containing 2 phr of MAH grafted PP fibers (E1C2PPMAH). The micrograph showed presence of epoxy-clay on the MAH grafted PP fibers. This indicated good coupling of PP fiber reinforcement with the epoxy matrix in the nanocomposite. The improvement in mechanical properties obtained for this nanocomposite system (E1C2PPMAH) may be attributed to these reasons.

The next chapter presents the results and discussion on the mechanical properties obtained in GFRP nanocomposites reinforced with polyethylene terephthalate fibers i.e. second type of micro-filler selected in the present research.

CHAPTER 5

RESULTS AND DISCUSSION OF POLYETHYLENE TEREPHTHALATE FIBER REINFORCED GFRP NANOCOMPOSITES

5.1 GENERAL

This chapter presents the impact testing and tensile testing results of PET fiber reinforced GFRP nanocomposites to determine their optimum composition along with the best surface treatment condition for PET fiber reinforcement providing maximum improvement in properties of resulting GFRPs. Further, the results of characterization procedures of XRD, SEM-EDS, TEM, and FTIR analysis to determine changes in surface morphology of fibers and also interfacial adhesion of constituents in nanocomposites is described in the chapter.

5.2 IMPACT STRENGTH

This section presents the results of impact testing of PET fiber reinforced GFRP nanocomposites. Table 5.1 shows the results of various mechanical properties evaluated for PET fiber reinforced GFRP nanocomposites.

The impact strength of epoxy based GFRP composite containing no clay and no PET fiber (reference sample, NE) was 161 kJ/m^2. On addition of 1 phr clay to the reference sample (i.e. E1C nanocomposite), a slight increase of 4% in impact strength (167 kJ/m^2) was observed, as reported in Section 4.2. Further, on addition of untreated polyethylene terephthalate fibers (PET) to this nanocomposite system, impact strength of the resulting nanocomposites viz. E1C1PET, E1C2PET, and E1C3PET (Table 3.6 provided details of these compositions) decreased (166 kJ/m^2, 130 kJ/m^2, and 110 kJ/m^2, respectively with an addition of 1 phr, 2 phr, and 3 phr untreated PET fibers). It is evident that impact strength deteriorated even on addition of a more ductile component i.e. untreated PET fibres. This may be attributed to lack of compatibility of PET fibers with other constituents of the composite system. For improving the compatibility, PET fibers were treated with two different silane agents separately viz. methacryloxypropyltrimethoxysilane (MS) and vinylytriethoxysilane (VS). The results showed that addition of silane treated PET fibers (as compared to untreated PET fibres) to the composite system significantly increased the impact

strength of GFRPs for a given composition (Table 5.1 and Figure 5.1). Further, interestingly it was observed that for all cases with PET fiber reinforcement (treated or untreated), the impact strength of GFRPs showed improvement till 2 phr PET fiber loading, and after this limit (i.e. for 3 phr PET loading), the impact strength deteriorated.

Table 5.1 Mechanical properties of PET fiber reinforced GFRP nanocomposites.

Sample Designation		Impact Strength (kJ/m^2)	Tensile Strength (MPa)	Tensile Modulus (MPa)
NE	*Avg**	161±2	269±3	7315±40
	s	4	7	81
E1C	*Avg**	167±15	313±6	7780±133
	s	30	12	265
E1C1PET	*Avg**	166±12	261±8	5953±215
	s	21	16	430
E1C1PETMS	*Avg**	182±1	259±3	5448±50
	s	3	6	99
E1C1PETVS	*Avg**	183±8	266±5	5788±60
	s	16	11	19
E1C2PET	*Avg**	130±3	234±7	4960±29
	s	6	14	57
E1C2PETMS	*Avg**	180±3	229±4	4895±68
	s	6	8	135
E1C2PETVS	*Avg**	**191±5**	258±4	5393±63
	s	9	8	126
E1C2PETMAH	*Avg**	175±6	262±16	6415±136
	s	11	31	272
E1C3PET	*Avg**	110±4	235±5	4703±52
	s	8	9	103
E1C3PETMS	*Avg**	172±3	186±10	4358±113
	s	7	21	226
E1C3PETVS	*Avg**	172±7	195±2	4138±48
	s	14	4	96

*Avg** = Mean value ± Range of values; *s* = Standard deviation of values

Decrease in impact strength of GFRP nanocomposites with 3 phr PET loading can be attributed to the poor dispersion of PET fibers in the composite system because of the concomitant high viscosity of resin at such a high concentration (i.e. 3 phr). For such systems, poor dispersion leads to lower aspect ratio of aggregates, and thus, lowers the impact strength.

Impact strength of reference sample was significantly improved with addition of treated PET fibers (i.e. compatibilized PET fibers). Maximum improvement of 19% in impact strength was achieved for GFRPs with reinforcement of 2 phr VS treated PET fibers. Since, maximum improvement in impact strength was observed for 2 phr PET loading (E1C2PETMS), only this PET concentration was selected for the other treatment of PET fibers i.e. maleic anhydride grafting (MAH). When maleic anhydride grafted PET fibers were used as reinforcement (2 phr of MAH grafted PET fibers), impact strength of resulting GFRP (i.e. E1C2PETMAH) showed improvement (9%, second only to E1C2PETVS) in impact strength as compared to the reference sample.

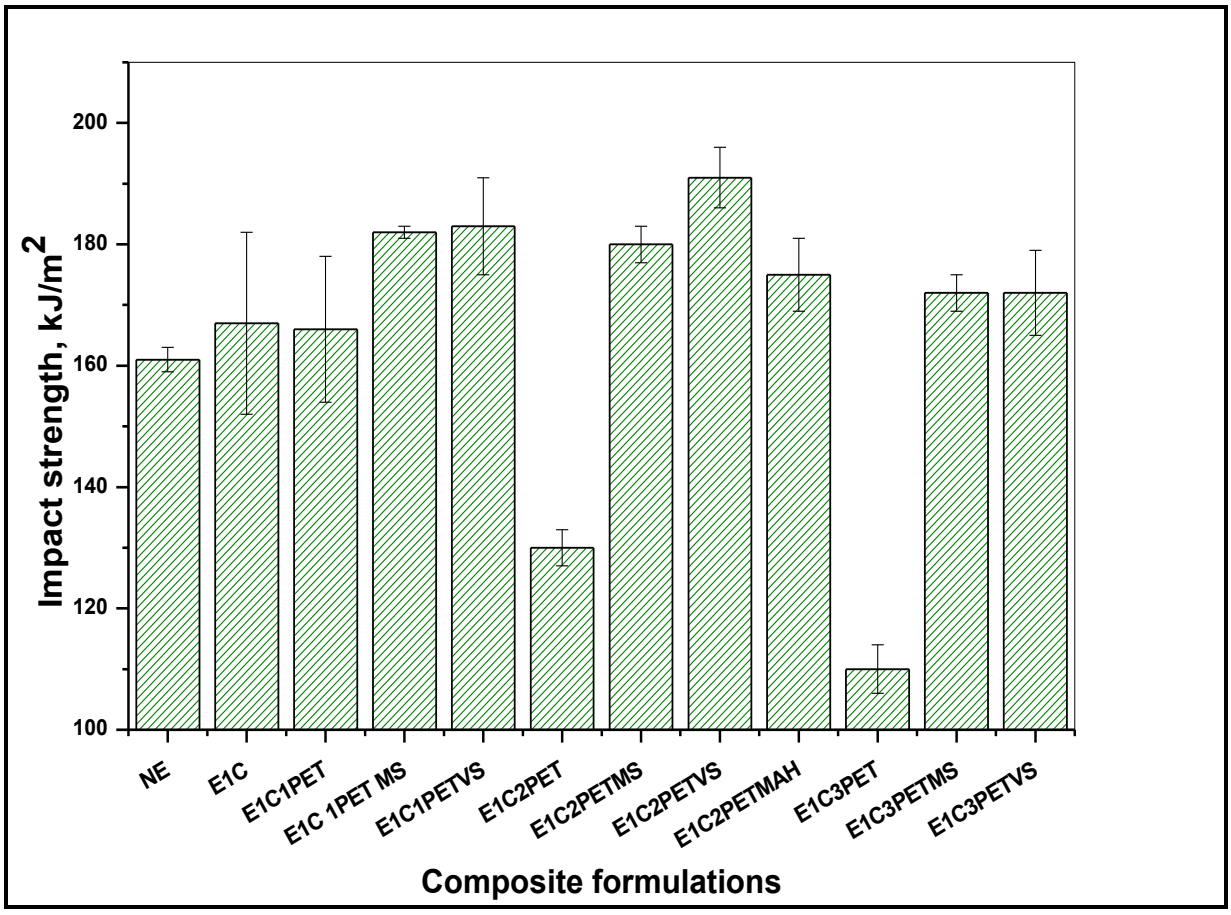

Figure 5.1 Impact testing results of PET fiber reinforced GFRP nanocomposites.

5.3 TENSILE PROPERTIES

The tensile strength and tensile modulus of the reference sample was observed as 269 MPa and 7315 MPa, respectively. On addition of 1 phr clay to the reference sample (i.e. E1C nanocomposite), an increase of 16% and 6% in tensile strength and modulus respectively was observed, as discussed in Section 4.3. Further, on addition of untreated PET fibers, to this nanocomposite system (viz. E1C1PET, E1C2PET, and E1C3PET), tensile strength and modulus values of the resulting nanocomposites decreased. Significantly, addition of treated PET fibers, restored the tensile properties of nanocomposites in most cases (as compared to untreated PET fiber reinforced nanocomposites); however the values were below those for the reference sample (NE).

For the nanocomposite at which maximum improvement in impact strength was observed (i.e. E1C2PETVS), the tensile strength and modulus values were 4% and 26% lower as compared to the reference sample. However, for the optimum concentration of 2 phr PET fiber loading, MAH grafted PET fiber reinforcement led to recovery in tensile properties of nanocomposites. For this E1C2PETMAH nanocomposite, tensile strength and modulus values were 3% and 12% less as compared to NE composition. So, the objective of significantly improving the impact strength of epoxy based GFRPs with addition of soft/ductile second phase filler (here PET fibers) without considerable loss in tensile properties was successfully achieved. Thus, optimized composition of GFRP combining 1 phr clay and 2 phr PET fiber treated with VS silane agent, showed a significant improvement of 19% in impact strength over the reference sample and a very slight drop in tensile strength. A detailed investigation was done to understand the reasons for the increase in the impact strength. These are discussed in the following sections (Section 5.4–5.7).

5.4 COMPATIBILIZATION

The main purpose of the present research was to enhance the impact strength of epoxy based GFRP nanocomposites. For improving the impact strength, second phase fillers in the form of PET fibers were added to the GFRP nanocomposite system containing nanoclay as the first filler. The results showed that addition of treated PET fibers (up to 2 phr) led to improvements in impact strength of the composite system. For nanocomposites reinforced with silane treated PET fibers, impact strength improvement was attributed to the improved compatibility between the inorganic glass

fibers and the organic PET fibers. It is well reported in literature that silane agents are silicon-based chemicals which act as an interface between an inorganic (here, glass fiber) and an organic material (here, PET fiber). Silanes contain two types of reactivities viz. inorganic and organic, which lead to increase in the interfacial bonding between two different materials. The grafting of silane agents onto polymeric chains helps in cross-linking these chains and also in forming stable covalent bonds with polar fillers [117, 152, 162, 163]. Further, for MAH grafted PET fibers, there was improvement in impact strength with appreciable restoration of tensile properties of nanocomposites. The enhancement in impact strength was attributed to the improved bonding of MAH grafted PET fibers to the epoxy matrix, as described in Section 4.4.

5.5 DISPERSION OF CLAY IN NANOCOMPOSITES

XRD and TEM analysis were used to examine the type of clay morphology (phase separated, intercalated, or exfoliated) obtained in the nanocomposites as a result of processing methodology. The epoxy system and clay used for fabrication of PET reinforced GFRPs and PP reinforced GFRPs were the same and also the processing methodology was same. Thus, for epoxy based PET reinforced GFRPs, it was concluded that the desirable exfoliated morphology was achieved, as described in Section 4.5.

5.6 CHANGES IN SURFACE MORPHOLOGY OF PET FIBERS

This section describes the changes observed in the surface morphology of PET fibers as a result of surface treatment of these fibers including silane treatment and MAH grafting.

5.6.1 SEM analysis of untreated fibers

SEM images of the as-received glass fibers and PET fibers are presented in Figure 5.2. Glass fibers showed a circular cross-section (diameter ~ 15 μm) whereas PET fibers showed a triangular cross-section (side ~ 37 μm). These details were helpful to differentiate between the glass fibers and PET fibers during SEM analysis of nanocomposite samples containing both these type of fibers.

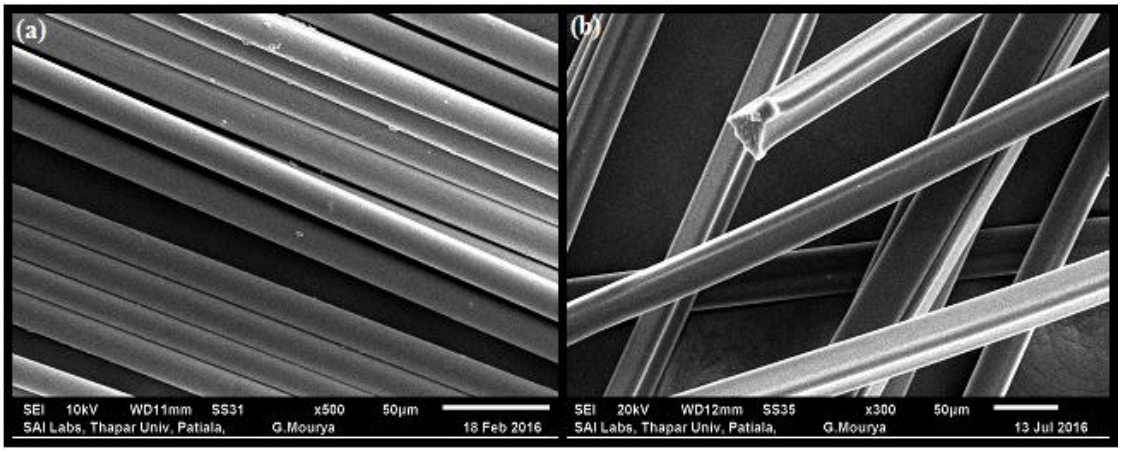

Figure 5.2 SEM images of the as-received (a) glass fibers, and (b) polyethylene terephthalate fibers.

5.6.2 SEM-EDS of silane treated polyethylene terephthalate fibers

Figure 5.3 shows the SEM images of untreated PET fibers (Figure 5.3a) and those treated with MS silane agent and VS silane agent respectively (Figure 5.3b–c). SEM micrographs confirmed the presence of a coating on the treated PET fibers.

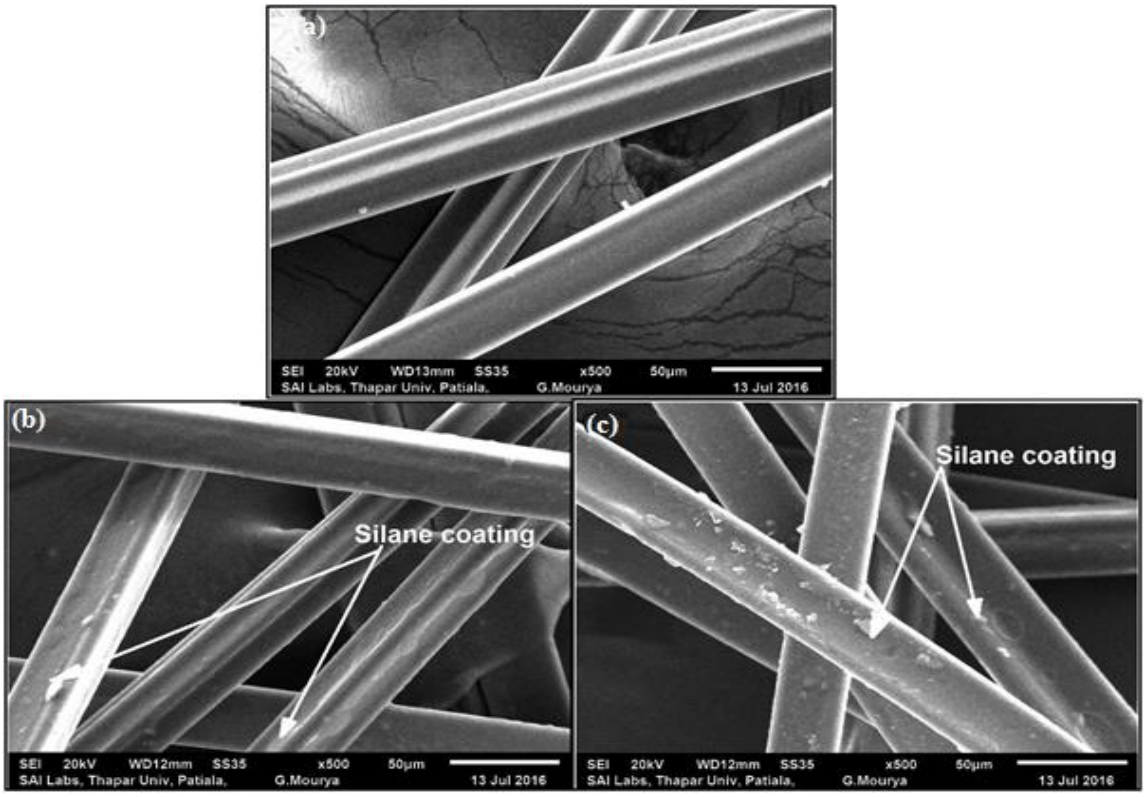

Figure 5.3 SEM micrographs showing surface of polyethylene terephthalate fibers in the condition (a) untreated, (b) MS silane treated, and (c) VS silane treated.

The composition of this coating was obtained from the energy dispersive spectroscopy (EDS) analysis. From EDS, it was confirmed that the coating present on the silane treated PP fibers was of silane agent as was evident by presence of silicon in the EDS spectra. Figure 5.4a–c shows the results of EDS analysis. The amount of silicon in the untreated, MS treated, and VS treated PP fibers was observed as 0, 3.27, and 3.65 wt. % respectively. The presence of silicon on the surface of treated PP fibers confirmed successful silane coating on the PET fibers.

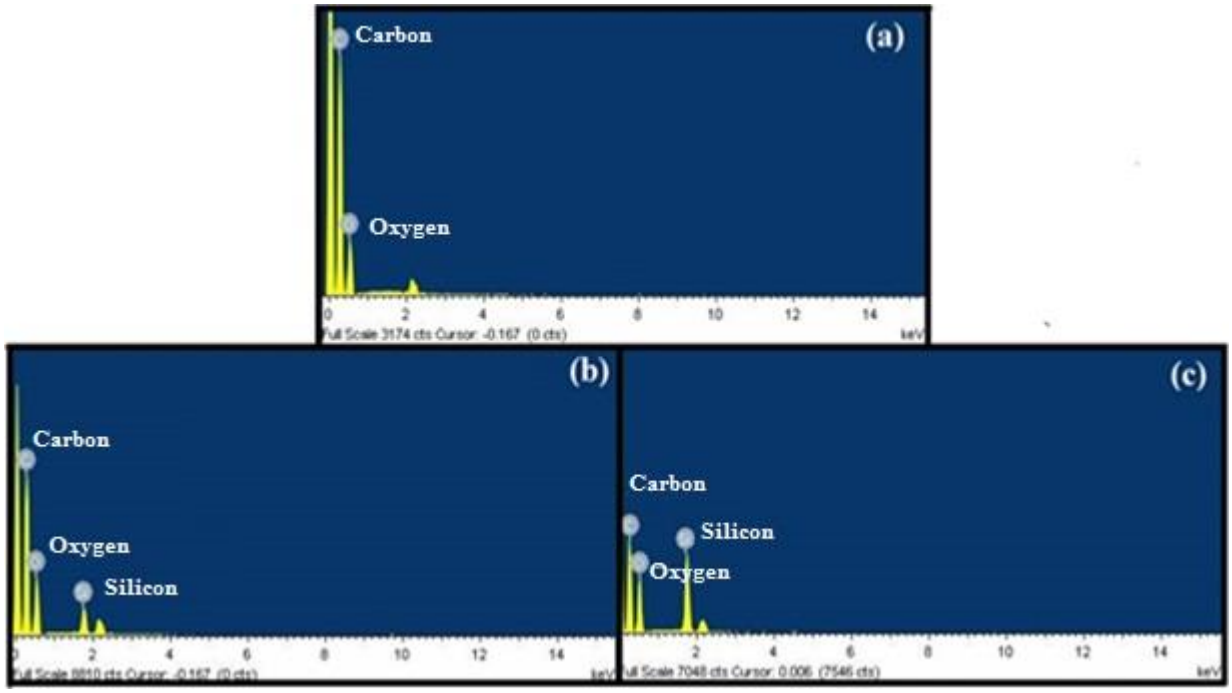

Figure 5.4 Results of EDS of polyethylene terephthalate fibers in the condition (a) untreated, (b) treated with VS silane agent, and (c) treated with MS silane agent.

5.6.3 SEM and FTIR analysis of MAH grafted polyethylene terephthalate fibers

As discussed earlier in Section 3.6.4.2, UV-assisted MAH grafting of PET fibers showed maximum weight gain for a treatment time of 8 h (3 g; Table 3.4). So for MAH grafting of PET fibers, the optimum treatment time was selected as 8 h.

To confirm MAH grafting on PET fibers, SEM analysis of untreated and MAH grafted PET fibers (treated for 8 h) was conducted (Figure 5.5). It was observed that the untreated fibers had a very smooth surface whereas the fibers grafted with MAH displayed a surface which was less smooth due to presence of MAH on it.

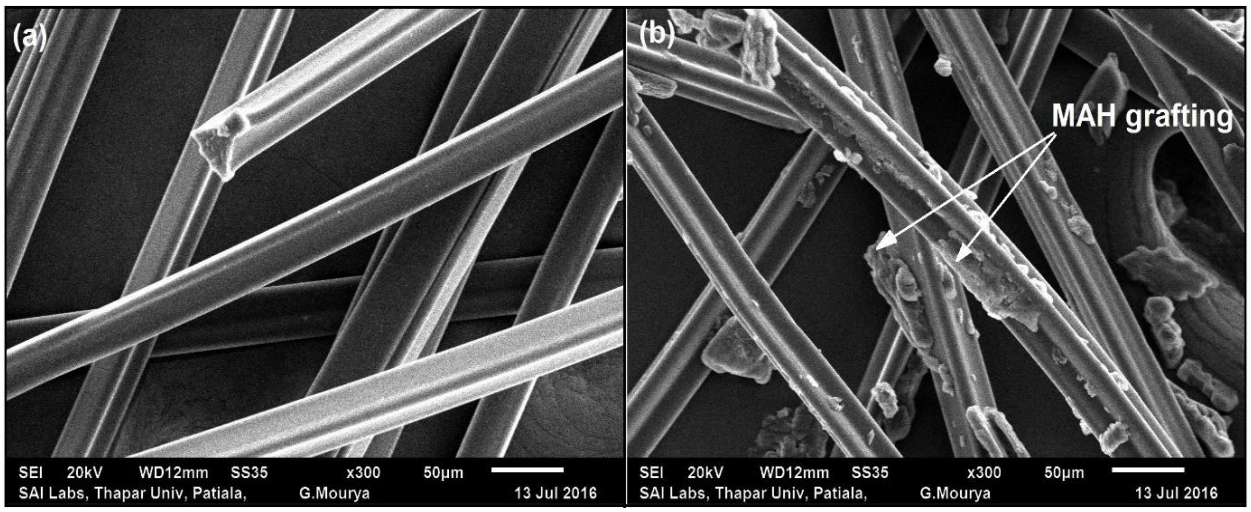

Figure 5.5 SEM images of PET fibers in the condition (a) untreated and (b) MAH grafted.

Further, FTIR analysis was conducted for MAH grafted PET fibers to confirm the grafting.

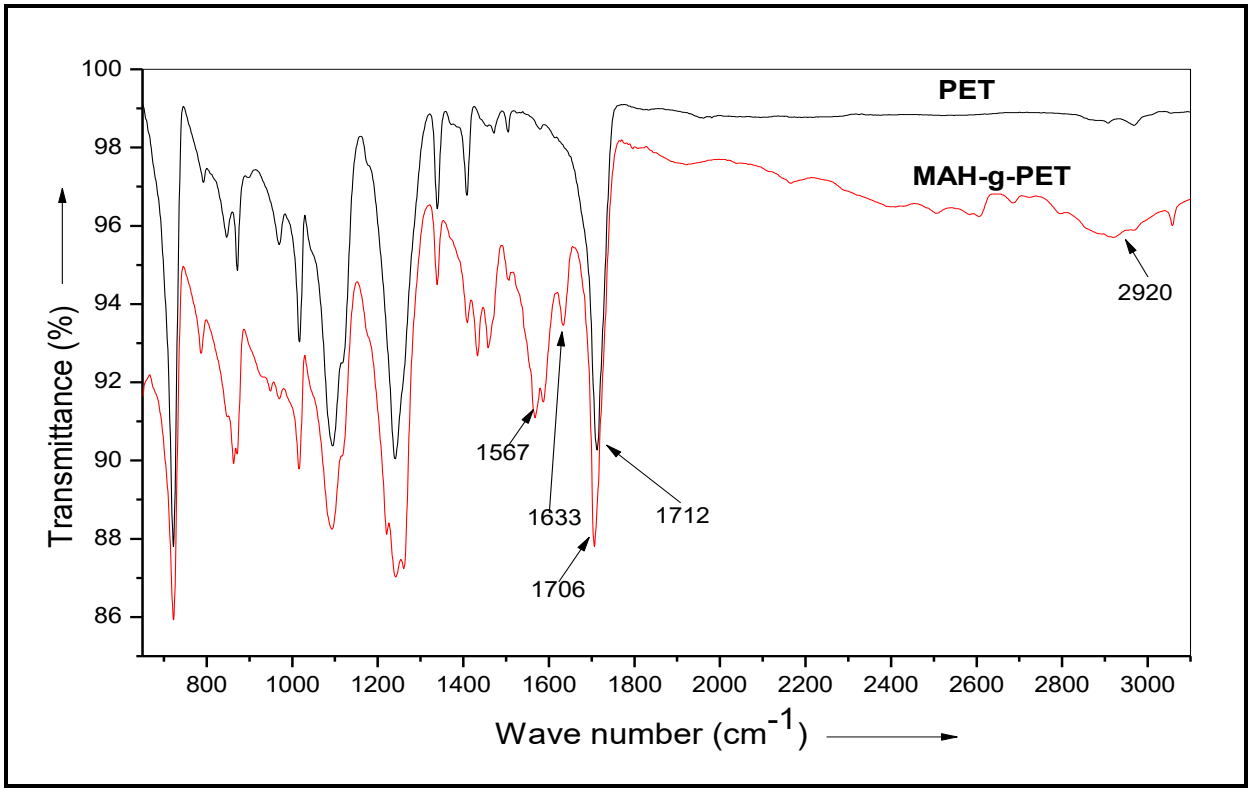

Figure 5.6 FTIR results of untreated and MAH grafted PET fibers. PET= untreated polyethylene terephthalate fibers, MAH-g-PET= MAH grafted polyethylene terephthalate fibers.

Figure 5.6 presents the FTIR results for the untreated PET fibers as well as MAH grafted PET fibers (treated for optimum period of 8 h). For MAH grafted samples, new peaks at 2920 cm^{-1}, 1633 cm^{-1}, and 1567 cm^{-1} were obtained for the MAH grafted samples (these peaks were absent in untreated fibers) and also a shift in the peak at 1712 cm^{-1} was observed. The new band which appeared at about 2920 cm^{-1} in the MAH grafted PET fibers was due to presence of C–H vibrations of methane. This peak was absent in the untreated fibers. The variation in peak at about 1712 cm^{-1} may be attributed to the C=O stretching of anhydride present in MAH. The appearance of a new absorption band at about 1633 cm^{-1} may be attributed to the formation of carboxy group by reaction of anhydro group with moisture. The appearance of an additional band at l567 cm^{-1} may be due to the presence of COOH group [116, 163–166]. Thus, MAH grafting on the surface of PET fibers was confirmed by the FTIR study.

5.7 SEM ANALYSIS OF FRACTURED IMPACT SPECIMENS

SEM micrographs of the fracture surface of impact tested specimens were investigated for some typical compositions (NE, E1C, and all nanocomposites containing 2 phr untreated/treated PET fibers) to understand the failure behaviour of composites.

SEM micrograph of fracture surface of impact specimen of reference composition (NE) revealed a lack of interaction between glass fibers and epoxy resin (Figure 5.7a). Also, the surface of epoxy appeared quite smooth which indicated less resistance to failure under impact loading [90, 173]. As compared to 'NE', the surface of epoxy in 'E1C' composite was more rough indicating greater resistance to impact loading before failure. Also, epoxy-nanoclay was seen on the glass fibers indicating better interaction among the 'E1C' constituents (Figure 5.7b).

Figure 5.7c–f presents the SEM micrographs showing fracture surfaces of impact specimens of 2 phr PET fiber reinforced GFRPs. SEM image of fracture surface of epoxy-clay GFRP nanocomposite containing 2 phr untreated PET fibers (E1C2PET) is presented in Figure 5.7c. It was observed that there is negligible interaction of PET fibers with other constituents which could be attributed to the inert nature of PET [108]. This lack of interaction resulted in poor impact strength of the resulting nanocomposite.

Figure 5.7d–e shows the SEM images of fracture surfaces of epoxy-clay GFRP nanocomposite sample containing 2 phr silane treated PET fibers (E1C2PETMS and EIC2PETVS respectively).

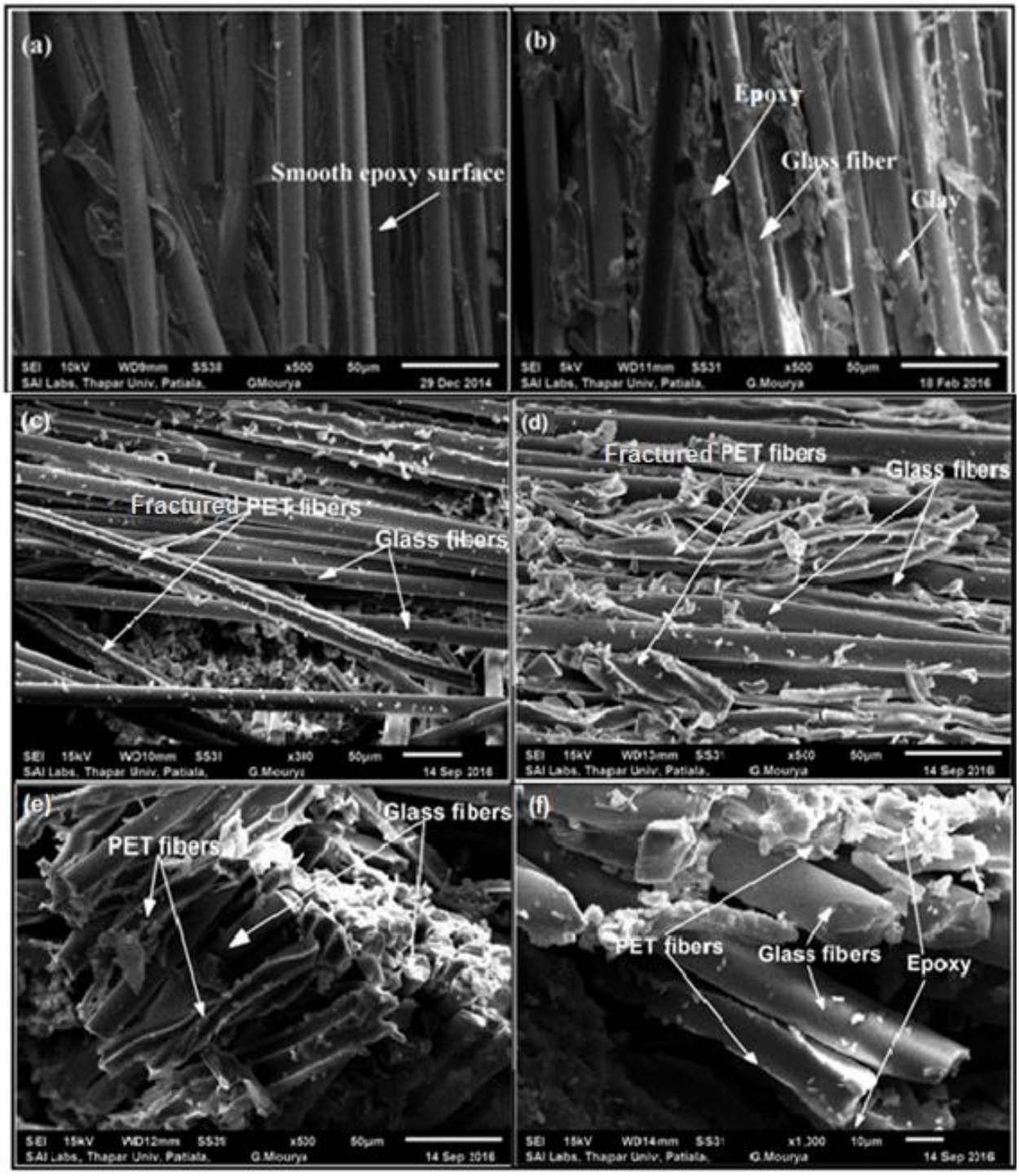

Figure 5.7 SEM micrographs showing fracture surfaces of impact specimens of (a) reference GFRP without clay and PET fibers (NE), (b) nanocomposite without PET fibers (E1C), (c) nanocomposite with 2 phr PET fibers (E1C2PET), (d) nanocomposite with 2 phr MS treated PET fibers (E1C2PETMS), (e) nanocomposite with 2 phr VS treated PET fibers (E1C2PETVS), and (f) nanocomposite with 2 phr MAH grafted PET fibers (E1C2MAHPET). PET = polyethylene terephthalate.

The micrographs showed improved interaction of the silane treated PET fibers with other constituents of the nanocomposite system. For the silane treated nanocomposites containing 2 phr PET fibers (E1C2PETMS and E1C2PETVS), a few regions even showed fractured PET fibers. This indicated that silane treated PET fibers used as reinforcement in the nanocomposites resisted the impact loading more effectively, thereby resulting in higher impact strength of the nanocomposite system. Figure 5.7f shows the SEM image of the impact tested surface of epoxy-clay GFRP nanocomposite sample containing 2 phr of MAH grafted PET fibers (E1C2PETMAH). The micrograph showed presence of epoxy-clay on the MAH grafted PET fibers. This indicated good coupling of PET fiber reinforcement with the epoxy matrix in the nanocomposite. The improvement in mechanical properties obtained for this nanocomposite system (E1C2PETMAH) may be attributed to these reasons.

The next chapter presents the results and discussion on the mechanical properties obtained in GFRP nanocomposites reinforced with ethylene propylene diene monomer rubber.

CHAPTER 6

RESULTS AND DISCUSSION OF ETHYLENE PROPYLENE DIENE MONOMER REINFORCED GFRP NANOCOMPOSITES

6.1 GENERAL

This chapter presents the results of impact testing and tensile testing of elastomer reinforced GFRP nanocomposites. The results of various characterization techniques utilized in the present research to ascertain the type of clay morphology obtained in the nanocomposites and also the chemical/interfacial changes in morphology of EPDM rubber particles due to compatibilization procedures have also been presented.

6.2 IMPACT STRENGTH

This section presents the results of impact testing of EPDM particle reinforced GFRP nanocomposites. Table 6.1 shows the results of various mechanical properties evaluated for the GFRP nanocomposites reinforced with rubber particles.

The impact strength of epoxy based GFRP composite without clay and EPDM particles (reference sample, NE_R) was 145 kJ/m^2. On addition of 1 phr clay to the reference sample (i.e. $E1C_R$ nanocomposite), an increase of 13% in impact strength (164 kJ/m^2) was observed. Further, on addition of untreated ethylene propylene diene monomer (EPDM) particles to this nanocomposite system, impact strength of the resulting nanocomposites viz. E1C2.5R, E1C5R, E1C7.5R, and E1C10R (Table 3.6 provided details of these compositions) were observed as 152 kJ/m^2, 184 kJ/m^2, 137 kJ/m^2 and 133 kJ/m^2, respectively with an addition of 2.5 phr, 5 phr, 7.5 phr, and 10 phr of untreated EPDM). For nanocomposites reinforced with untreated EPDM, maximum improvement in impact strength (25% higher than the reference sample) was achieved at 5 phr concentration. At higher concentrations of untreated EPDM (7.5 phr and 10 phr), the impact strength of resulting nanocomposites decreased. The decline in impact strength could be attributed to non-uniform dispersion of EPDM due to the concomitant higher viscosity of resin system at higher EPDM concentrations. For further improving the impact strength, EPDM was compatibilized using bis-(3-triethoxysilyl-propyl)-tetrasulfane (BS) silane agent. The results showed that addition of silane treated EPDM (as compared to untreated EPDM) to the composite

system significantly increased the impact strength of GFRPs for a given composition (Table 6.1 and Figure 6.1). Further, interestingly it was observed that silane treated EPDM modified system showed a significant improvement in impact strength of GFRP nanocomposites over the untreated EPDM modified system (for a given specific concentration of EPDM). The maximum improvement in impact strength of GFRPs was observed as 68% (over the reference sample) for 5 phr BS silane treated EPDM modified system.

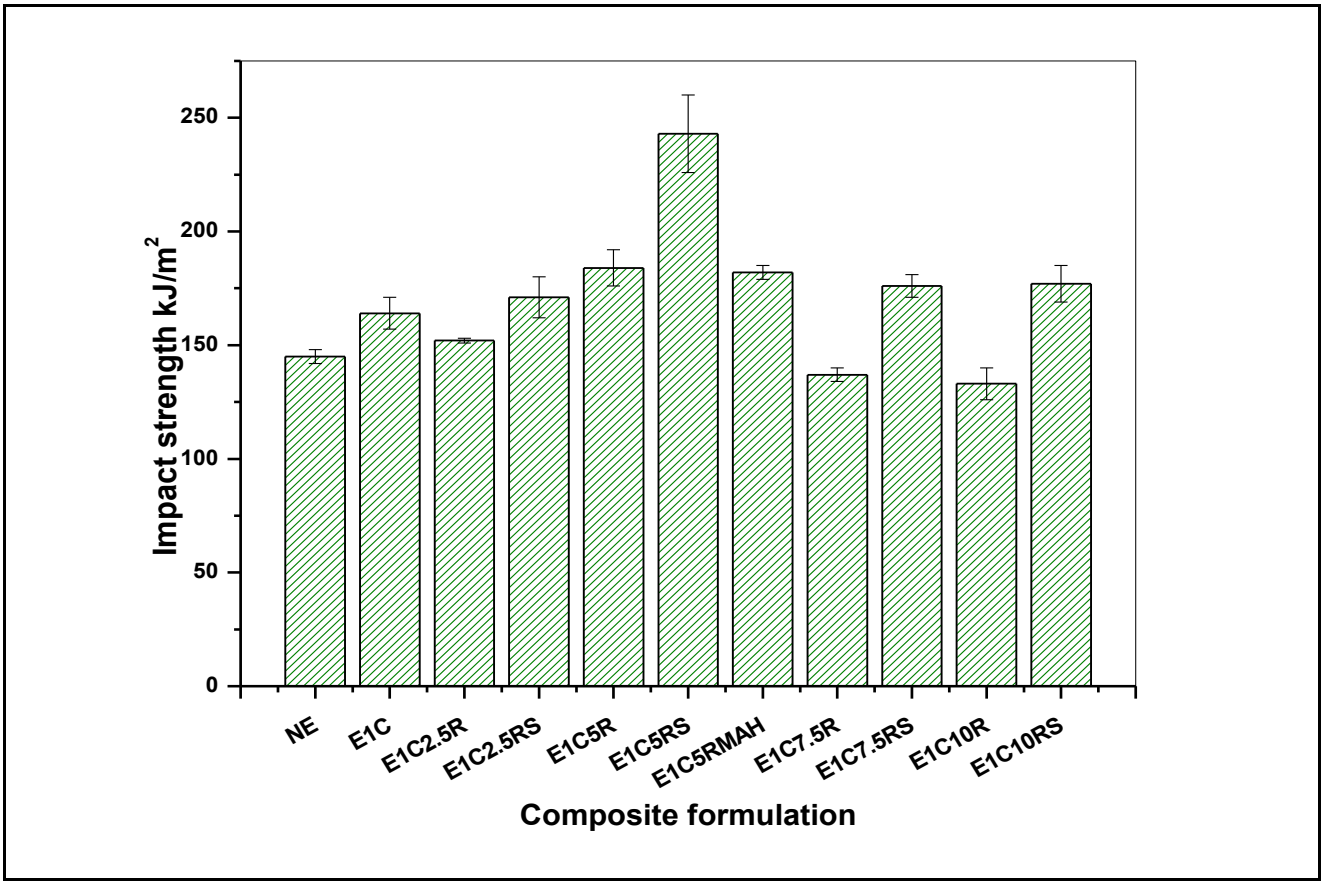

Figure 6.1 Impact testing results of EPDM reinforced GFRP nanocomposites.

Since, maximum improvement in impact strength was observed for 5 phr EPDM loading (E1C5RS), only this EPDM concentration was selected for the other surface treatment of EPDM i.e. maleic anhydride grafting (MAH). When maleic anhydride grafted EPDM particles were used as reinforcement (5 phr of MAH grafted EPDM particles), impact strength of resulting GFRP showed a significant improvement (26%) in impact strength as compared to the reference sample.

Thus, impact strength of reference sample was significantly improved with addition of treated EPDM filler. Maximum improvement of 68% in impact strength was achieved for GFRPs with reinforcement of 5 phr BS treated EPDM. Similarly, reinforcement of 5 phr MAH grafted EPDM filler also improved the impact strength (by 26%) of the reference composite sample.

Table 6.1. Mechanical properties of EPDM modified GFRP nanocomposites.

Sample Designation		*Impact Strength (kJ/m^2)*	*Tensile Strength (MPa)*	*Tensile Modulus (MPa)*
NE_R	*Avg**	145±3	291±15	6793±53
	s	6	29	105
$E1C_R$	*Avg**	164±7	320±16	7003±133
	s	13	31	266
E1C2.5R	*Avg**	152±1	306±3	6460±11
	s	2	6	22
E1C2.5RS	*Avg**	171±9	304±3	6300±189
	s	17	7	379
E1C5R	*Avg**	184±8	261±6	5820±67
	s	17	11	134
E1C5RS	*Avg**	**243±17**	253±14	5525±203
	s	33	28	406
E1C5RMAH	*Avg**	182±3	276±5	6080±110
	s	6	11	220
E1C7.5R	*Avg**	137±3	229±5	5068±104
	s	6	11	208
E1C7.5RS	*Avg**	176±5	221±6	4975±342
	s	10	12	684
E1C10R	*Avg**	133±7	204±8	4580±58
	s	13	16	117
E1C10RS	*Avg**	177±8	193±3	4420±32
	s	15	7	65

*Avg** = Mean value ± Range of values; *s* = Standard deviation of values

6.3 TENSILE PROPERTIES

The tensile strength and tensile modulus of the reference sample was observed as 291 MPa and 6793 MPa, respectively. On addition of 1 phr clay to the reference sample (i.e. E1C nanocomposite), an increase of 10% and 3% in tensile strength and modulus respectively was observed. Further, on addition of untreated EPDM particles to this nanocomposite system, tensile strength and modulus values of the resulting nanocomposites (viz. E1C2.5R, E1C5R, E1C7.5R, and E1C10R) showed decrease with increase in EPDM concentration. Addition of silane treated EPDM particles led to only marginal (insignificant) changes in tensile properties of nanocomposites as compared to untreated EPDM reinforced nanocomposites, for a given composition. It was observed that for nanocomposite at which maximum improvement in impact strength was observed (E1C5RS), the tensile strength and modulus values were 13% and 19% lower as compared to the reference sample. However, for the optimum concentration of 5 phr EPDM loading, MAH grafted EPDM reinforcement (E1C5RMAH) led to a recovery in tensile properties of nanocomposites. For this E1C5RMAH nanocomposite, tensile strength and modulus values were just 5% and 10% less as compared to the reference sample. Thus optimized composition of GFRP combining 1 phr clay and 5 phr EPDM treated with BS silane agent showed a significant improvement of 68% in impact strength with a drop of 13% in tensile strength. A detailed investigation was done to understand the reasons for the increase in the impact strength. These are discussed in the following sections (Section 6.4–6.7).

6.4 COMPATIBILIZATION

The main purpose of the present research was to enhance the impact strength of epoxy based GFRP nanocomposites. For improving the impact strength, second phase fillers in the form of EPDM particles were added to the GFRP nanocomposite system containing nanoclay as the first filler. The results showed that addition of treated EPDM (up to 5 phr) led to improvements in impact strength of the composite system. For nanocomposites modified with silane treated EPDM filler, impact strength enhancement was attributed to the improved compatibility between the inorganic glass fibers and the organic EPDM filler. It is well reported in literature that silane agents are used to improve compatibility between different components of a materials system (e.g. to improve interfacial adhesion between an organic constituent like elastomer and an inorganic constituent

like glass fiber). Silane agents possess two different types of reactivities viz. inorganic and organic. These distinct reactivities facilitate enhanced interfacial bonding between different constituents of a materials system [87, 138, 167]. Silane treatment of polymer/elastomer filler helps in cross-linking of polymer/elastomer chains and results in formation of stable covalent bonds with polar constituents of the material system, thereby improving the interfacial adhesion of constituents [152, 162, 163, 168].

Further, MAH grafting is a very effective method for compatibilization of elastomer/polymer filler to improve its interfacial adhesion with other constituents of a materials system [127, 169, 170]. MAH grafting procedure improves the compatibility of constituents through incorporation of maleic anhydride poly-functional group on the elastomer filler surface. MAH on being grafted to the polymer/elastomer filler surface improves its adhesion with the polar constituents of the composite system [149, 150]. MAH is grafted on the substrate surface in the presence of ultraviolet (UV) radiations [148, 149]. Under UV radiations, MAH produces the excimers viz. MAH^{+} and MAH^{-}. These excimers produced can abstract hydrogen atoms from elastomer molecules which induce cross-linking reaction leading to grafting of elastomer with MAH [148, 150].

6.5 DISPERSION OF CLAY IN NANOCOMPOSITES

X-ray diffraction (XRD) and transmission electron microscopy (TEM) were conducted to examine the type of clay morphology obtained in the nanocomposites as a result of processing methodology. These analysis helped in determining if the processing methodology used was able to achieve the desired clay morphology (i.e. exfoliated morphology) in the nanocomposites. The details of the results are as follows.

6.5.1 XRD analysis

XRD analysis was carried out for pristine nanoclay and for '$E1C_R$' nanocomposite. '$E1C_R$' composition was selected because the same processing method for clay dispersion was followed for all other nanocomposites as was for the '$E1C_R$' nanocomposite. It is well reported in literature that for nanocomposite systems, absence of peak in the XRD spectrum indicates exfoliated morphology [60, 71].

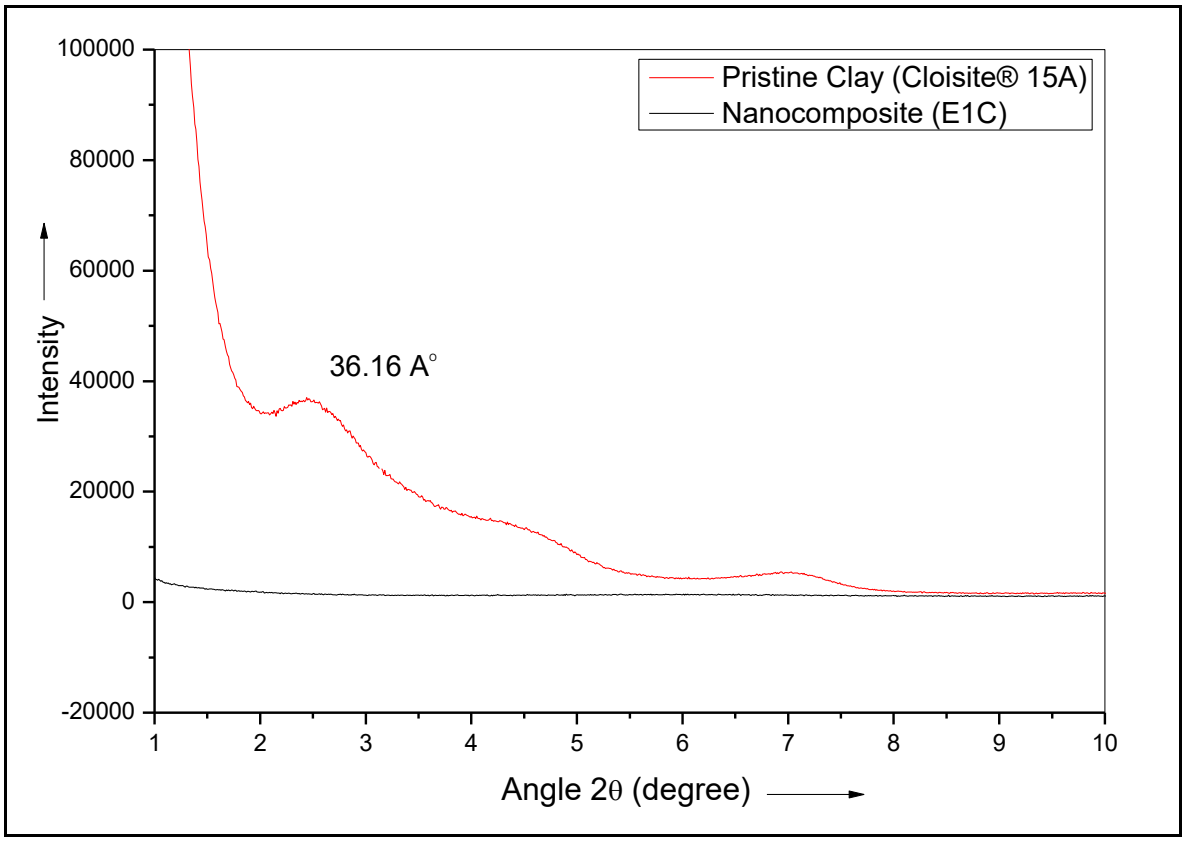

Figure 6.2. XRD patterns for the pristine nanoclay and the nanocomposite system.

Figure 6.2 shows the XRD patterns of pristine nanoclay (Cloisite 15A) and the '$E1C_R$' nanocomposite. As reported earlier in Section 4.5.1, XRD pattern of pristine clay showed peak (d_{001}) at 2.44 degree ($2\theta = 2.44°$) and d-spacing was calculated as 36.16 Å. However, XRD pattern of the nanocomposite system ($E1C_R$) showed absence of peak, indicating an exfoliated morphology of silicate layers in the nanocomposite system.

6.5.2 TEM analysis

To confirm the results obtained through X-ray diffraction pattern, TEM analysis was carried out for '$E1C_R$' composition at two different regions in the nanocomposite system. The dark/black lines represent the clay platelets and the grey background represents the epoxy matrix. Figure 6.3a–b presents the TEM micrographs of '$E1C_R$' composition at two different regions in the nanocomposite system. Figure 6.3a shows that clay layers are non-parallel and randomly aligned. Figure 6.3b shows a mixed type of clay morphology where some clay layers are evenly spaced with large inter-lamellar spacing, indicating uniform dispersion of silicate layers. Thus, TEM

images showed largely an exfoliated clay morphology with uniform dispersion interspersed with intercalated clay layers [78, 87, 154–157].

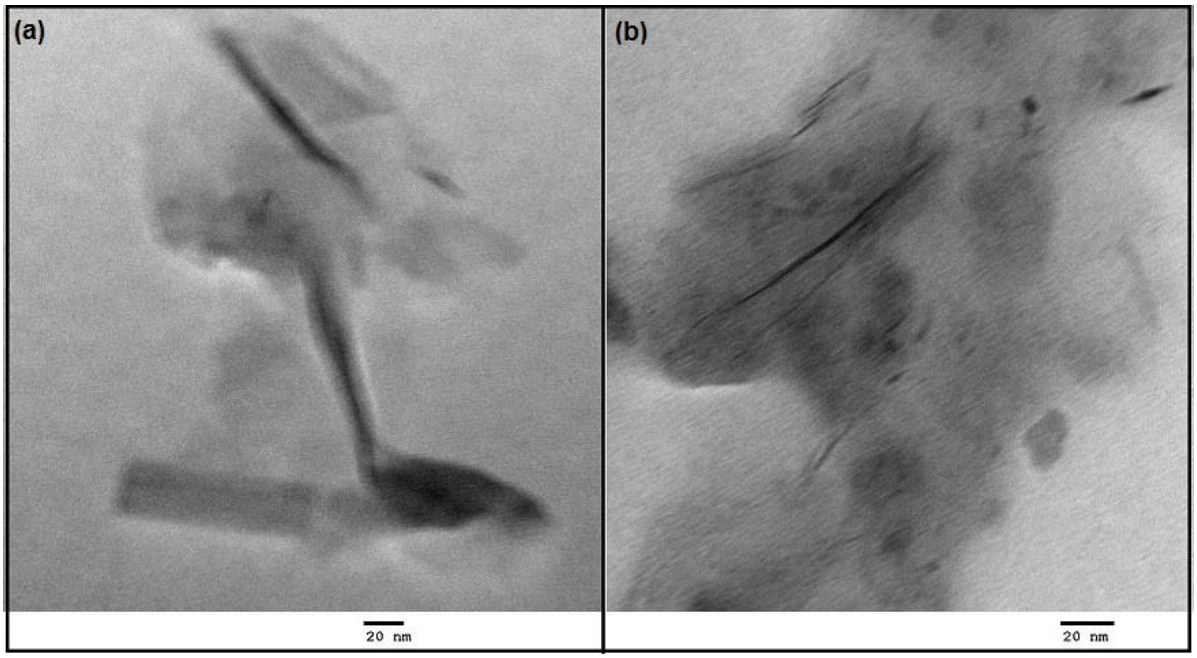

Figure 6.3. TEM micrographs of the epoxy-clay nanocomposite showing clay morphology.

XRD and TEM analysis justified that the processing method used in the present research was effective in dispersing the clay in the nanocomposite system.

6.6 CHANGES IN SURFACE MORPHOLOGY OF EPDM

This section describes the changes observed in the surface morphology of EPDM as a result of surface treatment of this filler including silane treatment and MAH grafting.

6.6.1 SEM-EDS of silane treated ethylene propylene diene monomer filler

Figure 6.4 shows the SEM images of untreated EPDM particles (Figure 6.4a) and those treated with BS silane agent (Figure 6.4b). SEM micrographs of untreated EPDM particles showed a number of large pores (Figure 6.4a). However, for the silane treated EPDM particles (Figure 6.4b), the number and size of pores decreased considerably giving a relatively dense and compact morphology which was attributed to the presence of compatibilizing agent. SEM micrographs, thus, confirmed the presence of silane agents on the treated EPDM.

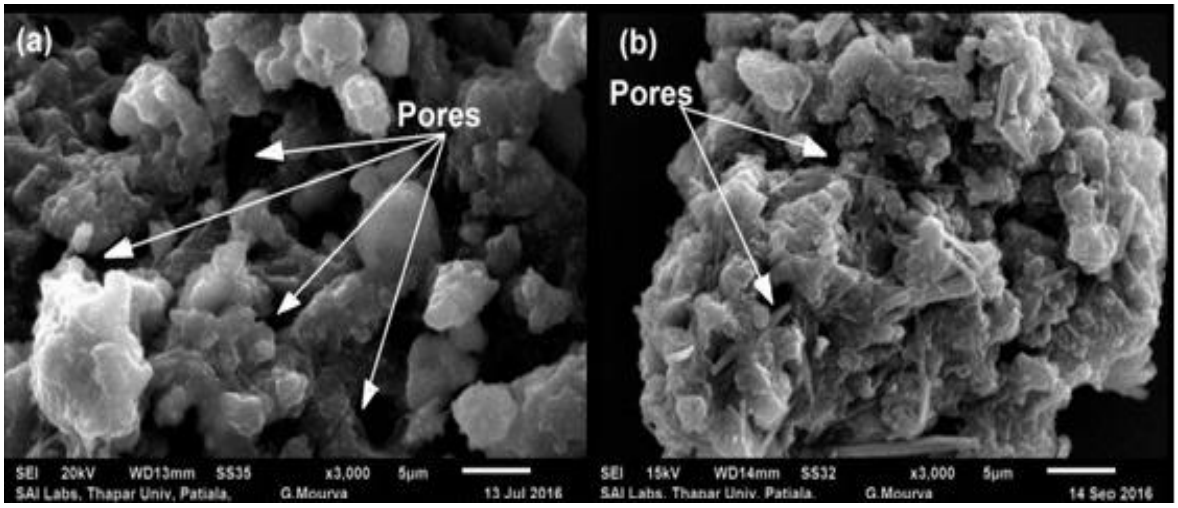

Figure 6.4 SEM micrographs showing surface of ethylene propylene diene monomer in the condition (a) untreated, (b) BS silane treated.

To confirm the SEM results with regards to silane treatment of EPDM particles, energy dispersive spectroscopy (EDS analysis) was conducted. The presence of silane agent on treated EPDM particles was confirmed by the presence of silicon on its surface. Figure 6.5a–b shows the results of EDS analysis. The amount of silicon in the untreated and BS treated EPDM particles was observed as 0 and 1.10 wt. % respectively. The presence of silicon on the surface of treated EPDM surface confirmed successful silane coating on the EPDM filler, and thus, the SEM results.

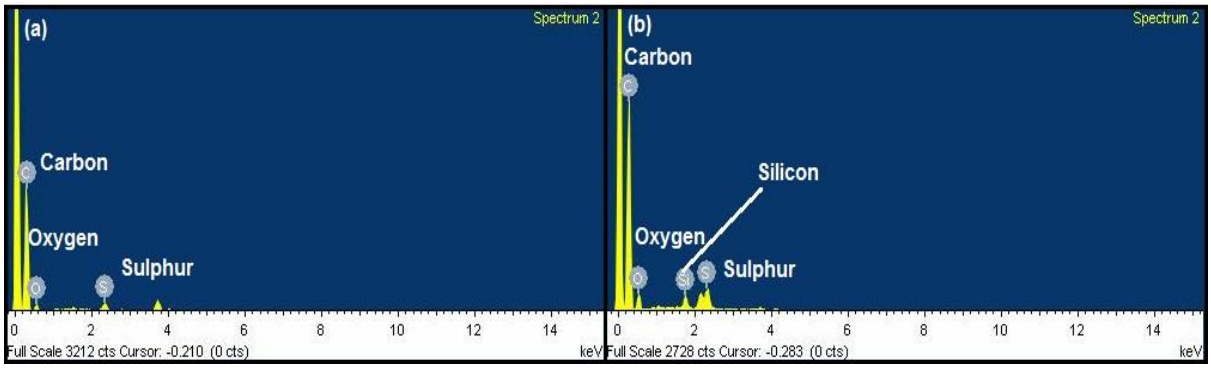

Figure 6.5 Results of EDS of ethylene propylene diene monomer particles in the condition a) untreated, (b) treated with BS silane agent.

6.6.2 SEM and FTIR analysis of MAH grafted ethylene propylene diene monomer filler

As discussed earlier in Section 3.6.4.2, UV-assisted MAH grafting of EPDM particles showed maximum weight gain for treatment time of 20 h (5 g; Table 3.5). So, for MAH grafting of EPDM particles, the optimum treatment time was selected as 20 h. To confirm MAH grafting on EPDM

surface, SEM analysis of untreated EPDM particles and MAH grafted EPDM particles (treated for optimum time period of 20 h) was conducted. SEM micrograph of MAH grafted EPDM (Figure 6.6b) revealed a relatively dense and compact morphology with significantly decreased number and size of pores compared to the morphology of untreated EPDM (Figure 6.6a). These changes were attributed to the presence of MAH on the surface of EPDM particles as a result of MAH grafting.

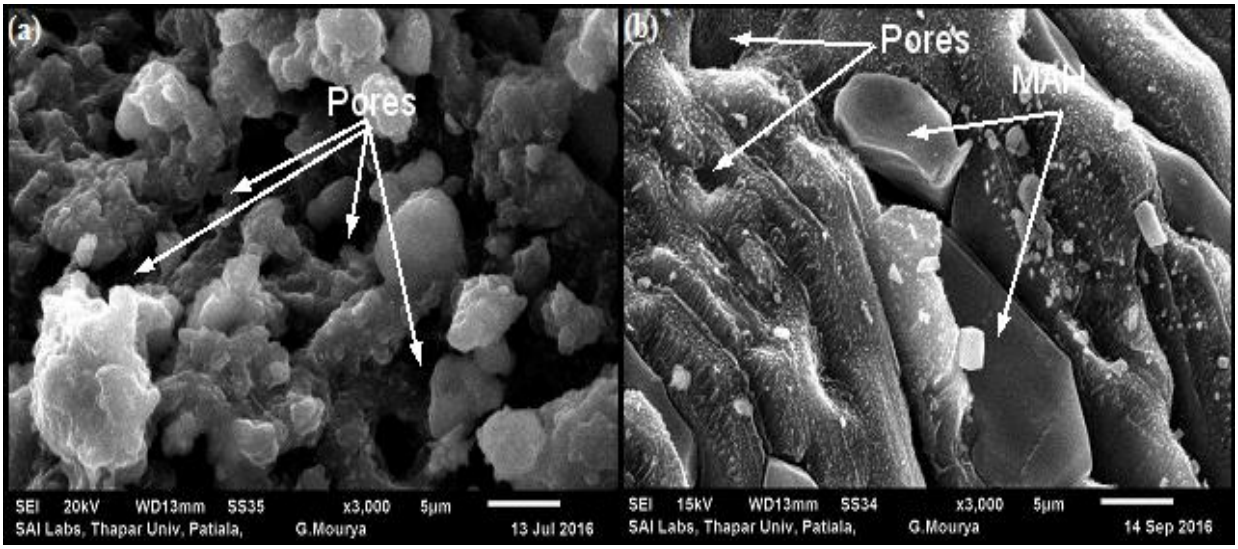

Figure 6.6 SEM micrographs showing ethylene propylene diene monomer in the condition (a) untreated and (b) grafted with MAH for 20 h.

Further, FTIR analysis was conducted for MAH grafted EPDM to confirm the grafting. Figure 6.7 presents the FTIR results for both the untreated EPDM as well as the MAH grafted EPDM particles (treated for optimum period of 20 h). For the MAH grafted rubber, the emergence of a new band at around 1703 cm^{-1} could be due to the C=O symmetric stretching bonds of hydrolysed MAH and existence of dimeric carboxylic acid in MAH grafted EPDM [122, 171, 172]. Further, appearance of another absorption band for the MAH grafted rubber at around 917 cm^{-1} indicated existence of OH group [122, 171]. Finally, the absence of absorption band for MAH grafted rubber at 707 cm^{-1} (which was present in the FTIR spectrum of untreated EPDM) may be related to the C=C bond of maleic anhydride [122]. These observations of FTIR spectra confirmed the grafting of MAH on EPDM rubber particles. Thus, MAH grafting on EPDM filler was confirmed by the FTIR study.

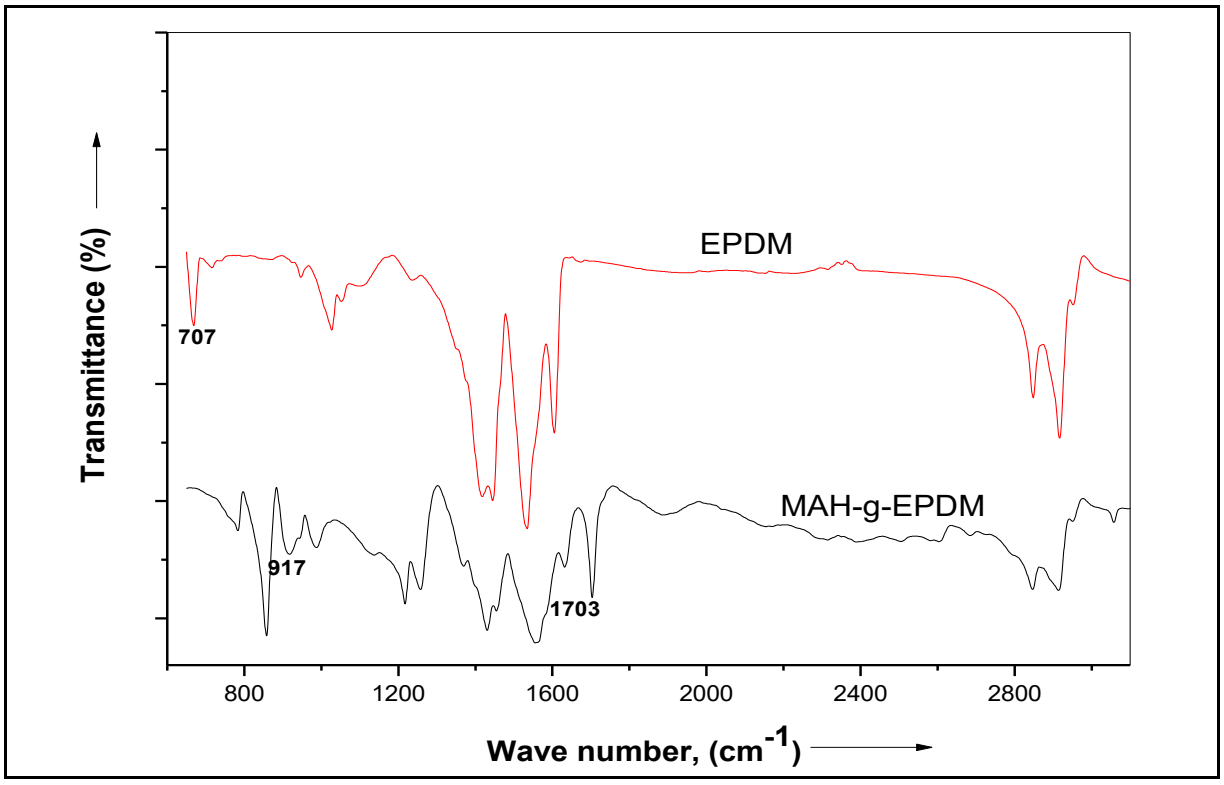

Figure 6.7 FTIR results of untreated and MAH grafted ethylene propylene diene monomer. EPDM = untreated ethylene propylene diene monomer, MAH-g-EPDM = MAH grafted ethylene propylene diene monomer.

6.7 SEM ANALYSIS OF FRACTURED IMPACT SPECIMENS

SEM micrographs of the fracture surface of impact tested specimens were investigated for some typical compositions (NE_R, $E1C_R$, and all nanocomposites containing 5 phr untreated/treated EPDM) to understand the failure behaviour of composites. Figure 6.8a–e presents the SEM micrographs showing fracture surfaces of impact specimens of various GFRPs reinforced with the elastomer filler. Figure 6.8a shows the fracture surface of reference sample 'NE_R'. The micrograph revealed a lack of interaction between the glass fibers and epoxy resin. Also, the surface of epoxy appeared quite smooth which indicated less resistance to failure under impact loading [90, 173]. Figure 6.8b shows the fracture surface of '$E1C_R$' nanocomposite. As compared to 'NE_R', the surface of epoxy in '$E1C_R$' composite was more rough indicating greater resistance to impact loading before failure. Also, epoxy-nanoclay was seen on the glass fibers indicating better interaction among the '$E1C_R$' constituents as compared to 'NE_R' constituents.

SEM image of fracture surface of impact specimen of epoxy-clay GFRP nanocomposite containing 5 phr of untreated EPDM (E1C5R) is presented in Figure 6.8c. Several cavities were observed in the SEM micrograph of fractured specimen which was a result of cavitation of rubber. The toughening mechanisms in rubber reinforced epoxy based composite systems are investigated in detail and well described in literature. On application of mechanical stress, the brittle epoxy is not able to dissipate the mechanical energy adequately. This causes over-stress resulting in formation of cracks. These cracks propagate easily and quickly through the epoxy, leading to brittle failure. To increase the toughness of epoxy based composites, it is required to provide some mechanism for dissipation of mechanical energy while simultaneously limiting the growth and breakdown of voids to prevent premature crack initiation. Under triaxial type of stresses, voids get initiated inside the rubber particles. On cavitation of rubber, the hydrostatic tension in material is relieved, with stress state in thin ligaments of matrix between the voids converting from a triaxial to uniaxial state. This new stress state favours initiation of shear bands, leading to ductile shear yielding mechanism. Cavitation of rubber particles as an energy-dissipating phenomenon significantly lowers the rates of crack propagation in epoxy based composite systems, and thus, leads to high impact strength [27, 30, 32, 170, 174, 175]. Manjunatha *et al*. [41] reported that suppressed matrix cracking along with decreased rate of crack growth (because of plastic deformation mechanisms and cavitation of rubber particles) contribute to improved mechanical performance of epoxy based GFRP composites reinforced with elastomeric filler. For the above stated reasons, the E1C5R nanocomposite showed improved impact strength. Figure 6.8d shows the SEM image of fracture surface of impact specimen of epoxy-clay GFRP nanocomposite sample containing 5 phr silane treated EPDM particles (E1C5RS). It was observed in the SEM micrograph that glass fibers were surrounded with silane treated EPDM reinforced epoxy. This indicated better interfacial adhesion of EPDM with glass fibers due to the silane treatment of EPDM particles. In the SEM image of silane treated EPDM reinforced GFRPs, some cavities like those seen in SEM image of untreated EPDM modified system were also observed.

Figure 6.8e shows the SEM image of 5 phr MAH grafted EPDM modified system. SEM micrographs showed presence of cavities and a rough fractured surface indicating better resistance to impact loading as compared to the reference sample. Also, MAH grafting of EPDM rubber resulted in improved interaction (interfacial adhesion) between compatibilized EPDM rubber

particles and epoxy in the nanocomposite system. The improved mechanical properties obtained for this nanocomposite system (E1C5RMAH) may be attributed to these reasons.

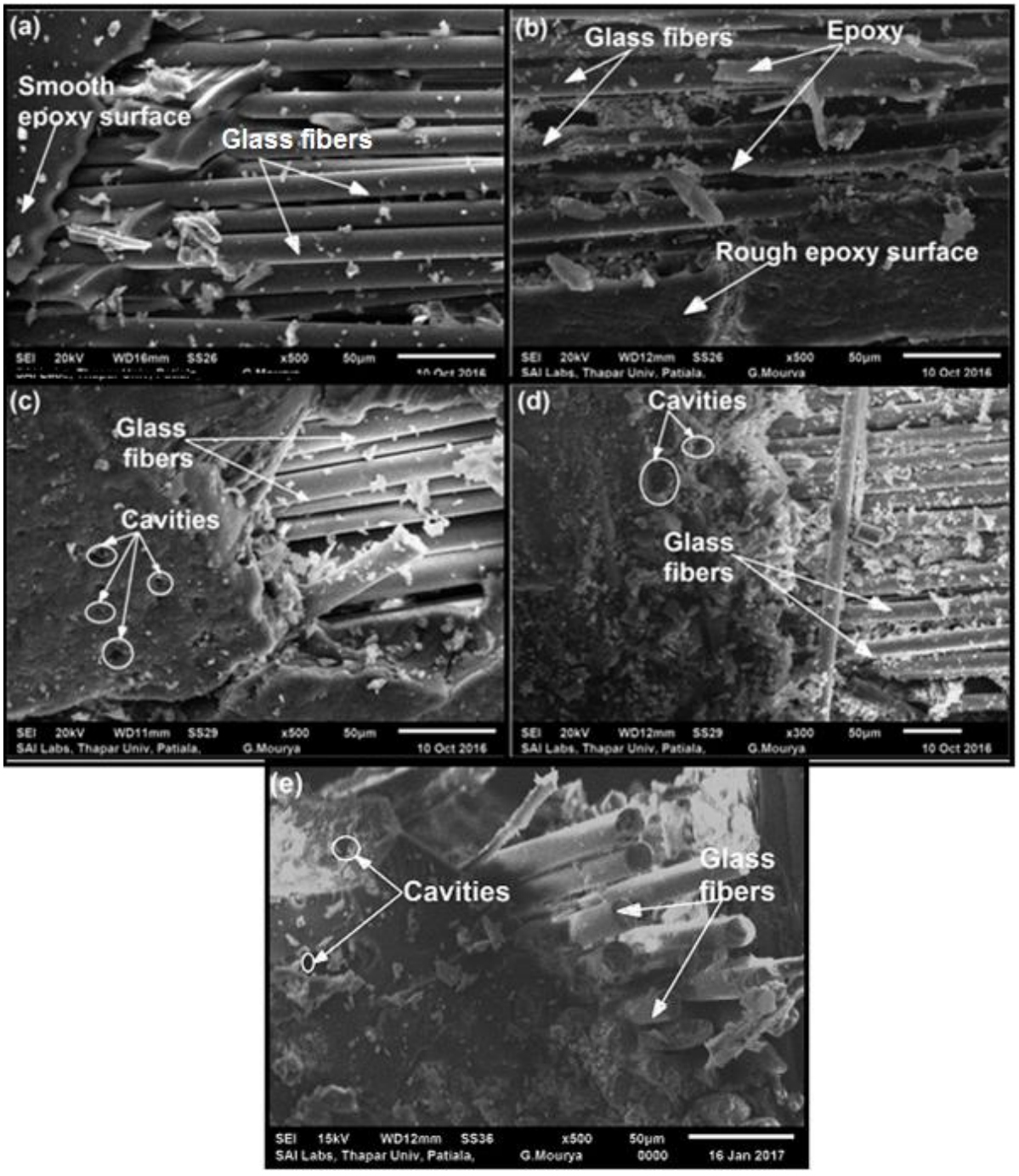

Figure 6.8 SEM micrographs showing fracture surfaces of impact specimens of (a) GFRP without clay and EPDM (NE_R), (b) nanocomposite without EPDM ($E1C_R$), (c) nanocomposite with 5 phr EPDM (E1C5R), (d) nanocomposite with 5 phr BS treated EPDM (E1C5RS), and (e) nanocomposite with 5 phr MAH grafted EPDM (E1C5RMAH). EPDM = Ethylene propylene diene monomer.

Thus, it was observed that, in addition to the phenomenon of cavitation of rubber particles, improvement in interfacial adhesion of constituents of nanocomposites because of surface treatment of elastomer filler resulted in improved impact strength. Silane treatment improved the interfacial adhesion between EPDM particles and glass fibers whereas MAH grafting improved the compatibility between EPDM particles and epoxy matrix.

The next chapter presents the conclusions to be drawn from the present study and future scope of research work.

CHAPTER 7

CONCLUSIONS AND RECOMMENDATIONS FOR FUTURE WORK

7.1 GENERAL

Epoxy based GFRP nanocomposites reinforced with clay as the nano-filler and thermoplastic fibers/elastomer particles as the micro-filler were processed using vacuum assisted hand lay-up technique. This multi-scale reinforcement combining a soft and ductile micro-reinforcement with a rigid nano-reinforcement proved successful in significantly improving the impact strength of epoxy based GFRPs.

The main conclusions drawn from the present research are discussed in the following sections.

7.2 PROCESSING OF EPOXY BASED NANOCOMPOSITES

The processing methodology including the sequence of steps and range of process parameters, used in the present work were effective in fabrication of epoxy based GFRPs possessing significantly improved mechanical performance.

- For dispersion of nano-reinforcement in the epoxy resin, homogenization followed by ultrasonication was performed. Homogenization at 20,000 rpm for 10 min and ultrasonication at 80% amplitude with pulse-on and pulse-off time periods as 40 s and 20 s respectively, were able to effectively disperse the nanoclay in the composite system. Further, for dispersion of micro-reinforcements, mechanical stirring at 500 rpm for 15 min was used for polymer fibers whereas homogenization at 20,000 rpm for 10 min was used for ethylene propylene diene monomer (EPDM) rubber particles. Finally, curing agent was added to the resin system by mechanical stirring at 500 rpm for 10 min.
- XRD results and TEM analysis showed that the processing methodology was effective in dispersing the nanoclay and obtaining the desired morphology for silicate layers in the nanocomposite system. XRD diffractograms showed absence of 'd_{001}' peak for the nanocomposites. TEM micrographs confirmed the XRD results and revealed largely an exfoliated morphology with individual clay layers randomly distributed, with some degree of intercalation also with increased inter-lamellar spacing.

- For compatibilization of micro-fillers i.e. improved interfacial adhesion of polymer fibers/elastomer particles with other constituents of the nanocomposite system, surface modification of micro-fillers using silane treatment and UV-assisted maleic anhydride (MAH) grafting was very effective.
- For MAH grafting of micro-fillers, optimum exposure time of MAH-acetone solution to UV radiations was determined as 30 h, 08 h, and 20 h for polypropylene (PP) fibers, polyethylene terephthalate (PET) fibers, and EPDM particles, respectively. These optimum time periods resulted in weight gain of 109%, 150%, and 125% for PP fibers, PET fibers, and EPDM particles respectively. It was observed that for exposure time periods in excess of the optimum time, the surface of micro-fillers ruptured due to prolonged exposure to UV radiations.

7.3 PROPERTIES OF SYNTHESIZED NANOCOMPOSITES

The epoxy based GFRP nanocomposites studied in the present work displayed significantly improved impact strength. The main conclusions with regards to mechanical performance of the processed GFRPs are as follows:

- Addition of 1 phr nanoclay to the reference GFRP slightly improved the impact strength by 4%. Addition of this nano-reinforcement improved the tensile strength and tensile modulus values of reference GFRP by 16% and 6%, respectively.
- Addition of untreated thermoplastic polymeric fibers (PP fibers/PET fibers) to the nanocomposite system resulted in deterioration of impact strength as well as tensile properties. This decrease was due to the inert nature of thermoplastic fibers resulting in their poor compatibility with other constituents of the nanocomposite system. However, addition of untreated elastomeric particles (EPDM rubber) to the nanocomposite system improved the impact strength (with maximum improvement of 27%) till an optimum concentration of 5 phr elastomer loading. This improvement was mainly due to cavitation of rubber particles in the nanocomposite system.
- Compatibilization procedures used for surface modification of micro-fillers were successful in bringing chemical as well as morphological changes on the surface of micro-fillers as was confirmed by SEM-EDS results and FTIR analysis. These changes enhanced the interfacial

adhesion of micro-fillers with other constituents of the composite system and resulted in significant improvements in impact strength of resulting GFRPs.

- Silane treatment of thermoplastic fibers/elastomeric particles improved the interfacial adhesion of these micro-fillers with glass fibers. As a result, for a given composition, impact strength and tensile properties of nanocomposites reinforced with silane treated polymer fibers/elastomer fillers was significantly higher than their counterparts reinforced with untreated micro-fillers.
- The optimum loading of polymer fibers (PP fibers/PET fibers) in the nanocomposite system for maximum improvement in impact strength was 2 phr. Addition of silane treated PP fibers and PET fibers resulted in maximum improvement in impact strength of nanocomposites by 44% (with 2 phr of MS silane treated PP fibers) and 19% (with 2 phr of VS silane treated PET fibers), respectively with a minor drop in tensile properties. For fiber concentration beyond this optimum value (i.e. at 3 phr), a decrease in impact strength was observed. This was attributed to the poor dispersion of PP fibers/PET fibers in nanocomposites because of the concomitant high viscosity of resin at such high concentration of reinforcement.
- The optimum loading of EPDM filler in nanocomposite system for maximum improvement in impact strength was 5 phr with BS silane treatment. Addition of silane treated EPDM rubber particles resulted in maximum improvement of 68% in impact strength of resulting nanocomposites. This significant increase in impact strength was due to the combined effect of improved compatibility between EPDM filler and glass fibers along with cavitation phenomenon of rubber particles.
- UV-assisted MAH grafting of thermoplastic fibers/elastomeric particles improved the interfacial adhesion of these micro-fillers with epoxy matrix. Similar to the case of silane treated micro-fillers, addition of MAH grafted micro-fillers also improved the impact strength and tensile properties of nanocomposites as compared to when nanocomposites were reinforced with untreated micro-fillers. Further, for a given composition of nanocomposites, improvement in impact strength with MAH grafted micro-fillers was lesser as compared to silane treated micro-fillers. However, MAH grafting resulted in better recovery of tensile properties of nanocomposites.

7.4 MAJOR CONCLUSIONS

For the first time, GFRP nanocomposites with glass fibers as the macro reinforcement, clay as the nano-filler, and compatibilized polymer fibers/elastomer particles as the micro-sized filler were fabricated successfully providing improved impact strength without much drop in tensile properties. This multi-scale reinforcement containing glass fibers and combining a soft micro-reinforcement with a rigid nano-reinforcement proved successful in improving the mechanical performance of epoxy based GFRP nanocomposite system.

- The present research was based on the premise that despite the lower strength and modulus of polymer/elastomer fillers, the impact strength of GFRPs reinforced with them would increase because of the good ductility of these micro-fillers, while tensile properties of GFRPs may decrease. However, impact strength deteriorated (except for elastomer modified GFRPs) even on addition of a more ductile component i.e. untreated micro-fillers. This was attributed to a lack of compatibility of polymer/elastomer fillers with other constituents of the composite system.
- All the compatibilization procedures used for surface modification of micro-fillers were effective in improving interfacial adhesion between constituents of composite system, thereby resulting in significant improvements in impact strength of nanocomposites. Silane treatment of polymer/elastomer filler was more effective than UV-assisted MAH grafting.
- The more ductile was the micro-filler reinforcement (EPDM rubber, PP, PET; in this order), greater was the improvement achieved in impact strength of nanocomposites. For the epoxy based GFRPs processed in the present work, maximum improvement obtained in impact strength was 68%, 44%, and 19% with micro-filler as EPDM rubber particles, PP fibers, and PET fibers, respectively.

It is concluded that several mechanisms including stress transfer capability of silicate layers, improved interfacial adhesion of micro-filler reinforcement with other constituents as a result of compatibilization procedures, and also cavitation of rubber particles in case of elastomer modified systems, resulted in an improved impact strength of epoxy based GFRP nanocomposites. The nanocomposite formulations processed in the present research were highly viscous as a result of multi-scale reinforcements. It was a tremendous processing challenge to fabricate uniform FRP sheets with minimal defects. Despite these processing difficulties, nanocomposites with

significantly enhanced impact behaviour were developed. The processing methodology developed in the present work, including (i) reinforcing compatibilized micro-fillers, and (ii) processing highly viscous systems, will open up new paths for further research to enhance the mechanical properties of epoxy based GFRP nanocomposites.

7.5 SCOPE OF FUTURE WORK

- In the present research, polymer fillers (PET and PP fibers) and elastomer filler (EPDM rubber particles) were used. A wide spectrum of thermoplastic/elastomeric fillers are available having different values of ductility, tensile strength, and impact strength. These fillers with diverse mechanical properties can be suitably reinforced after compatibilization into the epoxy-clay based GFRPs to obtain further enhancement in impact strength.
- In the present research, only the micro-filler was compatibilized for its improved adhesion with other constituents of composite system. There is a scope of further improvement in mechanical properties of nanocomposites by addition of compatibilized nano-clay or compatibilized glass fibers, or both. Even for the micro-fillers, various other surface modifications techniques available can be evaluated.
- The nano-clay content was kept constant at a low value of 1 phr keeping in view the resultant higher viscosity due to addition of thermoplastic fibers till 3 phr and elastomer filler till 10 phr. Further research can be done with different combinations of clay-filler concentration (with clay concentration higher than 1phr) for further improvement in mechanical properties of resulting nanocomposites.

REFERENCES

[1] Kotsilkova R, Pissis P, Silvestre C, Cimmino S, Duraccio D. editors. Thermoset Nanocomposites for Engineering Applications. UK: Smithers Rapra Technology Limited; 2007.

[2] Camargo P H C, Satayanarayana K G, Wypych F. Nanocomposites : synthesis, structure, properties and new application opportunities. Materials Research 2009; 12: 1–39. DOI: 10.1590/S1516-14392009000100002.

[3] Hamidi Y K, Aktas L, Altan M C. Composite materials effect of nanoclay content on void morphology in resin transfer. Journal of Thermoplastic Composite Materials 2008; 131: 1–11. DOI: 10.1177/0892705707083635.

[4] Karabulut M. Production and characterization of nanocomposite materials from recycled thermoplastics. Master of Science. The Middle East Technical University, Ankara, Turkey 2003.

[5] Li Y, Lu D, Wong C P. editors. Electrical conductive adhesives with nanotechnologies. Germany: Springer; 2010. DOI: 10.1007/978-0-387-88783-8_2.

[6] Utracki L A, Kamal M R. Clay-containing polymeric nanocomposites. The Arabian Journal for Science and Engineering 2002; 27: 43–67.

[7] Lee J H, Advani S G, Li-Yu L, Gye-Hyong Y. The preparation of clay/glass fiber/epoxy hybrid nanocomposites using VARTM. The 7th International Conference on Flow Process in Composite Materials, Newark, Delaware, USA, February 7–9, 2004.

[8] Asgari M and Sundararaj U. Silane functionalization of sodium montmorillonite: nanoclay: the effect of dispersing media on intercalation and chemical grafting. Applied Clay Science 2018; 153: 228–238. DOI: 10.1016/j.clay.2017.12.020.

[9] Sharma B, Chhibber R, Mehta R. Effect of mixing parameters, postcuring, and stoichiometry on mechanical properties of fiber reinforced epoxy–clay nanocomposites. Proceedings of the Institution of Mechanical Engineers, Part L: Journal of Materials: Design and Applications 2018. DOI: 10.1177/1464420717752023.

[10] Zabihi O, Ahmadi M, Nikafshar S, Chandrakumar P K, Naebe M. A technical review on epoxy-clay nanocomposites: Structure, properties, and their applications in fiber reinforced composites. Composites Part B: Engineering 2018; 135: 1–24. DOI: 10.1016/j.compositesb.2017.09.066.

[11] Alexandre M and Dubois P. Polymer layered-silicate nanocomposites: preparation,

properties and uses of a new class of materials. Materials Science and Engineering 2000; 28: 1–63. DOI: 10.1016/S0927-796X(00)00012-7.

[12] Chow W S. Water absorption of epoxy/glass fiber/organo-montmorillonite nanocomposites. Express Polymer Letters 2007; 1: 104–108. DOI: 10.3144/expresspolymlett.2007.18.

[13] Singh P, Kaushik A, Kaur K. Mechanical properties and swelling behavior of short glass fiber reinforced polyester composites. Journal of Thermoplastic Composite Materials 2005; 18: 543–559. DOI: 10.1177/0892705705055444.

[14] Ansari M M, Chakrabarti A. Influence of projectile nose shape and incidence angle on the ballistic perforation of laminated glass fiber composite plate. Composites Science and Technology 2017; 142: 107–116. DOI: 10.1016/j.compscitech.2016.12.033.

[15] Dhanapal D, Srinivasan A K, Ramalingam N. Role of POSS as coupling agent for DGEBA/GF reinforced nanocomposites. Silicon 2018; 10: 537–548. DOI: 10.1007/s12633-016-9487-8.

[16] Jahandideh S, Shirazi M J S, Tavakoli M. Mechanical and thermal properties of octadecylamine-functionalized graphene oxide reinforced epoxy nanocomposites. Fibers and Polymers 2017; 18: 1995–2004. DOI: 10.1007/s12221-017-7417-z.

[17] Kwon D J, Shin P S, Kim J H, Baek Y M, Park H S, DeVries K L, Park J M. Interfacial properties and thermal aging of glass fiber/epoxy composites reinforced with SiC and SiO_2 nanoparticles. Composites Part B: Engineering 2017; 130: 46–53. DOI: 10.1016/j.compositesb.2017.07.045.

[18] Singh P, Kaushik A, Gupta P. Characterization of short glass fiber-reinforced castor oil-based polyurethane polystyrene interpenetrating networks. International Journal of Polymeric Materials and Polymeric Biomaterials 2006; 55: 359–372. DOI: 10.1080/009140390968056.

[19] Lee J J, Nam I, Kim H. Thermal stability and physical properties of epoxy composite reinforced with silane treated basalt fiber. Fibers and Polymers 2017; 18: 140–147. DOI: 10.1007/s12221-017-6752-4.

[20] Safi S, Zadhoush A, Ahmadi M, Pedram S, Tehrani R. Hybrid silane-treated glass fabric/epoxy composites : tensile properties by micromechanical approach. Iranian Polymer Journal 2018; 27: 1–11. DOI: https://doi.org/10.1007/s13726-017-0578-1.

[21] Upadhyay A K, Pandey R, Shukla K K. Nonlinear flexural response of laminated composite plates under hygro-thermo-mechanical loading. Communications in Nonlinear Science and Numerical Simulation 2010; 15: 2634–2650.

DOI: 10.1016/j.cnsns.2009.08.026.

[22] Ansari M M, Chakrabarti A. Impact behaviour of GFRP and Kevlar/epoxy sandwich composite plate: experimental and FE analyses. Journal of Mechanical Science and Technology 2017; 31: 771–776. DOI: 10.1007/s12206-017-0128-y.

[23] Prusty R K, Rathore D K, Ray B C. CNT/polymer interface in polymeric composites and its sensitivity study at different environments. Advances in Colloidal and Interface Science 2017; 240: 77–106. DOI: https://doi.org/10.1016/j.cis.2016.12.008.

[24] Mittal G, Rhee K Y, Mi V, Hui D. Reinforcements in multi-scale polymer composites: processing, properties, and applications. Composites Part B: Engineering 2018; 138: 122–139. DOI: https://doi.org/10.1016/j.compositesb.2017.11.028.

[25] Bui T Q, Nguyen M N, Zhang C. An efficient meshfree method for vibration analysis of laminated composite plates. Computational Mechanics 2011; 48: 175–193. DOI: 10.1007/s00466-011-0591-8.

[26] Hamouda A M., Hashmi M S. Testing of composite materials at high rates of strain: advances and challenges. Journal of Materials Processing Technology 1998; 77: 327–336. DOI: 10.1016/S0924-0136(97)00436-6.

[27] Balakrishnan S and Raghavan D. Acrylic, elastomeric, particle-dispersed epoxy-clay hybrid nanocomposites: Mechanical properties. Macromolecular Rapid Communications 2004; 25: 481–485. DOI: 10.1002/marc.200300111.

[28] Balakrishnan S, Start P R, Raghavan D, Hudson S D. The influence of clay and elastomer concentration on the morphology and fracture energy of preformed acrylic rubber dispersed clay filled epoxy nanocomposites. Polymer 2005; 46: 11255–11262. DOI: 10.1016/j.polymer.2005.10.053.

[29] Lee K Y, Kim K Y, Hwang I R, Choi Y S, Hong C H. Thermal, tensile and morphological properties of gamma-ray irradiated epoxy-clay nanocomposites toughened with a liquid rubber. Polymer Testing 2010; 29: 139–146. DOI: 10.1016/j.polymertesting.2009.10.003.

[30] Manjunatha C M, Taylor A C, Kinloch A J, Sprenger S. The tensile fatigue behaviour of a silica nanoparticle-modified glass fibre reinforced epoxy composite. Composites Science and Technology 2010; 70: 193–199. DOI: 10.1016/j.compscitech.2009.10.012

[31] Pandey R, Upadhyay A K, Shukla K K, Jain A. Nonlinear dynamic response of elastically supported laminated composite plates. Mechanics of Advanced Materials and Structures 2012; 19: 397–420. DOI: 10.1080/15376494.2010.528161.

[32] Dadfar M R and Ghadami F. Effect of rubber modification on fracture toughness

properties of glass reinforced hot cured epoxy composites. Materials and Design 2013; 47: 16–20. DOI: 10.1016/j.matdes.2012.12.035.

[33] Ngah S A and Taylor A C. Toughening performance of glass fibre composites with core-shell rubber and silica nanoparticle modified matrices. Composites Part A: Applied Science and Manufacturing 2016; 80: 292–303. DOI: 10.1016/j.compositesa.2015.10.036.

[34] Flore D, Wegener K, Seel D, Oetting C C, Bublat T. Investigation of chemical ageing and its effect on static and fatigue strength of continuous fibre reinforced plastics. Composites Part A: Applied Science and Manufacturing 2016; 90: 359–370. DOI: 10.1016/j.compositesa.2016.08.001.

[35] Yasmin A, Abot J L, Daniel I M. Processing of clay/epoxy nanocomposites by shear mixing. Scripta Materialia 2003; 49: 81–86. DOI: 10.1016/S1359-6462(03)00173-8.

[36] Gupta N, Lin T C, Shapiro M. Clay/epoxy nanocomposites: processing and mechanical properties. Journal of the Minerals Metals and Materials Society 2007; 59: 61–65. DOI: https://doi.org/10.1007/s11837-007-0041-4.

[37] Yao X F, Zhou D, Yeh H Y. Macro/microscopic fracture characterizations of SiO_2/epoxy nanocomposites. Aerospace Science and Technology 2008; 12: 223–230. DOI: 10.1016/j.ast.2007.03.005.

[38] Ozdemir N G. Toughening of carbon fibre reinforced polymer composites with rubber nanoparticles for advanced industrial applications. Express Polymer Letters 2016; 10: 394–407. DOI: 10.3144/expresspolymlett.2016.37.

[39] Leelachai K, Kongkachuichay P, Dittanet P. Toughening of epoxy hybrid nanocomposites modified with silica nanoparticles and epoxidized natural rubber. Journal of Polymer Research 2017; 24: 1–13. DOI: 10.1007/s10965-017-1202-y.

[40] Liu W, Hoa S V, Pugh M. Morphology and performance of epoxy nanocomposites modified with organoclay and rubber. Polymer Engineering and Science 2004; 44: 1178–1186. DOI: 10.1002/pen.20111.

[41] Manjunatha C M, Sprenger S, Taylor A C, Kinloch A J. The Tensile fatigue behavior of a glass-fiber reinforced plastic composite using a hybrid-toughened epoxy matrix. Journal of Composite Materials 2010; 44: 2095–2109. DOI: 10.1177/0021998309360943.

[42] Dutra R C L, Soares B G, Campos E A, Melo J D G D, Silva J L G. Composite materials constituted by a modified polypropylene fiber and epoxy resin. Journal of Applied Polymer Science 1999; 73: 69–73. DOI: 10.1002/(SICI)1097-

4628(19990705)73:1<69::AID-APP8>3.0.CO;2-5.

[43] Dutra R C L, Soares B G, Campos E A., Silva J L G. Hybrid composites based on polypropylene and carbon fiber and epoxy matrix. Polymer 2000; 41: 3841–3849. DOI: 10.1016/S0032-3861(99)00552-2.

[44] Prabhu T N, Hemalatha Y J, Harish V, Prashantha K, Iyengar P. Thermal degradation of epoxy resin reinforced with polypropylene fibers. Journal of Applied Polymer Science 2007; 104: 500–503. DOI: 10.1002/app.25523.

[45] Ratna D. Toughened FRP composites reinforced with glass and carbon fiber. Composites Part A: Applied Science and Manufacturing 2008; 39: 462–469. DOI: 10.1016/j.compositesa.2007.12.005.

[46] Sanchez-Cabezudo M, Prolongo M G, Salom C, Cid M A G D, Masegosa R M. Ternary nanocomposites: curing, morphology, and mechanical properties of epoxy/thermoplastic/ organoclay systems. Polymers and Polymer Composites 2016; 37: 2184-2195. DOI: 10.1002/pc.23397.

[47] Xie Y, Hill C A S, Xiao Z, Militz H, Mai C. Silane coupling agents used for natural fiber/polymer composites: a review. Composites Part A: Applied Science and Manufacturing 2010; 41: 806–819. DOI: 10.1016/j.compositesa.2010.03.005.

[48] Punyamurthy R, Sampathkumar D. Abaca fiber reinforced epoxy composites: evaluation of impact strength. International Journal of Basic and Applied Sciences 2014; 18: 305–317.

[49] Mahjoub R, Yatim J M, Mohd Sam A R, Hashemi S H. Tensile properties of Kenaf fiber due to various conditions of chemical fiber surface modifications. Construction and Building Materials 2014; 55: 103–113. DOI: 10.1016/j.conbuildmat.2014.01.036.

[50] Fiore V, Di Bella G, Valenza A. The effect of alkaline treatment on mechanical properties of Kenaf fibers and their epoxy composites. Composites Part B: Engineering 2015; 68: 14–21. DOI: 10.1016/j.compositesb.2014.08.025.

[51] Nattapat M, Marimuthu S, Kamara A M, Esfahani M R N. Laser surface modification of carbon fiber reinforced composites. Materials and Manufacturing Processes 2015; 30: 1450–1456. DOI: 10.1080/10426914.2015.1019097.

[52] Rajan R, Rainosalo E. Modification of epoxy resin by silane-coupling agent to improve tensile properties of viscose fabric composites. Polymer Bulletin 2018; 75: 167–195. DOI: 10.1007/s00289-017-2022-2.

[53] Favis B D, Blanchard L P, Leonard J, Prud'Homme R E. The interaction of a cationic silane coupling agent with mica. Journal of Applied Polymer Science 1983; 28:

1235–1244. DOI: 10.1002/app.1983.070280327.

[54] Lu H, Roy S, Sampathkumar P J M. Characterization of the fracture behavior of epoxy nanocomposites. Proceedings of the 17th Annual Technical Conference of the American Society for Composites, Purude Univeristy, West Liafayette, Indidna, October 20–23, 2005.

[55] Liu T, Tjiu W C, Tong Y, He C, Goh S S, Chung T S. Morphology and fracture behavior of intercalated epoxy/clay nanocomposites. Journal of Applied Polymer Science 2004; 94: 1236–1244. DOI: 10.1002/app.21033.

[56] Wang K, Chen L, Wu J, Toh M L, He C, Yee A F. Epoxy nanocomposites with highly exfoliated clay: mechanical properties and fracture mechanisms. Macromolecules 2005; 38: 788–800. DOI: 10.1021/ma048465n.

[57] Ngo T D, Ton-That M T, Hoa S V. Preparation and properties of epoxy nanocomposites. Part I. The effect of premixing on dispersion of organoclay. Polymer Engineering and Science 2009; 49: 666–672. DOI: 10.1002/pen.

[58] Satapathy S and Mohanty G C. Synthesis and characterization of layered silicate/epoxy nanocomposite. Pelagia Research Library: Advances in Applied Science Research 2012; 3: 3981–3986.

[59] Kusmono, Wildan M W, Ishak Z A M. Preparation and properties of clay-reinforced epoxy nanocomposites. International Journal of Polymer Science 2013; 2013: 1–7. DOI: http://dx.doi.org/10.1155/2013/690675.

[60] Sharmila T K B, Ayswarya E P, Abraham B T, Begum P M S, Thachil E T. Fabrication of partially exfoliated and disordered intercalated cloisite epoxy nanocomposites via in situ polymerization: mechanical, dynamic mechanical, thermal and barrier properties. Applied Clay Science 2014; 102: 220–230. DOI: 10.1016/j.clay.2014.09.043.

[61] Ying Z, Xianggao L, Bin C, Fei C, Jing F. Highly exfoliated epoxy/clay nanocomposites : mechanism of exfoliation and thermal/mechanical properties. Composite Structures 2015; 132: 44–49. DOI: 10.1016/j.compstruct.2015.05.017.

[62] Sharifi M, Ebrahimi S J M. Preparation and characterization of a high performance powder coating based on epoxy/clay nanocomposite. Progress in Organic Coatings 2017; 106: 69–76. DOI: https://doi.org/10.1016/j.porgcoat.2017.02.013.

[63] Isik I, Yilmazer U, Bayram G. Impact modified epoxy/montmorillonite nanocomposites: synthesis and characterization. Polymer 2003; 44: 6371–6377. DOI: 10.1016/S0032-3861(03)00634-7.

[64] Lam C K, Cheung H Y, Lau K T, Zhou L M, Ho M W, Hui D. Cluster size effect in

hardness of nanoclay/epoxy composites. Composites Part B: Engineering 2005; 36: 263–269. DOI: 10.1016/j.compositesb.2004.09.006.

[65] Akbari B and Bagheri R. Deformation mechanism of epoxy/clay nanocomposite. European Polymer Journal 2007; 43: 782–788. DOI: 10.1016/j.eurpolymj.2006.11.028.

[66] Lim S R and Chow W S. Fracture toughness enhancement of epoxy by organo-montmorillonite. Polymer-Plastics Technology and Engineering 2011; 50: 182–189. DOI: 10.1080/03602559.2010.531427.

[67] Mouloud A, Cherif R, Fellahi S, Grohens Y, Pillin I. Study of morphological and mechanical performance of amine-cured glassy epoxy–clay nanocomposites. Journal of Applied Polymer Science 2012; 124: 4729–4739. DOI: 10.1002/app.

[68] Ngo T D, Ton-That M T, Hoa S V. Preparation and properties of epoxy nanocomposites. Part 2: The effect of dispersion and intercalation/exfoliation of organoclay on mechanical properties. Polymer Engineering and Science 2012; 52: 607–614. DOI: 10.1002/pen.21359.

[69] Olad A, Azar R H, Babaluo A A. Investigation on the mechanical and thermal properties of intercalated epoxy/layered silicate nanocomposites. International Journal of Polymeric Materials 2012; 61: 1035–1049. DOI: 10.1080/00914037.2011.617333.

[70] Ying Z, Xianggao L, Bin C, Fei C, Jing F. Highly exfoliated epoxy/clay nanocomposites: mechanism of exfoliation and thermal/mechanical properties. Composite Structures 2015; 132: 44–49. DOI: 10.1016/j.compstruct.2015.05.017.

[71] Al-Qadhi M, Merah N, Gasem Z M. Mechanical properties and water uptake of epoxy-clay nanocomposites containing different clay loadings. Journal of Materials Science 2013; 48: 3798–3804. DOI: 10.1007/s10853-013-7180-5.

[72] Al-Qadhi M, Merah N, Gasem Z M, Abu-Dheir N. Effect of water and crude oil on mechanical and thermal properties of epoxy-clay nanocomposites. Polymer Composites 2014; 35: 318–326. DOI: 10.1002/pc.22664.

[73] Pascual-Sánchez V, Barrientos-Ramirez S, Martín-Martínez J M. Comparative study of the effect of addition of silica and silicate nanofillers on the properties of epoxy coatings. Composite Interfaces 2010; 17: 513–532. DOI: 10.1163/092764410X513477.

[74] Becker O, Varley R J, Simon G P. Thermal stability and water uptake of high performance epoxy layered silicate nanocomposites. European Polymer Journal 2004; 40: 187–195. DOI: 10.1016/j.eurpolymj.2003.09.008.

[75] Mittal V. Epoxyg-vermiculite nanocomposites as gas permeation barrier. Journal of Composite Materials 2008; 42: 2829–2839. DOI: 10.1177/0021998308096954.

[76] Paul D R, Robeson L M. Polymer nanotechnology: nanocomposites. Polymer 2008; 49: 3187–3204. DOI: 10.1016/j.polymer.2008.04.017.

[77] Rafiq A, Al-Qadhi M, Merah N, Ali Y. Mechanical behavior of hybrid glass fibre/epoxy clay nanocomposites. Advanced Materials Research 2014; 894: 336–341. DOI: 10.4028/www.scientific.net/AMR.894.336.

[78] Bashar M, Mertiny P, Sundararaj U. Effect of nanocomposite structures on fracture behavior of epoxy-clay nanocomposites prepared by different dispersion methods. Journal of Nanomaterials 2014; 2014: 1–13. DOI: http://dx.doi.org/10.1155/2014/312813.

[79] Bucknall C B, Partridge I K. Phase separation in epoxy resins containing polyethersulphone. Polymer 1983; 24: 639–644. DOI: 10.1016/0032-3861(83)90120-9.

[80] Bucknall C B, Gilbert A H. Toughening tetrafunctional epoxy resins using polyetherimide. Polymer 1989; 30: 213–217. DOI: 10.1016/0032-3861(89)90107-9.

[81] Shih W C, Ma C C M, Yang J C, Chen H De. Polydimethylsiloxane containing isocyanate group-modified epoxy resin: curing, characterization, and properties. Journal of Applied Polymer Science 1999; 73: 2739–2747. DOI: 10.1002/(SICI)1097-4628(19990923)73:13<2739::AID-APP22>3.0.CO;2-F.

[82] Franco M, Mondragon I, Bucknall C B. Blends of epoxy resin with amine-terminated polyoxypropylene elastomer: morphology and properties. Journal of Applied Polymer Science 1999; 72: 427–434. DOI: https://doi.org/10.1002/(SICI)1097-4628(19990418)72:3<427::AID-APP12>3.0.CO;2-4.

[83] Kornmann X, Rees M, Thomann Y, Necola A, Barbezat M, Thomann R. Epoxy-layered silicate nanocomposites as matrix in glass fibre-reinforced composites. Composites Science and Technology 2005; 65: 2259–2268. DOI: 10.1016/j.compscitech.2005.02.006.

[84] Avila A, Duarte H V., Soares M I. The nanoclay influence on impact response of laminated plates. Latin American Journal of Solids and Structures 2005; 3: 3–20.

[85] Tsai J L, Kuo J C, Hsu S M. Organoclay effect on transverse compressive strength of glass/epoxy nanocomposites. Journal of Materials Science 2006; 41: 7406–7412. DOI: 10.1007/s10853-006-0800-6.

[86] Lingaraju D, Ramji K, Devi M P, Lakshmi U R. Mechanical and tribological studies of polymer hybrid nanocomposites with nano reinforcements. Bulletin of Materials Science 2011; 34: 705–712. DOI: 10.1007/s12034-011-0185-2.

[87] Withers G J, Yu Y, Khabashesku V N, Cercone L, Hadjiev V G, Souza J M. Improved

mechanical properties of an epoxy glass-fiber composite reinforced with surface organomodified nanoclays. Composites Part B: Engineering 2015; 72: 175–182. DOI: 10.1016/j.compositesb.2014.12.008.

[88] Reddy C V, Babu P R, Ramnarayanan R. Effect of various filler materials on interlaminar shear strength (ILSS) of glass/epoxy composite materials. International Journal of Engineering and Manufacturing 2016; 6: 22–29. DOI: 10.5815/ijem.2016.05.03.

[89] Lin L Y, Lee J H, Hong C E, Yoo G H, Advani S G. Preparation and characterization of layered silicate/glass fiber/epoxy hybrid nanocomposites via vacuum-assisted resin transfer molding (VARTM). Composites Science and Technology 2006; 66: 2116–2125. DOI: 10.1016/j.compscitech.2005.12.025.

[90] Bozkurt E, Kaya E, Tanoğlu M. Mechanical and thermal behavior of non-crimp glass fiber reinforced layered clay/epoxy nanocomposites. Composites Science and Technology 2007; 67: 3394–3403. DOI: 10.1016/j.compscitech.2007.03.021.

[91] Kumar M A, Reddy K H, Reddy Y V M, Reddy G R, Naidu S V. Improvement of tensile and flexural properties in epoxy/clay nanocomposites reinforced with weave glass fiber reel. International Journal of Polymeric Materials 2010; 59: 854–862. DOI: 10.1080/00914037.2010.504144.

[92] Agubra V, Owuor P, Hosur M. Influence of nanoclay dispersion methods on the mechanical behavior of E-glass/epoxy nanocomposites. Nanomaterials 2013; 3: 550–563. DOI: 10.3390/nano3030550.

[93] Devendra K, Rangaswamy T. Evaluation of thermal properties of E-glass/epoxy composites filled by different filler materials. International Journal of Computational Engineering Research 2012; 2: 1708–1714.

[94] Channapagoudra M N, Joshi A G, Thaned S, Patil M. Effect of hematite filler material on mechanical properties of glass/epoxy composites. International Journal of Innovative Research in Science 2013; 2: 6229–6234.

[95] Shettar M, Chauhan V R. Investigation on mechanical properties of E-glass, epoxy resin with asbestos filled/hybrid composites. Global Journal of Engineering Science and Research Management 2015; 2: 31–35.

[96] Cid M A G D, Prolongo M G, Salom C, Arribas C, Sánchez-Cabezudo M, Masegosa R M. The effect of stoichiometry on curing and properties of epoxy-clay nanocomposites. Journal of Thermal Analysis and Calorimetry 2012; 108: 741–749. DOI: 10.1007/s10973-012-2215-8.

[97] Kumar D S, Shukla M J, Mahato K K, Rathore D K, Prusty R K, Ray B C. Effect of post-

curing on thermal and mechanical behavior of GFRP composites. Materials Science and Engineering 2015; 75: 1–6. DOI: 10.1088/1757-899X/75/1/012012.

[98] Minty R F, Thomason J L, Yang L. The role of the epoxy resin: curing agent ratio on composite interfacial strength and thermal performance. ECCM17-17th European Conference on Composite Materials, Munich, Germany, June 26–30, 2016.

[99] Sharma B, Chhibber R, Mehta R. Curing studies and mechanical properties of glass fiber reinforced composites based on silanized clay minerals. Applied Clay Science 2017; 138: 89–99. DOI: 10.1016/j.clay.2016.12.038.

[100] Santos P and Pezzin S H. Mechanical properties of polypropylene reinforced with recycled-PET fibres. Journal of Materials Processing Technology 2003; 143–144: 517–520. DOI: 10.1016/S0924-0136(03)00391-1.

[101] Guan G H, Li C C, Zhang D. Spinning and properties of poly(ethylene terephthalate)/ organomontmorillonite nanocomposite fibers. Journal of Applied Polymer Science 2005; 95: 1443–1447. DOI: 10.1002/app.21387.

[102] Arikan V and Sayman O. Comparative study on repeated impact response of E-glass fiber reinforced polypropylene & epoxy matrix composites. Composites Part B: Engineering 2015; 83: 1–6. DOI: 10.1016/j.compositesb.2015.08.051.

[103] Carolan D, Ivankovic A, Kinloch A J, Sprenger S, Taylor A C. Toughening of epoxy-based hybrid nanocomposites. Polymer 2016; 97: 179–190. DOI: 10.1016/j.polymer.2016.05.007.

[104] Nguyen T K L, Soares B G, Duchet-Rumeau J, Livi S. Dual functions of ILs in the core-shell particle reinforced epoxy networks: curing agent vs dispersion aids. Composites Science and Technology 2017; 140: 30–38. DOI: 10.1016/j.compscitech.2016.12.021.

[105] Teh S F, Liu T, Wang L, He C. Fracture behaviour of poly(ethylene terephthalate) fiber toughened epoxy composites. Composites Part A: Applied Science and Manufacturing 2005; 36: 1167–1173. DOI: 10.1016/j.compositesa.2004.08.007.

[106] Khanchaitit P and Aht-Ong D. Continuous surface modification process with ultraviolet/ozone for improving interfacial adhesion of poly(ethylene terephthalate)/epoxy composites. Polymer Composites 2006; 27: 484–490. DOI: 10.1002/pc.20216.

[107] Jindal Y. Polyethylene terephthalate fiber reinforced epoxy nanocomposites. Master of Engineering. Thapar University, Patiala, Punjab, India 2013.

[108] Raturi M. Fabrication and property evaluation of a epoxy-clay-PET nanocomposite system. Master of Engineering. Thapar University, Patiala, Punjab, India 2014.

[109] Wang L, Shui X, Zheng X, You J, Li Y. Investigations on the morphologies and properties of epoxy/acrylic rubber/nanoclay nanocomposites for adhesive films. Composites Science and Technology 2014; 93: 46–53. DOI: 10.1016/j.compscitech.2013.12.023.

[110] Demir T and Tinçer T. Preparation and characterization of poly(ethylene terephthalate) powder-filled high-density polyethylene in the presence of silane coupling agents. Journal of Applied Polymer Science 2001; 79: 827–835. DOI: 10.1002/1097-4628(20010131)79:5<827::AID-APP70>3.0.CO;2-4.

[111] Cioffi M O H, Voorwald H J C, Mota R P. Surface energy increase of oxygen-plasma-treated PET. Materials Characterization 2003; 50: 209–215. DOI: 10.1016/S1044-5803(03)00094-9.

[112] Fernandez-Blazquez J P, Setzer S, Del Campo A. Nanostructured polymer fibers with enhanced adhesion to epoxy matrices. Plasma Processes and Polymers 2013; 10: 207–212. DOI: 10.1002/ppap.201200105.

[113] Liu X D, Sheng D K, Gao X M, Li T B, Yang Y M. UV-assisted surface modification of PET fiber for adhesion improvement. Applied Surface Science 2013; 264: 61–69. DOI: 10.1016/j.apsusc.2012.09.107.

[114] Jiang X, Huang H, Zhang Y, Zhang Y. Dynamically cured polypropylene/epoxy blends. Journal of Applied Polymer Science 2004; 92: 1437–1448. DOI: https://doi.org/10.1002/app.13700

[115] Pan B, Viswanathan K, Hoyle C E, Moore R B. Photoinitiated grafting of maleic anhydride onto polypropylene. Journal of Polymer Science Part A: Polymer Chemistry 2004; 42: 1953–1962. DOI: 10.1002/pola.20038.

[116] Abacha N and Fellahi S. Synthesis of polypropylene-graft-maleic anhydride compatibilizer and evaluation of nylon 6/polypropylene blend properties. Polymer International 2005; 54: 909–916. DOI: 10.1002/pi.1788.

[117] Aboudzadeh M A, Mirabedini S M, Atai M. Effect of silane-based treatment on the adhesion strength of acrylic lacquers on the PP surfaces. International Journal of Adhesion and Adhesives 2007; 27: 519–526. DOI: 10.1016/j.ijadhadh.2006.09.012.

[118] Castel C D, Jr T P, Barbosa R V, Liberman S A, Mauler R S. Properties of silane grafted polypropylene/montmorillonite nanocomposites. Composites Part A: Applied Science and Manufacturing 2010; 41: 185–191. DOI: 10.1016/j.compositesa.2009.09.017.

[119] Roh J U, Ma S W, Lee W I, Hahn H T, Lee D W. Electrical and mechanical properties of graphite/maleic anhydride grafted polypropylene nanocomposites. Composites Part B:

Engineering 2013; 45: 1548–1553. DOI: 10.1016/j.compositesb.2012.09.062.

[120] Tsuji K, Nakaya M, Uedono A, Hotta A. Enhancement of the gas barrier property of polypropylene by introducing plasma-treated silane coating with SiO_x-modified top-surface. Surface and Coatings Technology 2015; 284: 377–383. DOI: 10.1016/j.surfcoat.2015.10.027.

[121] Kaynak C, Celikbilek C, Akovali G. Use of silane coupling agents to improve epoxy-rubber interface. European Polymer Journal 2003; 39: 1125–1132. DOI: 10.1016/S0014-3057(02)00381-6.

[122] Pasbakhsh P, Ismail H, Fauzi M N A, Bakar A A. Influence of maleic anhydride grafted ethylene propylene diene monomer (MAH-g-EPDM) on the properties of EPDM nanocomposites reinforced by halloysite nanotubes. Polymer Testing 2009; 28: 548–559. DOI: 10.1016/j.polymertesting.2009.04.004.

[123] Satapathy S, Nag A, Nando G B. Thermoplastic elastomers from waste polyethylene and reclaim rubber blends and their composites with fly ash. Process Safety and Environmental Protection 2010; 88: 131–141. DOI: 10.1016/j.psep.2009.12.001.

[124] Zhou Y, Wang W, Dou R, Li L, Yin B, Yang M. Effect of EPDM-g-MAH on the morphology and properties of PA6/EPDM/HDPE ternary blends. Polymer Engineering and Science 2013; 53: 1845–1855. DOI: 10.1002/pen.23445.

[125] Sarkawi S S, Dierkes W K, Noordermeer J W M. Elucidation of filler-to-filler and filler-to-rubber interactions in silica-reinforced natural rubber by TEM network visualization. European Polymer Journal 2014; 54: 118–127. DOI: 10.1016/j.eurpolymj.2014.02.015.

[126] Jantanasakulwong K, Rohindra D, Mori K, Kuboyama K, Ougizawa T. Thermoplastic elastomer by reactive blending of poly(butylene succinate) with ethylene-propylene-diene terpolymer and ethylene-1-butene rubbers. Journal of Elastomers and Plastics 2015; 47: 2–12. DOI: 10.1177/0095244313507805.

[127] Bazli L, Khavandi A, Ali M, Karrabi M. Correlation between viscoelastic behavior and morphology of nanocomposites based on SR/EPDM blends compatibilized by maleic anhydride. Polymer 2017; 113: 156–166. DOI: 10.1016/j.polymer.2017.02.057.

[128] Hadjizadeh A, Ajji A, Bureau M N. Preparation and characterization of NaOH treated micro-fibrous polyethylene terephthalate nonwovens for biomedical application. Journal of the Mechanical Behavior of Biomedical Materials 2010; 3: 574–583. DOI: 10.1016/j.jmbbm.2010.07.002.

[129] Fadeev A Y and Mccarthy T J. Surface modification of poly (ethylene terephthalate) to prepare surfaces with silica-like reactivity. Langmuir 1998; 14: 5586–5593.

DOI: 10.1021/la980512f.

[130] Kusuktham B. Surface modification of polyester fabrics with vinyltriethoxysilane. Journal of Metals, Materials and Minerals 2010; 20: 85–88.

[131] Goh C S, Tan S C, Ngoh S L, Wei J. Surface treatment of polyethylene terephthalate (PET) film for lamination of flexible photovoltaic devices. Energy Procedia 2012; 428–435. DOI: 10.1016/j.egypro.2012.02.052.

[132] Paunikallio T, Suvanto M, Pakkanen T T. Grafting of 3-(trimethoxysilyl)propyl methacrylate onto polypropylene and use as a coupling agent in viscose fiber/polypropylene composites. Reactive and Functional Polymers 2008; 68: 797–808. DOI: 10.1016/j.reactfunctpolym.2007.11.018.

[133] Zhou S, Hu M, Hu Y, Wang Z. Influence of coagents on the silane grafting and cross-linking of polypropylene. Polymer-Plastics Technology and Engineering 2009; 48: 193–200. DOI: 10.1080/03602550802634543.

[134] Jiang X L, Sun K, Zhang Y X. Effects of dynamical cure and compatibilization on the morphology and properties of the PP/epoxy blends. Express Polymer Letters 2007; 1: 283–291. DOI: 10.3144/expresspolymlett.2007.41.

[135] Hujuri U, Chattopadhay S K, Uppaluri R, Ghoshal A K. Effect of maleic anhydride grafted polypropylene on the mechanical and morphological properties of chemically modified short-pineapple-leaf-fiber-reinforced polypropylene composites. Journal of Applied Polymer Science 2008; 107: 1507–1516. DOI: 10.1002/app.27156.

[136] Igarza E, Pardo S G, Abad M J, Cano J, Galante M J, Pettarin V, Bernal C. Structure-fracture properties relationship for polypropylene reinforced with fly ash with and without maleic anhydride functionalized isotactic polypropylene as coupling agent. Materials and Design 2014; 55: 85–92. DOI: 10.1016/j.matdes.2013.09.055.

[137] Msekh M A, Cuong N H, Zi G, Areias P, Zhuang X, Rabczuk T. Fracture properties prediction of clay/epoxy nanocomposites with interphase zones using a phase field model. Engineering Fracture Mechanics 2018; 188: 287–299. DOI: 10.1016/j.engfracmech.2017.08.002.

[138] Garg M, Sharma S, Mehta R. Processing of functionalized and pristine carbon nanotube epoxy composites with silane treated glass fiber. Materials and Manufacturing Processes 2016; 31: 2044–2056. DOI: 10.1080/10426914.2016.1176186.

[139] Sharma B, Chhibber R, Mehta R. Effect of surface treatment of nanoclay on the mechanical properties of epoxy/glass fiber/clay nanocomposites. Composite Interfaces 2016; 23: 623–640. DOI: 10.1080/09276440.2016.1165522.

[140] Demjen Z, Pukanszky B, Nagy J. Possible coupling reactions of functional silanes and polypropylene. Polymer 1999; 40: 1763–1773. DOI: 10.1016/S0032-3861(98)00396-6.

[141] Park S and Jin J. Effect of silane coupling agent on mechanical interfacial properties of glass fiber-reinforced unsaturated polyester. Journal of Polymer Science Part B: Polymer Physics 2002; 41: 55–62. DOI: https://doi.org/10.1002/polb.10359.

[142] Alkadasi N A N, Sarwade B D, Hundiwale D G, Kapadi U R. Studies on the effect of titanate coupling agent (2.0 %) on the mechanical properties of flyash-filled polybutadiene rubber. Polymer 2003; 63: 603–609. DOI: 10.1002/app.20548.

[143] Alkadasi N A N, Sarwade B D, Hundiwale D G, Kapadi U R. Effect of coupling agent on the mechanical properties of fly ash-filled polybutadiene rubber. Journal of Applied Polymer Science 2004; 91: 1322–1328. DOI: https://doi.org/10.1002/app.13280.

[144] Li Y. Processing of Sisal Fiber Reinforced Composites by Resin Transfer Molding. Materials and Manufacturing Processes 2006; 21: 181–190. DOI: 10.1081/AMP-200068669.

[145] Sever K, Sarikanat M, Seki Y, Cecen V, Tavman I H. Effects of fiber surface treatments on mechanical properties of epoxy composites reinforced with glass fabric. Journal of Materials Science 2008; 43: 4666–4672. DOI: 10.1007/s10853-008-2679-x.

[146] Cohen N, Dotan A, Dodiuk H, Kenig S. Superhydrophobic coatings and their durability. Materials and Manufacturing Processes 2015; 31: 1143–1155. DOI: 10.1080/10426914.2015.1090600.

[147] Deng J P, Yang W T, Ranby B. Surface photografting polymerization of vinyl acetate (VAc), maleic anhydride, and their charge transfer complex . I . VAc (1). Journal of Applied Polymer Science 2000; 77: 1522–1531. DOI: 10.1002/app.21877.

[148] Deng J P and Yang W T. Self-initiating performance of maleic anhydride on surface photografting polymerization. Journal of Polymer Science Part A: Polymer Chemistry 2001; 39: 3246–3249. DOI: 10.1002/pola.1307.

[149] Rzayev Z M O. Graft copolymers of maleic anhydride and its isostructural analogues: high performance engineering materials. International Review of Chemical Engineering 2011; 3: 153–215.

[150] Deng J, Wang L, Liu L, Yang W. Developments and new applications of UV-induced surface graft polymerizations. Progress in Polymer Science 2009; 34: 156–193. DOI: 10.1016/j.progpolymsci.2008.06.002.

[151] Kordoghli B, Khiari R, Dhaouadi H, Belgacem M N, Mhenni M F, Sakli F. UV irradiation-assisted grafting of poly(ethylene terephthalate) fabrics. Colloids and

Surfaces A: Physicochemical and Engineering Aspects 2014; 441: 606–613. DOI: 10.1016/j.colsurfa.2013.10.032.

[152] Asumani O M L, Reid R G, Paskaramoorthy R. The effects of alkali-silane treatment on the tensile and flexural properties of short fibre non-woven Kenaf reinforced polypropylene composites. Composites Part A: Applied Science and Manufacturing 2012; 43: 1431–1440. DOI: 10.1016/j.compositesa.2012.04.007.

[153] Jaeger B D and Gleria M. editors. Inorganic Polymers. New York: Nova Science Publishers; 2007.

[154] Wang K, Chen L, Kotaki M, He C. Preparation, microstructure and thermal mechanical properties of epoxy/crude clay nanocomposites. Composites Part A: Applied Science and Manufacturing 2007; 38: 192–197. DOI: 10.1016/j.compositesa.2006.01.008.

[155] Lei W. Preparation, morphology and thermal/mechanical properties of epoxy-nanoclay composites. Doctorate of Philospohy. National University of Singapore, Singapore 2005.

[156] Camino G, Tartaglione G, Frache A, Manferti C, Costa G. Thermal and combustion behaviour of layered silicate-epoxy nanocomposites. Polymer Degradation and Stability 2005; 90: 354–362. DOI: 10.1016/j.polymdegradstab.2005.02.022.

[157] Chung S K, Wie J J, Park B Y, Kim S C. Synthesis of reactive organifier for the epoxy/layered silicate nanocomposite and the properties of the epoxy nanocomposites. Journal of Macromolecular Science, Part A: Pure and Applied Chemistry 2009; 46: 205–214. DOI: 10.1080/10601320802595185.

[158] Dicastillo A C L D, Castro M M, Vilarino J M L, Gonzalez R M V. Study of the interaction between a natural antioxidant and anhidride maleic modified polypropylene formulations. 5th International Synopsium on Food Packing Scientific Developments Supporting Safety and Innovation, Berlin, Germany, November 14–16, 2012.

[159] Conzatti L, Giunco F, Stagnaro P, Patrucco A, Tonin C, Marano C, Rink M, Marsano E. Wool fibres functionalised with a silane-based coupling agent for reinforced polypropylene composites. Composites Part A: Applied Science and Manufacturing 2014; 61: 51–59. DOI:10.1016/j.compositesa.2014.02.005.

[160] Oever M V D and Peijs T. Continuous-glass-fibre-reinforced polypropylene composites II. Influence of maleic-anhydride modified polypropylene on fatigue behaviour. Composites Part A: Applied Science and Manufacturing 1998; 29: 227–239. DOI: 10.1016/S1359-835X(97)00089-4.

[161] Li M, Wen X, Liu J, Tang T. Synergetic effect of epoxy resin and maleic anhydride grafted polypropylene on improving mechanical properties of polypropylene/short

carbon fiber composites. Composites Part A: Applied Science and Manufacturing 2014; 67: 212–220. DOI: 10.1016/j.compositesa.2014.09.001.

[162] Posthumus W, Magusin P C M M, Brokken-Zijp J C M, Tinnemans A H A, Linde R V D. Surface modification of oxidic nanoparticles using 3-methacryloxypropyltrimethoxysilane. Journal of Colloid and Interface Science 2004; 269: 109–116. DOI: 10.1016/j.jcis.2003.07.008.

[163] Yeh S K, Hsieh C C, Chang H C, Yen C C C, Chang Y C. Synergistic effect of coupling agents and fiber treatments on mechanical properties and moisture absorption of polypropylene-rice husk composites and their foam. Composites Part A: Applied Science and Manufacturing 2015; 68: 313–322. DOI: 10.1016/j.compositesa.2014.10.019.

[164] Severini F, Pegoraro M, Yuan L, Ricca G, Fanti N. Free radical grafting of maleic anhydride in vapour phase on polypropylene film. Polymer 1999; 40: 7059–7064. DOI: https://doi.org/10.1016/S0032-3861(99)00113-5.

[165] Meola C, Giorleo G, Prisco U. Experimental evaluation of properties of cross-linked polyethylene. Materials and Manufacturing Processes 2003; 18: 135–144. DOI: 10.1081/Amp-120017595.

[166] Abdolahifard M, Bahrami S H, Malek R M A. Surface modification of PET fabric by graft copolymerization with acrylic acid and its antibacterial properties. International Scholarly Research Network Organic Chemistry 2011; 2011: 1–8. DOI: 10.5402/2011/265415.

[167] Koohestani B, Ganetri I, Yilmaz E. Effects of silane modified minerals on mechanical, microstructural, thermal, and rheological properties of wood plastic composites. Composites Part B: Engineering 2017; 111: 103–111. DOI: 10.1016/j.compositesb.2016.12.021.

[168] Nien Y H, Yeh P H, Shih Y F, Wang X P, Huang L Y. Modification of the structure of EPDM by chemically grafting inorganic species. Journal of Sol-Gel Science and Technology 2015; 73: 350–357. DOI: 10.1007/s10971-014-3539-6.

[169] Wang K, Chen Y, Zhang Y. Effects of organoclay platelets on morphology and mechanical properties in PTT/EPDM-g-MA/organoclay ternary nanocomposites. Polymer 2008; 49: 3301–3309. DOI: 10.1016/j.polymer.2008.05.025.

[170] Shen C, Zhou Y, Dou R, Wang W, Yin B, Yang M. Effect of the core-forming polymer on phase morphology and mechanical properties of PA6/EPDM-g-MA/HDPE ternary blends. Polymer 2015; 56: 395–405. DOI: 10.1016/j.polymer.2014.11.027.

[171] Barra G M O, Crespo J S, Bertolino J R, Soldi V, Pires A T N. Maleic anhydride grafting

on EPDM: qualitative and qunatative determination. Journal of the Brazilian Chemical Society 1999; 10: 31–34. DOI: http://dx.doi.org/10.1590/S0103-50531999000100006.

[172] Dou R, Zhou Y, Shen C, Li L P, Yin B, Yang M B. Toughening of PA6/EPDM-g-MAH/HDPE ternary blends via controlling EPDM-g-MAH grafting degree: the role of core–shell particle size and shell thickness. Polymer Bulletin 2014; 72: 177–193. DOI: 10.1007/s00289-014-1266-3.

[173] Kornmann X, Rees M, Thomann Y, Necola A, Barbezat M, Thomann R. Epoxy-layered silicate nanocomposites as matrix in glass fibre-reinforced composites. Composites Science and Technology 2005; 65: 2259–2268. DOI: 10.1016/j.compscitech.2005.02.006.

[174] Jansen B J P, Tamminga K Y, Meijer H E H, Lemstra P J. Preparation of thermoset rubbery epoxy particles as novel toughening modifiers for glassy epoxy resins. Polymer 1999; 40: 5601–5607. DOI: https://doi.org/10.1016/S0032-3861(98)00774-5.

[175] Ratna D. editor. Handbook of Thermoset Resins. UK: Smithers Rapra Technology Limited; 2009.